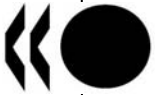


**Unclassified**

**NEA/CSNI/R(2008)2**



Organisation de Coopération et de Développement Economiques  
Organisation for Economic Co-operation and Development

**18-Sep-2008**

**English text only**

**NUCLEAR ENERGY AGENCY  
COMMITTEE ON THE SAFETY OF NUCLEAR INSTALLATIONS**

**NEA/CSNI/R(2008)1  
Unclassified**

**OECD-IAEA Paks Fuel Project Final Report**

**English text only**

Document complet disponible sur OLIS dans son format d'origine  
Complete document available on OLIS in its original format

## ORGANISATION FOR ECONOMIC CO-OPERATION AND DEVELOPMENT

The OECD is a unique forum where the governments of 30 democracies work together to address the economic, social and environmental challenges of globalisation. The OECD is also at the forefront of efforts to understand and to help governments respond to new developments and concerns, such as corporate governance, the information economy and the challenges of an ageing population. The Organisation provides a setting where governments can compare policy experiences, seek answers to common problems, identify good practice and work to co-ordinate domestic and international policies.

The OECD member countries are: Australia, Austria, Belgium, Canada, the Czech Republic, Denmark, Finland, France, Germany, Greece, Hungary, Iceland, Ireland, Italy, Japan, Korea, Luxembourg, Mexico, the Netherlands, New Zealand, Norway, Poland, Portugal, the Slovak Republic, Spain, Sweden, Switzerland, Turkey, the United Kingdom and the United States. The Commission of the European Communities takes part in the work of the OECD.

OECD Publishing disseminates widely the results of the Organisation's statistics gathering and research on economic, social and environmental issues, as well as the conventions, guidelines and standards agreed by its members.

\* \* \*

*This work is published on the responsibility of the Secretary-General of the OECD. The opinions expressed and arguments employed herein do not necessarily reflect the official views of the Organisation or of the governments of its member countries.*

## NUCLEAR ENERGY AGENCY

The OECD Nuclear Energy Agency (NEA) was established on 1<sup>st</sup> February 1958 under the name of the OEEC European Nuclear Energy Agency. It received its present designation on 20<sup>th</sup> April 1972, when Japan became its first non-European full member. NEA membership today consists of 28 OECD member countries: Australia, Austria, Belgium, Canada, the Czech Republic, Denmark, Finland, France, Germany, Greece, Hungary, Iceland, Ireland, Italy, Japan, Luxembourg, Mexico, the Netherlands, Norway, Portugal, Republic of Korea, the Slovak Republic, Spain, Sweden, Switzerland, Turkey, the United Kingdom and the United States. The Commission of the European Communities also takes part in the work of the Agency.

The mission of the NEA is:

- to assist its member countries in maintaining and further developing, through international co-operation, the scientific, technological and legal bases required for a safe, environmentally friendly and economical use of nuclear energy for peaceful purposes, as well as
- to provide authoritative assessments and to forge common understandings on key issues, as input to government decisions on nuclear energy policy and to broader OECD policy analyses in areas such as energy and sustainable development.

Specific areas of competence of the NEA include safety and regulation of nuclear activities, radioactive waste management, radiological protection, nuclear science, economic and technical analyses of the nuclear fuel cycle, nuclear law and liability, and public information. The NEA Data Bank provides nuclear data and computer program services for participating countries.

In these and related tasks, the NEA works in close collaboration with the International Atomic Energy Agency in Vienna, with which it has a Co-operation Agreement, as well as with other international organisations in the nuclear field.

### © OECD 2008

No reproduction, copy, transmission or translation of this publication may be made without written permission. Applications should be sent to OECD Publishing: [rights@oecd.org](mailto:rights@oecd.org) or by fax (+33-1) 45 24 99 30. Permission to photocopy a portion of this work should be addressed to the Centre Français d'exploitation du droit de Copie (CFC), 20 rue des Grands-Augustins, 75006 Paris, France, fax (+33-1) 46 34 67 19, ([contact@cfcopies.com](mailto:contact@cfcopies.com)) or (for US only) to Copyright Clearance Center (CCC), 222 Rosewood Drive Danvers, MA 01923, USA, fax +1 978 646 8600, [info@copyright.com](mailto:info@copyright.com).

## COMMITTEE ON THE SAFETY OF NUCLEAR INSTALLATIONS

The NEA Committee on the Safety of Nuclear Installations (CSNI) is an international committee made up of senior scientists and engineers, with broad responsibilities for safety technology and research programmes, and representatives from regulatory authorities. It was set up in 1973 to develop and co-ordinate the activities of the NEA concerning the technical aspects of the design, construction and operation of nuclear installations insofar as they affect the safety of such installations.

The committee's purpose is to foster international co-operation in nuclear safety amongst the OECD member countries. The CSNI's main tasks are to exchange technical information and to promote collaboration between research, development, engineering and regulatory organisations; to review operating experience and the state of knowledge on selected topics of nuclear safety technology and safety assessment; to initiate and conduct programmes to overcome discrepancies, develop improvements and research consensus on technical issues; to promote the coordination of work that serve maintaining competence in the nuclear safety matters, including the establishment of joint undertakings.

The committee shall focus primarily on existing power reactors and other nuclear installations; it shall also consider the safety implications of scientific and technical developments of new reactor designs.

In implementing its programme, the CSNI establishes co-operative mechanisms with NEA's Committee on Nuclear Regulatory Activities (CNRA) responsible for the program of the Agency concerning the regulation, licensing and inspection of nuclear installations with regard to safety. It also co-operates with NEA's Committee on Radiation Protection and Public Health (CRPPH), NEA's Radioactive Waste Management Committee (RWMC) and NEA's Nuclear Science Committee (NSC) on matters of common interest.

## FOREWORD

It is important for nuclear power plant (NPP) designers, operators and regulators to effectively use lessons learned from an event occurred at NPPs, since in general, it is impossible to reproduce the event using experimental facilities. In particular, evaluation of the event using accident analysis codes is expected to contribute to improve understanding of phenomena during the events and to facilitate the validation of computer codes through simulation analyses.

During a fuel crud removal operation on the Paks-2 unit on 10 April 2003 several fuel assemblies were severely damaged. The assemblies were being cleaned in a special tank of the Paks Nuclear Power Plant, Hungary under deep water level in a service pit connected to the spent fuel storage pool. The first sign of fuel failures was the detection of some fission gases released from the cleaning tank. Later visual inspection revealed that most of the thirty fuel assemblies suffered heavy oxidation and fragmentation. The first evaluation of the event showed that the severe fuel damage happened due to inadequate cooling.

The Paks-2 event was discussed in various committees of the OECD Nuclear Energy Agency (OECD/NEA) and of the International Atomic Energy Agency (IAEA). Recommendations were made to undertake actions to improve the understanding of the incident sequence and of the consequence this had on the fuel. It was considered that the Paks-2 event may constitute a useful case for a comparative exercise on safety codes, in particular for models devised to predict fuel damage and potential releases under abnormal cooling conditions and the analyses on the Paks-2 event may provide information which is relevant for in-reactor and spent fuel storage safety evaluations.

The OECD-IAEA Paks Fuel Project was established in 2005 as a joint project between the IAEA and the OECD/NEA. The IAEA provided financial support to the operating agent (Hungarian Academy of Sciences KFKI Atomic Energy Research Institute (AEKI)) and reviewed the progress of the project within the framework of the TC Project, RER9076 “Strengthening Safety and Reliability of Fuel and Material in Nuclear Power Plants”. Thirty organizations from sixteen countries participated in the project. The following participants performed analyses of the event using numerical models based on a common database:

- AEKI (Hungary),
- BME NTI (Hungary),
- GRS (Germany),
- IRSN (France),
- IVS (Slovak Republic),
- KI (Russian Federation),
- SUEZ – TRACTEBEL ENGINEERING (Belgium),
- US NRC (United States of America),
- VEIKI (Hungary),
- VTT (Finland),
- VUJE (Slovak Republic).

The main results of calculations are summarised in the present report.

The report is published as a joint product between the IAEA and the OECD/NEA. The IAEA and the OECD/NEA acknowledge the work of the participating experts and wish to thank them to their valuable contribution to this publication. The IAEA and the OECD/NEA officers responsible for the preparation of this document were Y. Makihara and C. Vitanza, respectively.

## CONTENTS

FOREWORD .....	2
EXECUTIVE SUMMARY .....	1
1 INTRODUCTION .....	2
2 DESCRIPTION OF THE INCIDENT .....	6
2.1 Preliminaries .....	7
2.2 Operation of the cleaning tank .....	8
2.3 Chronology of the incident .....	12
2.3.1 Formation of steam volume .....	13
2.3.2 Plastic deformation of cladding and high temperature oxidation .....	14
2.3.3 Quench .....	15
2.4 State of damaged fuel .....	16
2.5 Post-incident investigations .....	17
2.6 The recovery work .....	18
3 MAJOR RESULTS OF ANALYSES .....	23
3.1 Participant SUEZ - TRACTEBEL ENGINEERING .....	23
3.1.1 Code description .....	23
3.1.2 Model description .....	23
3.1.3 Chronology of main events .....	26
3.1.4 Conclusions .....	27
3.2 Participant VTT .....	27
3.2.1 Introduction and case description .....	27
3.2.2 Calculation results .....	31
3.2.3 Conclusions .....	32
3.3 Participant GRS .....	33
3.3.1 Code description .....	33
3.3.2 Files delivered for the comparison .....	33
3.3.3 Nodalisation and input model .....	33
3.3.4 Results of calculation .....	34
3.4 Participant AEKI .....	35
3.4.1 Thermal hydraulic analysis .....	35
3.4.2 Thermal hydraulic analysis with the RELAP code .....	35
3.4.3 Thermal hydraulic analysis with the ATHLET code .....	38
3.4.4 Fuel behaviour calculation .....	39
3.4.5 Calculation of activity release .....	40
3.4.6 Summary of calculated results .....	41
3.5 Participant BME NTI .....	42
3.5.1 The 3D CFD models of the cleaning tank .....	42
3.5.2 Boundary conditions, parameters of the model .....	42
3.5.3 Computational results .....	43
3.6 Participant VEIKI .....	44
3.6.1 MELCOR PWR and BWR models of the cleaning tank .....	44
3.6.2 Safe envelope of operation .....	46
3.6.3 Transient calculations .....	47
3.6.4 Conclusions .....	48

3.7	Participant KI/IRSN .....	48
3.7.1	Code description .....	49
3.7.2	Thermal hydraulic phase of the transient.....	49
3.7.3	SFD phase of the transient .....	49
3.8	Participant IVS .....	51
3.8.1	Code description .....	51
3.8.2	Nodalisation scheme .....	52
3.8.3	Main results.....	53
3.9	Participant VUJE .....	54
3.9.1	Description of the input model .....	54
3.9.2	Initial and boundary conditions .....	55
3.9.3	Description of results .....	56
3.10	Participant USNRC.....	57
3.10.1	Code description .....	57
3.10.2	Thermal hydraulic Response .....	57
3.10.3	Fission Product Release .....	59
4	COMPARISON OF CALCULATED RESULTS .....	61
4.1	Thermal hydraulics .....	63
4.2	Fuel behaviour .....	64
4.3	Activity release .....	67
4.4	Plots of selected parameters .....	69
5	RECOMMENDATIONS.....	88
6	CONCLUSIONS .....	90
	ABBREVIATIONS.....	91
	CONTRIBUTORS TO DRAFTING AND REVIEW .....	92

## **EXECUTIVE SUMMARY**

The OECD-IAEA Paks Fuel Project aimed to support the understanding of fuel behaviour in accident conditions on the basis of analyses of the Paks-2 event. Numerical simulation of the most relevant aspects of the event and comparison of the calculation results with the available information was carried out between 2006 and 2007. A database was collected to provide input data for the code calculations. The activities covered the following three areas:

- Thermal hydraulic calculations described the cooling conditions possibly established during the incident.
- Simulation of fuel behaviour described the oxidation and degradation mechanisms of fuel assemblies.
- The release of fission products from the failed fuel rods was estimated and compared to available measured data.

The produced numerical results improved the understanding of the causes and mechanisms of fuel failures during the Paks-2 incident and provided new information on the behaviour of nuclear fuel under accident conditions.

## 1 INTRODUCTION

On the 10th April 2003 severe damage of fuel assemblies took place during an incident at Unit 2 of Paks Nuclear Power Plant in Hungary. The assemblies were being cleaned in a special tank below the water level of the spent fuel storage pool in order to remove crud buildup. That afternoon, the chemical cleaning of assemblies was completed and the fuel rods were being cooled by circulation of spent fuel storage pool water. The first sign of fuel failure was the detection of some fission gases released from the cleaning tank during that evening. The cleaning tank cover locks were released after midnight and this operation was followed by a sudden increase in activity concentrations. The visual inspection revealed that all 30 fuel assemblies were severely damaged. The first evaluation of the event showed that the severe fuel damage happened due to inadequate coolant circulation within the cleaning tank. The damaged fuel assemblies were removed from the cleaning tank in 2006 and are stored in special canisters in the spent fuel storage pool of the Paks NPP.

The event was reported to the IAEA and classified as a Level 3 (severe) incident on the International Nuclear Event Scale (INES). The IAEA sent an expert review mission to investigate the incident in June 2003.

First information on the Paks-2 incidents was provided to the CSNI in its June 2003 meeting, two months after the incident. At that time the CSNI requested the NEA secretariat to coordinate actions with Hungarian and Russian parties aimed to assess the extent to which possible fuel investigations would benefit the nuclear community while helping clarifying the conditions experienced by the fuel during the incident. As a first step in this direction, a meeting was organised in Budapest on 18 August 2003 under the auspices of the NEA. Visual examinations of the damaged assemblies as well as analyses were presented on that occasion. The participants agreed that international collaboration should be pursued to the extent feasible. Recommendations were made that the NEA and the IAEA try to organise a joint project in co-ordination with Russian and Hungarian organisations, provided that useful information could be gathered through such initiative.

The experts of the Hungarian Academy of Sciences KFKI Atomic Energy Research Institute (AEKI) and of the Russian Research Centre Kurchatov Institute (KI) prepared the first draft of the potential international project in 2004. An Experts' meeting of potential participants was organised in November 2004 in Studsvik that represented a crucial point in the process of launching the project. The participants were requested to assess the technical validity of the proposed project, suggest improvements if needed and provide a first indication of technical interest in the proposal. It was intended to organise the project in two phases, i.e.:

- Phase 1 focussing on analytical activities.
- Phase 2 focussing on the fuel examinations.

The analytical part of the project was intended to cover a database collection which would have served as basis for code calculations, for the selection of the fuel to be examined and for preparing the list of fuel examinations to be carried out. The fuel examination phase would have involved poolside activities first, then the shipping from Paks to hot cells in Russia and then the hot cells examinations.

Phase 1 of the project was launched in the framework of the OECD-IAEA Paks Fuel Project in 2006 aimed to investigate fuel behaviour in accident conditions on the basis of analyses of the Paks-2 event. The project was co-ordinated by the OECD NEA and by the IAEA. The

meetings were chaired by GRS, Germany. The tasks of the Operating Agent were fulfilled by the Hungarian AEKI.

There was no formal agreement signed by all participants for the OECD-IAEA Paks Fuel Project. The participation in the project was available through national nuclear regulatory organisations with the approval of OECD NEA and IAEA. During the two years duration of the project 58 experts from 34 organisations of 16 countries were listed among the participants. All participants had access to the materials of the project including the database and the presentations given at the meetings. In the frame of the RER/9/076 “Strengthening Safety and Reliability of Nuclear Fuel and Materials in Nuclear Power Plants” project the IAEA had made three contracts with AEKI in order to support financially the activities of the Operating Agent.

The kick-off meeting of the project was held in January 2006 in Budapest. The presentations on the earlier analytical work performed by some participants revealed that there were big differences in the calculation results, since most of calculations were done just after the event in 2003 and little information was provided to the analysts. Nevertheless, it was found in the thermal hydraulic calculations, that the by-pass flow would play an essential role for the prediction of uncover time. The fuel properties analysis also showed that the results were strongly dependent on the assumptions adopted by the analysts. In particular, decay heat and treatment of zirconium-water reactions would give a strong impact on the results. It was also revealed that the steam starvation effect may have stabilized the heat-up phase, which is strongly dependent on the assumed gas leakage rate from the tank. It was agreed that new calculations would be carried out by the participants using a common database. The scope of calculations would cover thermal hydraulic, fuel behaviour and activity release phenomena:

- Thermal hydraulic calculations to describe how the inadequate cooling conditions could have established during the incident.
- Fuel behaviour simulation to describe the oxidation and degradation mechanisms of fuel assemblies.
- Activity release and transport calculations to simulate the release of fission products from the failed fuel rods.

After the first meeting the AEKI collected the database, established a website for the project and prepared a proposal for the requirements for output data.

The database (Appendix A/I) included the following main parts:

- Design characteristics of VVER-440 fuel assemblies (main geometrical data, some mechanical properties, oxidation kinetics of E110 cladding, and integral data of assemblies). The source of these data was mainly the open literature publications of the VVER fuel supplier. Special experimental data on the high temperature behaviour of E110 alloy including oxidation in hydrogen rich steam were provided by the AEKI.
- Operational data of damaged fuel assemblies (power histories of fuel assemblies, burnup, fuel rod internal pressure, isotope inventories, decay heat and axial power distribution). These data included the main parameters of the damaged fuel assemblies during their normal operation in the reactors. The parameters describing the fuel state before the incident were produced by the experts of Paks NPP and AEKI using the KARATE,

SCALE, ORIGEN, TIBSO and TRANSURANUS codes. During the project some control calculations on fuel behaviour were calculated by VTT, Finland using the FRAPCON code (Appendix B/III).

- Design characteristics of the cleaning tank were provided by the tank designer AREVA NP GmbH.
- Measured data during the incident: (temperature, water level measurements, cleaning tank outlet flowrates).
- Activity measurements (measured coolant activity concentrations, activity release through the chimney, flowrate of water make-up system, released activities). These data included not only the incident, but the period of wet storage of damaged fuel until their removal from the service pit.
- Reports (describing results of investigations, chronology).
- Status of fuel (results of visual observations).

The database and the materials of the meetings were available on a password protected website (Appendix A/II) for the participants who received individual userid and password to enter the site. The content of the website was several times updated during the project.

The list of requested output parameters (Appendix A/III) was specified in order to make possible the comparison of the results of calculations carried out by different organisations. The approach applied in this project was similar as in International Standard Problem (ISP) projects. The total number of requested parameters was more than one-hundred. The main groups of parameters were the followings:

- histories of thermal hydraulic parameters,
- profiles of thermal hydraulic parameters by the time the maximum cladding temperature exceeds 800°C,
- histories of fuel parameters,
- profiles of fuel parameters before quenching and
- histories of activity release from the fuel rods.

The requirements specified also the scope of written presentations of the results according to which the participants prepared individual chapters on their work. These materials were collected into chapter 3 of the present report. More detailed description of each calculation is available in Appendix B.

The second meeting of the project was held in October 2006 in Budapest. The agenda included presentations with preliminary results of thermal hydraulic analyses, fuel behaviour analyses and activity release calculations. Most of the presented results had preliminary character and it was agreed that the participants would continue the numerical calculations. The participants of the second meeting agreed that the thermal hydraulic calculations should be completed by the end of March 2007, and the fuel behaviour and activity calculations by the end of April 2007.

The final meeting of the project was held in April 2007 in Budapest. Individual presentations were given on the latest calculated results by the participants. The first comparison of selected parameters was also discussed in details. The participants agreed on the table of contents of the report and that the report will be published as a joint IAEA-OECD Project Report.

The preparation of fuel examination in Phase 2 of the project was discussed during each meeting. Experts of the Paks NPP regularly informed the project on the state of fuel and the actions related to the removal of damaged fuel from the cleaning tank and its further storage. Hungarian experts prepared a proposal on the selection of fuel assembly for hot cell examinations. The damaged fuel is stored in the Paks NPP today. The hot cell examinations could be carried out in Dimitrovgrad, Russia. Until the time of the writing of the present report no formal proposal had been developed for the examination of damaged fuel in Phase 2.

## 2 DESCRIPTION OF THE INCIDENT

The Paks Nuclear Power Plant has four VVER-440 type reactor units of 440 MW original capacities per each. These units serve nearly 40% of the Hungarian electricity demand. The four units were installed between 1983 and 1987.

On 10<sup>th</sup> of April, 2003 a serious incident (classified as Level 3 on the INES scale) caused heavy damage of 30 fuel assemblies in the Unit 2 of the Paks NPP. During the previous years, Units 1, 2 and 3 were burdened with considerable magnetite corrosion product deposition. Parallel to the annual maintenance, the deposited fuel assemblies were cleaned in a special cleaning tank which was constructed by a large European company and was installed into the so-called refuelling pit just beside the reactor.

The cleaning processes were performed on batches of 30 fuel assemblies. On 10<sup>th</sup> of April, 2003, the cleaning of the sixth batch was finished. During the cleaning process itself, the cooling of the fuel was ensured by high mass flow rate coolant circulation. However, after finishing the 6<sup>th</sup> batch's cleaning process the fuel was not removed from the cleaning tank immediately since the crane was busy with another tasks. In the meantime, the coolant was circulated by a submersible pump with much lower mass flow rate according to the service regulations.

The later inspection has revealed that due to the special design of the cleaning tank and the characteristic of the fuel assemblies, the cooling of the submersible pump of lower mass flow was insufficient. The coolant was not capable for removing the bulk of the decay heat and this resulted in a complicated natural convection flow in the cleaning tank and the fuel assemblies. The temperature stratification blocked the flow therefore the coolant temperature reached the saturation temperature in the upper part of the cleaning tank. Then the steam-formation pushed the main volume of the coolant out of the cleaning tank vessel due to the disadvantageous design of the instrument. This way, the fuel assemblies were left without cooling for hours and heated up to above 1000°C which resulted in severe damage and oxidation of the fuel assemblies' structure.

The radioactive noble gases escaped from the damaged fuel assemblies were released into the environment through the reactor hall stack. However, the impact on the environment was negligible thanks to the small released quantity.

In this chapter the main technical causes, the course of the incident and the steps of the recovery work are drafted.

## 2.1 Preliminaries

The first steps towards the incident could be the chemical decontamination processes of the steam generators which were performed in large number in the 90's. At that time corrosion-erosion caused problems in the feed water distributors of the steam generators which resulted in the series of distributor replacements (see Figure 2.1). During these operations, the maintenance staff had to work inside the steam generator secondary side. For radiological protection of the staff, chemical decontamination of the SGs' primary side were adopted. (This method was used only on Units 1, 2 and 3. In case of Unit 4, the so called physical shielding technique subsequently used based on methods developed abroad.)

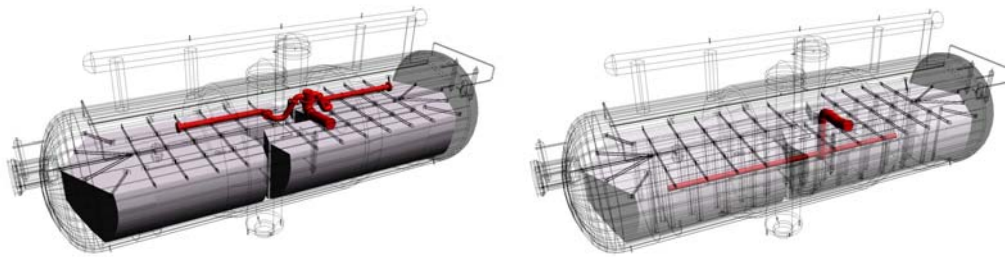


Figure 2.1. The old (left) and the new (right) distributors in the steam generator secondary side [14]

The widely used chemical decontaminations resulted in unacceptable aftermath: the dissolution of corrosion products accelerated to a large measure and the coolant transported the dissolved corrosion products into the reactor core. This yielded magnetite deposition on the surfaces of the fuel assemblies. In certain positions, these magnetite depositions blocked the part of the flow area, therefore the mass flow through these assemblies decreased and the maximum outlet temperature increased.

Significant deposits were experienced first time in the Unit 2 of Paks NPP in 1996. Until 1998 the quantity of the depositions was significant enough to require the replacement of the entire reactor core fuel with fresh assemblies for Unit 2. By 2000, the troubles with depositions affected Units 1, 2 and 3. In February of 2003, during the cycle, an entire reactor core fuel replacement had to be done in Unit 3. (In contrast, Unit 4, which used the physical shielding method, did not have any deposition problems.)

To comply with the Technical Operating Regulations and other specifications, the Paks NPP adopted the following measures: the power of the concerned units was limited in accordance with the limitations for the fuel assembly outlet temperatures, the dropping times of the absorber elements were verified, and the increased difficulties concerning the visual investigations of the reactors' inner components were taken into account.

The validity of safety analyses performed earlier was reviewed. The Russian firm Hydropress performed the analysis of the operation with magnetite deposits burdened fuel assemblies [1] for both normal and incidental conditions of the reactor units. These investigations have

shown that the deformations of the fuel assembly shrouds might be attained much easier if the shroud temperature exceeds 355°C.

The Hydropress report suggested new operational limits: the relative mass flow of the assemblies could not fall under 86% of the average value, because at lower mass flow rates, the shroud temperatures might exceed the problematic temperature value of 355°C. For controlling the mass flow limitations, the modification of the VERONA reactor core monitoring system was also necessary. In addition, the Hydropress suggested to plan the refuelling with extreme caution.

As a consequence of the above drafted events, the plant management decided to clean the affected fuel assemblies, first time on the turn of the millennium. In the years 2000 and 2001, the chemical cleaning of a total sum of 170 fuel assemblies was performed successfully in an instrument designed by Siemens KWU, which was capable for housing 7 fuel assemblies simultaneously [15]. In accordance with the preliminary expectations, this instrument operated effectively. (From the viewpoint of the events discussed below, it is important to mention that the cleaned fuel assemblies were removed from the core two years before the cleaning process started and they had low residual heat. Furthermore, this equipment would have been able to ensure the cooling of fuel assemblies of much higher thermal power. This cleaning tank had inlet junction in the bottom and outlet junction on the top of the vessel. The safety criteria specified by the Paks NPP experts were fulfilled for this equipment as it was proved by the main constructor Hydropress.)

In November of 2002, the Paks NPP commissioned a reputed Western-European nuclear company to design, construct and operate a new chemical cleaning equipment of larger dimensions. With this new cleaning tank the operators were able to perform the chemical cleaning of 30 fuel assemblies simultaneously with the same permanganate-oxalic-acid method. The instrument arrived to Hungary in the beginning of 2003 and was placed into the refuelling pit beside the reactor of Unit 2 in the Phase 1 of the Paks NPP (see Figure 2.2). The cleaning of the first batch of 30 fuel assemblies was started on 20<sup>th</sup> of March. Prior to the incident, five batches were cleaned successfully. The 1<sup>st</sup>, 2<sup>nd</sup>, and 4<sup>th</sup> batches consisted of fuel assemblies removed a few years earlier, but the 3<sup>rd</sup> and 5<sup>th</sup> batches contained fuel assemblies with significant residual power (removed from the reactor on those days).

## **2.2 Operation of the cleaning tank**

The AMDA (acronym of the German phrase: Automatic Mobile Decontaminating Instrument) cleaning tank was installed into the refuelling pit of Unit 2 (see Figure 2.2). The refuelling pit was filled up with borated water and so it was in a common water space with the spent fuel pool. The fuel assemblies were loaded into and removed from the cleaning tank by the refuelling machine of the Paks NPP. During the normal operational mode when the chemical cleaning was in progress (operational mode “C”), the oxalic acid solution – which played both the role of cleaning and cooling medium – circulated in a closed loop with a mass flow rate of 200-250 t/h (see Fig. 2.4). The heat exchanger built in the AMDA system ensured the removal of the fuel assemblies’ decay heat.

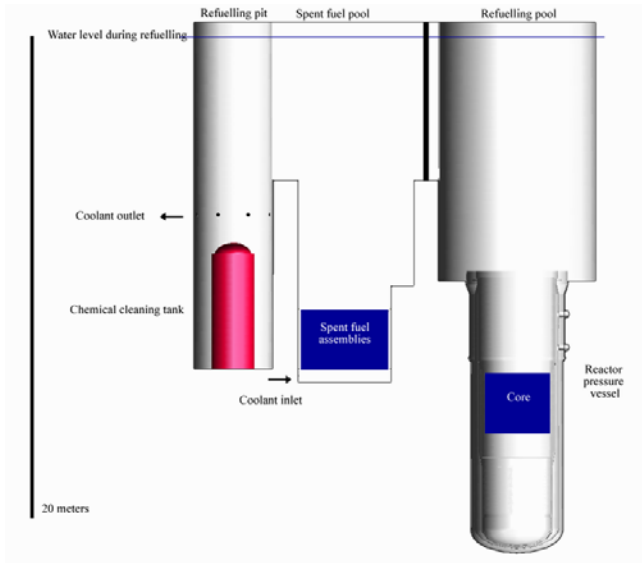


Figure 2.2. The cleaning tank's position in Unit 2 [6]

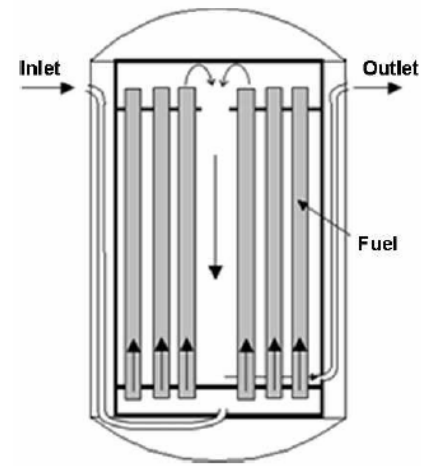


Figure 2.3. Flow scheme of the cleaning tank [6]

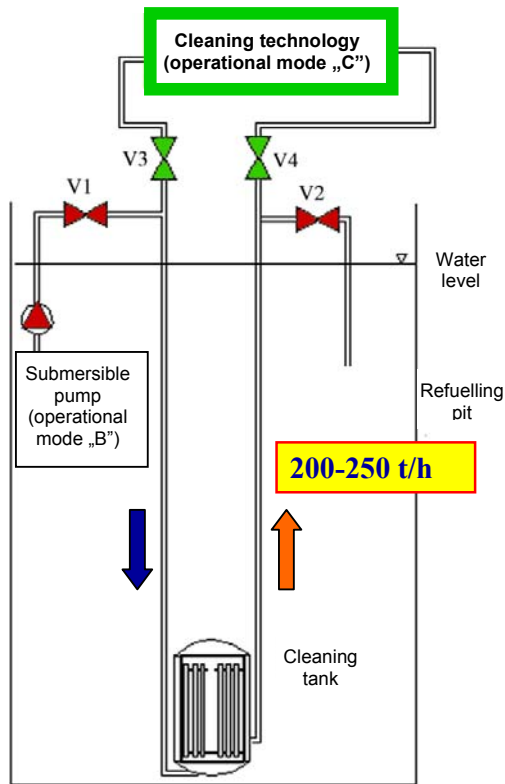


Figure 2.4. Coolant flow during the "C" operational mode (Valves V1, V2 are closed, V3, V4 are opened) [13]

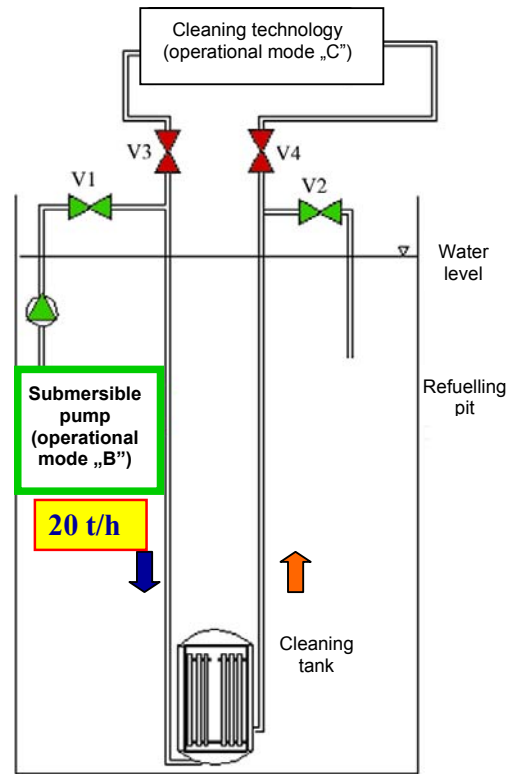


Figure 2.5. Coolant flow during the "B" operational mode (Valves V1, V2 are opened, V3, V4 are closed) [13]

Figure 2.3 shows the flow pattern of the oxalic acid solution coolant inside the cleaning tank during the cleaning process: the coolant flowed down through a pipe in the gap between the inner and outer vessels of the double mantled cleaning tank. Then it entered the inner domain at the bottom. The coolant flowed up inside the fuel assemblies and down among them. The coolant left the inner volume via the outlet nozzles in the bottom part of the cleaning tank, at a similar level, as the inlet nozzles. (This design solution was applied in order to avoid the accumulation of the crud on the lower plate of the tank, since such problems were observed during the operation of the small cleaning tank with seven fuel assemblies.) After that, the medium of mass flow rate of 200-250 t/h entered the cleaning module of the AMDA system (see Figure 2.4), where the dissolved magnetite and heat were removed from the solute.

After finishing the cleaning process, the system was changed over to the so-called “B” operational mode, which was rather different from the above described “C” mode (see Figure 2.5): a submersible pump of 20 t/h mass flow capacity circulated the coolant of the refuelling pit through the cleaning tank in an open loop. During the cleaning tank opening process – using the reactor hall crane – and during the loading and removing of the fuel assemblies, the AMDA system was cooled in the “B” operational mode.

The subsequent visual surveys after the incident showed clearly that oxidation in high temperature steam took place in the cleaning tank for several hours which resulted in the embrittlement of the fuel assembly shrouds and the fuel pin claddings. At the opening of the cleaning tank, the injection of cold coolant caused the breaking up of the embrittled shrouds and fuel pin claddings. The phenomenon of the high temperature oxidation indicates that the cooling of the fuel assemblies was insufficient. The investigations revealed two possible reasons for it:

1. Development of significant by-pass flow through the bottom perforations of the fuel assembly shrouds.

In the VVER-440 type reactors, two kinds of fuel assemblies are used: the normal “working” assemblies and the so-called follower assemblies. The follower assemblies are positioned under the 37 absorber elements and attached to them. During the reactor operation, these follower assemblies move together with the absorber elements and are positioned partly or entirely in the reactor core. Otherwise, they can be found below the reactor core. The other 312 fuel assemblies are working assemblies, which have fix positions in the reactor core.

The two fuel assembly types differ from each other in their head and leg parts. From the viewpoint of the incident, the most important difference is that the working assemblies’ shrouds are perforated by 12 and 12 holes of 9 mm diameter in the top and bottom parts. The 6<sup>th</sup> batch – which suffered the incident – consisted of 11 working and 19 follower assemblies. The subsequent investigations pointed out that with the rather low mass flow rate ensured by the submersible pump in the “B” operational mode, the bulk of the coolant might flow to the outlet through the bottom perforations of the working assemblies without flowing along and cooling the fuel assemblies. The special flow pattern which might cause this phenomenon is discussed in section 3.2.

## 2. Displacement of one or more fuel assemblies.

The bottom positioning and support plate was formed such a manner that both the working and follower assemblies were able to engage into the 30 seats on it (see Figure 2.7). According to the different formation of the two assembly types, the seats contain three flanges with different diameters. Unfortunately, the seats were not furnished with such instruments which would have been able to signal the proper engagement of the fuel assemblies into the seats. Furthermore, the proper positioning of the assemblies was assured by only one, the so-called upper positioning plate. Consequently, there was a real possibility that one or more of the 6<sup>th</sup> batch fuel assemblies were put inaccurately into their seat positions. In case of an entirely displaced fuel assembly, it could result in a by-pass cross section of 13-20 cm<sup>2</sup> (see Fig. 2.7).

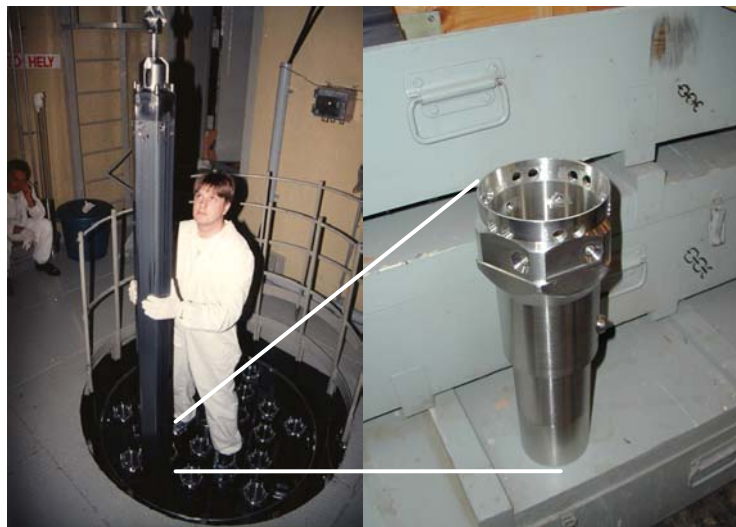


Figure 2.6. Working fuel assembly and its leg part [13]

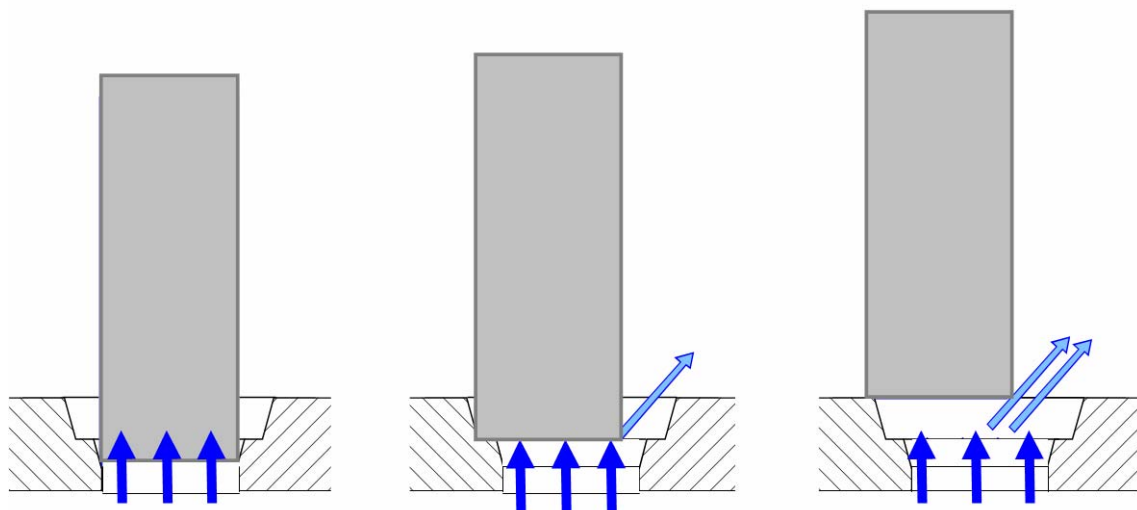


Figure 2.7. Possible by-pass orifices from displacements

For evaluating the design deficiencies of the cleaning tank it must be mentioned that no instrumentation (such as thermocouples, pressure transducers or water level measurements) were installed inside the tank. Therefore, the operating staff could not recognize the insufficiency of the cooling and the increase of the inner temperature.

### 2.3 Chronology of the incident

Unit 2 of the Paks NPP was shut down for refuelling on the 29<sup>th</sup> March 2003. The cleaning operation was carried out in refuelling pit of the spent fuel storage pool of unit No. 2. Five batches of fuel assemblies with crud were cleaned without any indication of fuel failure. Later investigation pointed out that the intermediate cooling mode was applied only for a short time in most of the five cases and the tank was open very soon after the completion of cleaning.

On the 10th April batch No. 6 was cleaned, the total decay heat of the 30 assemblies was 241 kW [16,17]. The chemical cleaning was completed at 16.00 and the intermediate cooling (operational mode “B” in Fig. 2.5) was started at 16.40 (Fig. 2.8). The opening of the tank was postponed, because the crane was used for other operations.

After 19.00 a slight increase of water level was recorded at the pressurizer. The change was only a few cm, but considering the common surface of the system it meant 4 m<sup>3</sup> water volume. As the total volume of the tank was 6 m<sup>3</sup>, the 4 m<sup>3</sup> volume indicated that the main part of the fuel rods were in dry conditions after this elevation change.

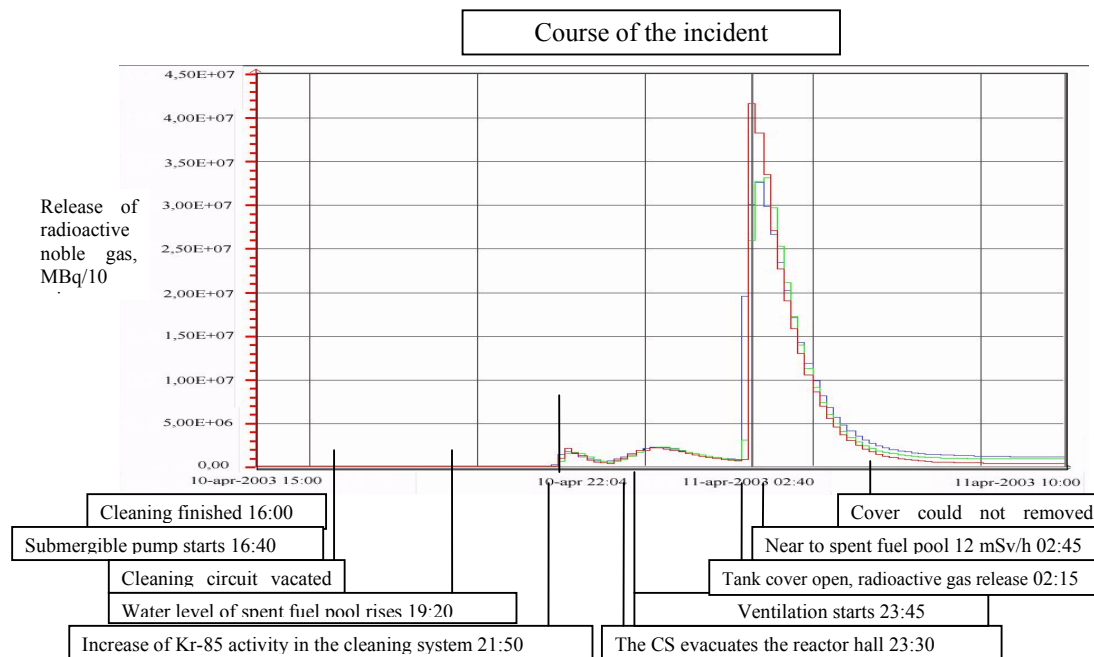


Figure 2.8. The course of the incident in time [3, 7]

The first indication of fuel failure was detected by the analyser device of the air letdown system at 21.50 as activity increase of <sup>85</sup>Kr. The operational team decided to open the tank to understand the cause of activity release.

The hydraulic interlock of the cover was opened at 2.15 after midnight. The cover removed from its original position without lifting up and a large gas bubble emerged from the tank. The detectors indicated high noble gas activity in the reactor hall and in the ventilation chimney. At 4.20h an attempt was made to remove the cover, but the rope of the crane was broken. The tank remained in partially open position. The first activity concentration measurements showed high ( $10^7$ - $10^8$  Bq/l) coolant activity in the spent fuel storage pool for several fission product isotopes. The cover was lifted on the 16<sup>th</sup> April.

Thermal hydraulic calculations pointed out that the main reason for the insufficient cooling in the cleaning tank was a design problem: both inlet and outlet junctions were located in the lower part of the tank and a by-pass flow could be formed between them [4]. Due to the low flowrate of the intermediate cooling pump and because of the low Reynolds number in the bundle, the by-pass flow through the perforations in the assembly shroud and at the bottom of the imperfectly seated assemblies became much more significant, than it was during the cleaning operation with high flowrate (Fig. 4.). The numerical analysis showed that the heating of the water led to saturation state in the top of the tank. The production of 4 m<sup>3</sup> steam could take place rather quickly, considering the high decay heat of the assemblies, and the formation of water level in the cleaning tank took only some minutes after saturation was reached. The fuel behaviour calculations proved that the loss of fuel integrity in 5 hours after the initiation of intermediate cooling mode was a result of fuel rod ballooning and burst [18]. The fuel rods could heat up above 800 °C by that time and the high internal pressure in some rods resulted in plastic deformation and burst. The calculation of zirconium oxidation pointed out that the volume of produced hydrogen could be much larger, than the volume of the cleaning tank. For this reason most of the hydrogen should have been released through the air letdown valve. Since the produced hydrogen could be released from the tank only with some time delay, the high temperature oxidation of fuel assemblies took place in hydrogen rich steam [19].

As there were no measurements inside of the cleaning tank the reconstruction of the event involved many uncertainties. The following scenario (see Fig. 2.8) was put together from the mosaics of numerical analysis, high temperature experimental work and observations of the fuel state [20,21]. The Paks-2 incident contained three main phases.

### **2.3.1 Formation of steam volume**

After the initiation of intermediate cooling mode with 20 t/h flowrate part of the coolant could by-pass the fuel assemblies and did not take part in the removal of decay heat. Two paths were identified for the by-pass flow (Fig. 2.7):

- The working type VVER-440 fuel assemblies have perforation holes in the shroud.
- The perfect seating of the assemblies was not controlled and some gaps could exist between the bottom of the assemblies and the lower plate.

The development of the thermal stratification and the increasing by-pass flow rate were not detectable from the outlet temperature measurement signal. The above described process conducted to the boiling of the coolant in two hours (see Figure 2.9.c). Then, the generated steam pushed out the water from the bulk volume of the cleaning tank between 19:00 and 19:20. This process was shown by the increase of pressurizer level of the unit. However, it was revealed only by the post-incident investigations.

The flow through the assemblies was not enough to remove the 241 kW decay heat and the temperature in the upper part of the tank started to increase. When the saturation temperature was reached the formation of a steam volume took place in short time. The subsequent heat-up period lasted about 2.5 hours.

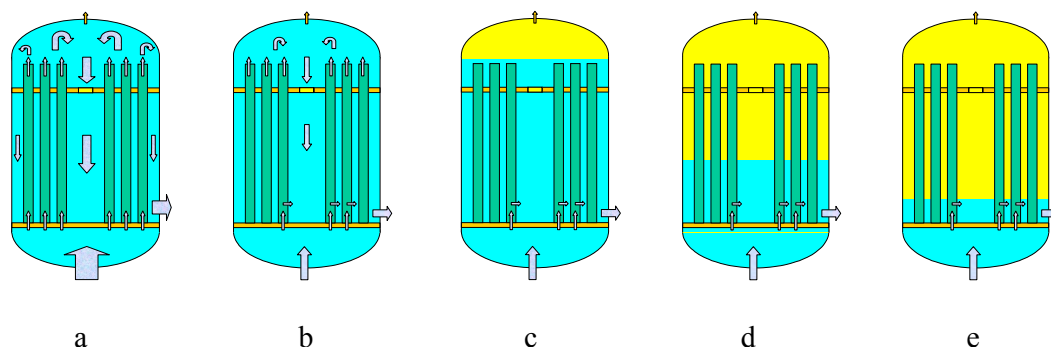


Figure 2.9. Flow path of coolant in the cleaning tank during normal cleaning operation (a), at the beginning of intermediate cooling mode (b) and the steps of steam volume formation (c,d,e)

### 2.3.2 *Plastic deformation of cladding and high temperature oxidation*

Continuous temperature increase started in the tank, when the upper part of the fuel rods was not cooled by water. The heat removal from the tank to the surrounding water was very low, because the vessel was isolated by the double wall system. The temperature increase led to the increase of pressure inside of the fuel rods. At 800-900 °C the internal pressure could reach 30-40 bars. In this range of pressure and temperature plastic deformation of the cladding can take place and the ballooning can lead to bursts and activity release from the fuel. It is very probable that this type of fuel failure was responsible for the activity release measured by the  $^{85}\text{Kr}$  detectors. (Very long ballooned areas were found in the later visual inspection of the fuel.) The first fuel rod ruptures were detected at 21:50, when the  $^{85}\text{Kr}$  measurement of the AMDA system showed an unexpected jump in the signal (see Fig. 2.8) and a few minutes later the noble gas detectors of the unit were also alerted.

The further increase of temperature accelerated the oxidation of zirconium components. The maximum cladding temperature reached 1200-1300 °C. The oxidation produced high hydrogen content in the stagnant steam volume. Most of the hydrogen could escape through the air letdown valve, but the high hydrogen concentration resulted in significant hydrogen uptake by the cladding and shroud. This period lasted for 7 hours. The upper part of the assemblies became oxidised and picked-up large amounts of hydrogen. The bottom part was cooled by water and suffered no significant changes.

The temperature distribution in the vessel was non-uniform. Probably there were significant differences between the temperature of peripheral and central fuel assemblies. Large variation of axial temperature can be supposed, since the bottom part of the fuel rods was cooled by water. For these reasons the plastic deformation at 800-900 °C and the intense oxidation above 900 °C could take place at the same time in the fuel assemblies.

As a result of hydrogen production in the Zr oxidation process the upper part of the cleaning tank was filled with steam-gas mixture. Probably most of the produced hydrogen was

released through the air letdown valve, but there was no reliable information on the operation of this device and on the released gas flowrate.

### 2.3.3 Quench

The severe fuel damage took place during the quench phase that was accompanied by large activity release. No signs of temperature escalation or hydrogen production were found, probably because of the high degree of oxidation before quench. The quench was a combination of top and bottom injection and the flow path had complex three-dimensional picture.

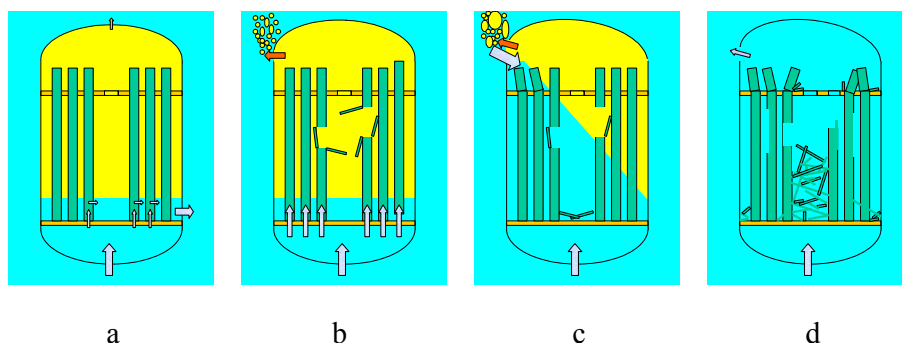


Figure 2.10. The main phases of quenching: intermediate cooling mode with formation of by-pass and 7 hours of oxidation (a), opening of the cover, gas release to the pool and water injection from the bottom (b), cold water injection from the top (c), stable final state (d).

The possible quench scenario included the following steps:

- The opening of the hydraulic locks created a small gap between the cover and the vessel.
- Some gas was released through the gap from tank into the spent fuel storage pool and the pressure in the tank decreased (Fig. 2.10b).
- Water injection through the inlet line could reach higher elevations than before the opening of the cover due to low pressure.
- Intense steam production took place when the cold water evaporated on the hot surface of the fuel. Probably this process resulted in vertical upward movements of the assemblies that were recognised by the signs of interactions between the inner surface of the cover and the assembly heads. These signs were found after the removal of the cover.
- The pressure increase in the tank led to the rising of the cover and increase of the gap between cover and vessel.
- The large gap size facilitated water penetration from the surrounding pool and so large amount of water quenched the fuel assemblies from the top (Fig. 2.10c).
- Finally the tank was filled up by water and stable circulation of coolant was established with the pump (Fig. 2.10d).

The thermal and mechanical loads resulted in the fragmentation of many fuel rods. Several assemblies suffered full cross section break, many parts of shroud plates were missing with signs of brittle failure. The high noble gas activity release indicated that many fuel rods lost their integrity during quench.

## 2.4 State of damaged fuel

After the incident detailed visual examination was carried out with the help of video cameras. The examination indicated that most of the fuel assemblies suffered damage. Brittle failure and fragmentation of fuel assemblies was observed. Above the upper plate several assembly heads were broken, standing in inclined position (Fig. 2.11). One assembly header was found far from its original place. Many assemblies were broken and fragmented below the upper plate, too. Some assemblies were fractured in their entirety. Fuel rod fragments and shroud pieces accumulated on the lower plate between the assemblies. Many fuel rod pieces and fragments of assembly shroud were spread in the tank. Some fuel pellets fell out of fuel rods, their form remained mainly intact. Heavy oxidation of the zirconium components was identified. Less oxidation was found in the periphery than in the centre. The bottom part of the fuel remained intact.

The visual investigations have also shown that the fuel assemblies positioned closer to the vertical axis suffered heavier damage, in some cases long parts were simply broken out from them. Thanks to the better position for the radiative heat transfer, the outermost assemblies suffered less heavy damage. The broken fuel pins, shrouds and fallen down fuel pellets formed a heap of debris on the bottom positioning and support plate.

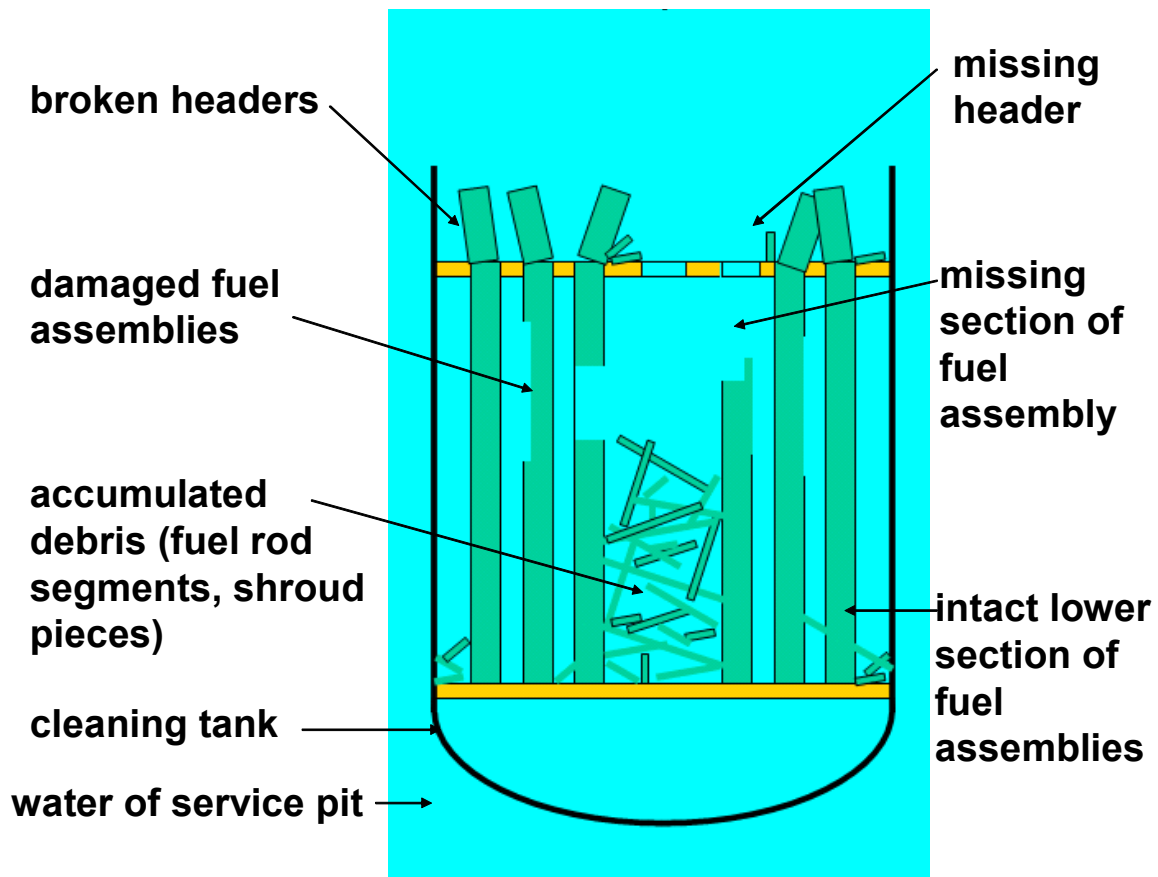


Figure 2.11. Distribution of damaged fuel in the cleaning tank

There were no signs of melting or formation of zirconium-steel eutectics on the surface of stainless steel components. This fact indicates that the maximum temperature during the incident remained below  $\approx 1400$  °C.

Isotope	Released activity	Relative release
<sup>133</sup> Xe	6.6e+14Bq	1.19%
<sup>131</sup> I	5.9e+14Bq	1.41%
<sup>106</sup> Ru	8.7e+12Bq	0.03%
<sup>134</sup> Cs	4.2e+13Bq	0.74%
<sup>137</sup> Cs	3.8e+13Bq	0.53%
<sup>140</sup> Ba	1.8e+14Bq	0.16%
<sup>144</sup> Ce	7.2e+13Bq	0.06%

Table 2.1. Activity release from damaged fuel during the incident

The activity concentrations in the coolant and the release through the chimney are regularly measured and such data were available after the incident, too. The incident happened two weeks after reactor shutdown, for this reason the release of isotopes with short half-life was very low. Integrating the activity concentrations over time and coolant volume in the pool, and summarising the release through the chimney in time, the total activity release from the fuel was determined for several isotopes. Most of the activity remained in the water, since the incident took place under 13 m water level, only the noble gases were released through the chimney. The integrated activity release was compared to the calculated inventories and the release rate was determined. In case of gaseous and volatile isotopes the release rate was roughly 1% (the precise data are given in Table 2.1). The release rate of non-volatile isotopes was much less. The ≈1% iodine, cesium and noble gas release indicated that the temperatures in the cleaning tank could not be very high, otherwise larger release should have been recorded. Considering these release rates the maximum temperature was estimated about 1200-1300 °C. This temperature range can explain as well that the local oxidation reached 100% in some positions.

The hot cell examination of the damaged fuel could not be carried out at the Paks NPP, since the power plant does not have the necessary equipment and facilities for the detailed investigation of irradiated fuel.

The very brittle state of the damaged fuel was observed during the removal operations. Several fuel assemblies and fuel rods were fragmented when the damaged fuel was removed from the cleaning tank and placed in the containers.

## 2.5 Post-incident investigations

The cleaning tank cover was removed on 16<sup>th</sup> of April [3]. Until that time, the operators of the AMDA system suspected only leakage from a few fuel rods. After the removal of the cover it has become clear that almost all fuel assemblies suffered heavy damage. The characteristics of the damage referred to that the insufficiency of the cooling would be the main cause. Regarding to the extent of the damage, the classification of the incident was changed to INES-3 from the previous rating of INES-2 which classification was based on the radioactive release [4].

The subsequent criticality calculations [10] showed that the multiplication factor of the damaged system was 0.595 by 20 g/kg boric acid concentration, so the system was in a deep subcritical state following the incident. The sophisticated 3D reactor-physical analyses pointed out that ensuring a minimal boric acid concentration of 16 g/kg, there had not been an arrangement of the fissile material that could have become critical.

The subsequent calculations [11] have also revealed that the geometrical arrangement which formed during the incident and the boric acid concentration level at the time of the incident

made the criticality impossible. The maximum value of the multiplication factor could be 0.66 during the incident. The radioactive release data also exclude the progress of uncontrolled chain reaction.

The calculations based on measurement data showed that the extra doses will not exceed the value of 0.13  $\mu\text{Sv}$  for the most affected population group. This value corresponds to the dose which accumulates from the natural background for 1.5 hours. On the other hand, the annual limitation of the artificial dose for the population nearby the NPP is 90  $\mu\text{Sv}$ , while the natural background caused annual doses are 2300-3000  $\mu\text{Sv}/\text{person}$ . On the basis of these values it can be stated that the extra doses from the incident are negligible.

As a consequence of the incident, a significant radioactive contamination occurred in only one case: the face of an NPP worker was contaminated in such a way that it caused an extra dose much below the annual dose limitation (0.059 mSv external and 0.55 mSv internal doses [3]). Personal injury did not occur during the incident.

Between 16-25 June, 2005, an examiner group mandated by the International Atomic Energy Agency visited the Paks NPP in accordance with the Hungarian government's wish, in order to help to reveal objectively the causes of the incident. The investigation of the group pointed out that the main reason of the incident was the insufficiency of the cleaning tank cooling system and, among others, revealed the below listed design deficiencies [2]:

- The submersible pump of the "B" operational mode was under sized and also did not have any redundancy or reserve.
- The by-pass flows of the fuel assemblies were not taken into account during the thermal hydraulic design of the cleaning tank.
- The further possibility for developing by-pass flow through orifices that could come because of the possible fuel displacements were realized but were not handled effectively.
- The measurement instrumentation, the parameter trend observation and the alarm system were not designed sufficiently.

The examiner group recommended several correcting measures for both the power plant and the Hungarian regulatory. Among others they made suggestions connected to the licensing of new technologies and methods, the improvement of the safety culture, the education of the staff, development of emergency plans and the feedback of operational experiences. A strong recommendation was that the safety of an important operating activity should not be given to a contractor without the supervision of the operator. The international examiner group also proposed to strengthen the communication between the operator and the regulatory.

The performance of these recommendations was investigated by a new examiner group [5] in February 2005, and 71% was classified as "performed" and the remaining as "adequately progressing".

## **2.6 The recovery work**

For the recovery of the incident, the Paks NPP established a working group (Recovery Project) which is charged with the removal of the damaged fuel. This group was previously charged with the normalization of the state of the system, and the preparation for and licensing of the recovery work.

During the normalization of the system's state the following main steps were made:

- Separation of the refuelling pit with the damaged cleaning tank and the spent fuel pool from the reactor.
- Increase of the boric acid concentration up to 20 g/kg in the refuelling pit.
- Development of the safety borating system of the cleaning tank.
- Construction of an independent cooling system of the cleaning tank.
- Separation of the refuelling pit from the spent fuel pool.
- Installation of redundant temperature, coolant level and neutron measurement instrumentation in order to make the refuelling pit an independently operated system.
- Visual exploration of the state and geometry of the damaged fuel assemblies and the cleaning tank in deep details.

In the summer of 2003, the Russian TVEL company was chosen for the execution of the technical tasks concerning the recovery of the damaged system.

During the removal, the pieces of the damaged fuel were picked up by manipulators which are operated by a staff standing on the so-called working and lifting platforms which were positioned into the refuelling pit. The picked up pieces were placed into special casks and containers which presumably will be stored in the spent fuel pool for five years.

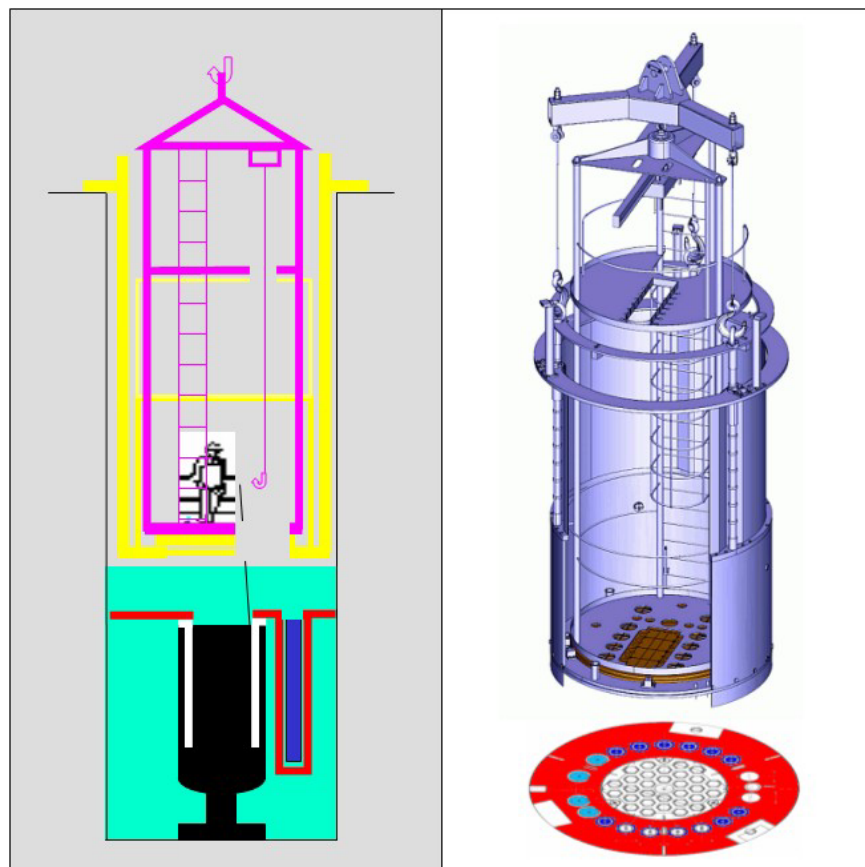


Figure 2.12. Instruments installed into the service pit during the recovery work [12]

The article [12] describes the technical equipments which were used during the recovery work. Fig. 2.12 shows the different equipments which were installed into the refuelling pit. The so-called middle flange and the protective flange (coloured with white and red in Fig.

2.12) were placed onto the split plane of the cleaning tank. The middle flange holds the temperature and neutron measuring equipments which are placed into the cleaning tank. The protective flange was a horizontal plate that was held by the consoles of the refuelling pit wall and it closed the domain between the split plane of the cleaning tank and the pit wall. Between the bottom and upper part of the refuelling pit the flow domain was connected by the TV shaft. Among others, the protective flange contained a mechanical filter, and holding structures for positioning 17 casks or containers constructed for storing the removed fuel assemblies and fuel pieces.

For the time period of the removal process itself, the coolant level was decreased. Above this decreased level, the working and lifting platforms were placed (coloured by yellow and violet on the left side of Fig. 2.12). The working platform was hold by the reactor-podium, and it could be set to different levels as it was needed. The bottom plate of this platform could be rotated and a working aperture was constructed on it. The lifting platform was put onto the rotating plate of the working platform. The lifting platform also had overlapping working aperture. During the removal process, the working staff was standing on the lifting platform. In case of emergency, the staff could exit on the ladder, or the platform could be lifted out by the reactor hall crane. The lifting platform was lifted out every time when the casks or containers hold by the protective flange got filled and the refuelling machine transported them into the spent fuel cooling pond.

During the recovery work, first the upper positioning plate of the cleaning tank was cleaned and removed. Then, the fuel assembly top parts were removed. The removing of the fuel assemblies followed a way from the inner parts to the outermost assemblies. For lifting out the fuel assemblies, the leg parts had to be disengaged. After that, the proper seats on the bottom positioning and supporting plate were closed by special plugs. The leg parts were cut off and the fuel pin batches were placed into the casks. After removing of the fuel assemblies, the bottom positioning and supporting plate was cleaned. Then the elliptical bottom part of the fuel tank was cleaned with vacuum-suction method. At the end, the cleaning tank was chemically decontaminated and lifted out from the refuelling pit. Also the chemical decontamination and the entire cleaning of the refuelling pit were necessary.

After the recovery work the damaged fuel is stored altogether in 24 wide and 44 narrow containers in the spent fuel pool of the unit 2 of Paks NPP.

## References to Chapter 2.

- [1] OKB Hydromash: Analysis of operation of fuel assemblies with reduced flow rate due to deposit in the Paks NPP (final technical report), U-213-TI-1762, 2003, in Hungarian
- [2] Report of the expert group on „Evaluation of examination results of the Hungarian Atomic Energy Agency on the incident in Paks NPP during fuel cleaning on 10. April 2003”, TC Project: HUN/9/022, IAEA-TCR-01769 (in Hungarian)
- [3] “Inquiry report of fuel damage in the cleaning facility of FANP on 10-11. April 2003”, Report for HAEA NSD, NBI 03.11, B20301, Paks NPP, Event Investigation Group, 11. Mai 2003, (in Hungarian)
- [4] Report for the Chairman of the Hungarian Atomic Energy Committee on the investigation of the incident in Paks NPP on 10. April 2003 (Event identification number: 1120), Hungarian Atomic Energy Authority, 23. Mai 2003, in Hungarian, [www.haea.gov.hu](http://www.haea.gov.hu)

- [5] Report of the Expert Mission „To Assess the Results of the Hungarian Atomic Energy Authorities Investigation of the 10 April 2003 Fuel Cleaning Incident at Paks NPP” 16 - 25 June 2003 And Operational Safety Review Team (OSART) Mission 8 - 25 October 2001 to the Hungarian Atomic Energy Authority and Paks Nuclear Power Plant Hungary and Follow-Up Visit, TC Project HUN/9/022, IAEA-TCR-02581, IAEA-NSNI-112F
- [6] Attila Aszódi, Ildikó Boros, András Csige, Gábor Légrádi: Thermal hydraulic analysis of the incident in the Paks NPP on 10th April 2003, 13th Symposium of AER on VVER Reactor Physics and Reactor Safety, Dresden, Germany, 2003., pp. 737-754, ISBN 963-372-630-1
- [7] Attila Aszódi, Ildikó Boros, András Csige, Gábor Légrádi: Thermal hydraulic analysis of the Paks incident, 2<sup>nd</sup> Symposium of Nuclear Technology, 4-5 December 2003, Budapest, CD Proceedings, BME NTI, ISBN 963 420 843 6 (in Hungarian)
- [8] Attila Aszódi, Gábor Légrádi, Bogdán Yamaji: Properties of the fuel damage during the Paks-2 incident, 2<sup>nd</sup> Symposium of Nuclear Technology, 4-5 December 2003, Budapest, CD Proceedings, BME NTI, ISBN 963 420 843 6 (in Hungarian)
- [9] Zoltán Hózer, Csaba Győri, Péter Windberg, Lajos Matus: Fuel behaviour during the Paks-2 incident, 2<sup>nd</sup> Symposium of Nuclear Technology, 4-5 December 2003, Budapest, CD Proceedings, BME NTI, ISBN 963 420 843 6 (in Hungarian)
- [10] Sándor Fehér, József Kópházi, Szabolcs Czifrus, Tamás Berki: Detailed 3D subcriticality analysis of the damaged fuel; Internal Research Report of TU Budapest, BME-NTI-281/2004, 20 May 2004, (in Hungarian)
- [11] József Kópházi, Sándor Fehér, Szabolcs Czifrus, Tamás Berki, Gyula Csom: Detailed 3D analysis of the reactor physics of the damaged fuel inside the cleaning tank, 3<sup>rd</sup> Symposium of Nuclear Technology, 2-3 December 2004, Budapest, CD Proceedings, BME NTI, ISBN 963 420 843 6
- [12] András Cserhádi: The technology of the recovery work in Paks Unit 2, 3<sup>rd</sup> Symposium of Nuclear Technology, 2-3 December 2004, Budapest, CD Proceedings, BME NTI, ISBN 963 420 843 6
- [13] Attila Aszódi: The Paks-2 incident, the planned recovery work and the restart of Unit 2, 47<sup>th</sup> Symposium of Hungarian Secondary School Physics Teachers, Miskolc, Hungary, 6 April 2004 (in Hungarian)
- [14] GMO CAD group of the of the Paks NPP
- [15] J.Schunk, M.Beier, F. Kovács, S. Mikó, P. Tilky, H.O. Berthold, I. Janzik, G. Marquardt: Fuel Assembly Chemical Cleaning at Paks Nuclear Power Plant, IAEA Meeting on fuel failures and Mitigation, Bratislava 2002
- [16] G. Vámos (Paks NPP): Investigation report on the fuel damage occurred on 10-11 April within the cleaning equipment of FANP, Report to OAH-NBI, NBI 03.11 B20301, (available on <http://www.npp.hu>)
- [17] Report to the Chairman of the Hungarian Atomic Energy Commission on the Authority's investigation of the incident at Paks Nuclear Power Plant on 10 April 2003, HAEA, 23 May 2003 (available on <http://www.haea.gov.hu>)
- [18] Cs. Győri, Z. Hózer, I. Tóth, I. Trosztel: Analyses of the 10<sup>th</sup> April 2003 Paks Incident, May 2003, AEKI (in Hungarian)

- [19] E. Perez-Feró, P. Windberg, Z. Hózer, M. Horváth, I. Nagy, A. Pintér-Csordás, E. Szabó, K. Kulacsy: Experimental Database of E110 Cladding Oxidised in Hydrogen Rich Steam, Transactions of TOPFUEL 2006, pp. 605-609
- [20] Zoltán Hózer: Fuel Failures During the Paks-2 Incident, Enlarged Halden Programme Group Meeting, Storefjell, Norway, 11-16 March 2007, Proceedings of the Fuels and Materials Sessions, HPR 366 Vol. 2, paper F4.1
- [21] Zoltán Hózer, Péter Windberg, Imre Nagy, András Vimi, Nóra Vér, Lajos Matus and Mihály Kunstár: Experimental Simulation of the Paks-2 Cleaning Tank Incident, Transactions, SMiRT 19, Toronto, August 2007, paper No. C02/5

### 3 MAJOR RESULTS OF ANALYSES

Ten organisations provided calculated data on their analyses of the Paks-2 event. Each partner produced a short summary on the work performed and the results received with the following content:

- short description of the code applied,
- short description of the input model, nodalisation scheme, specific options,
- description of total decay power, power of assembly groups, axial power distribution,
- description of inlet flow (mass flow, temperature) and external (pool) temperature,
- description of pressure boundary condition of cleaning tank.

It was requested to provide the chronology of main events considering the followings:

- saturation in the cleaning tank,
- water level drop in the cleaning tank,
- maximum cladding temperature exceeds 800°C,
- maximum cladding temperature exceeds 1200°C,
- start of intense Zr oxidation,
- failure of the first fuel rod due to ballooning,
- failure of the last fuel rod before quenching.

The short summary produced by each participating organisation is given in this chapter in the alphabetical order of the countries.

#### 3.1 Participant SUEZ - TRACTEBEL ENGINEERING

##### 3.1.1 Code description

Suez-Tractebel Engineering used the integral code MELCOR 1.8.5 to perform the calculations in the framework of the “OECD-IAEA Paks Fuel Project”. MELCOR 1.8.5 is a severe accident code developed by Sandia National Laboratories (SNL), which allows the user to perform integral severe accident calculations. As a result, MELCOR 1.8.5 is not only capable to calculate the thermal hydraulic behaviour of a facility, but also the possible degradation of the fuel assemblies and fission product releases.

##### 3.1.2 Model description

###### 3.1.2.1 Nodalisation scheme

An overview of the nodalisation scheme can be found in Fig. 3.1.1. Control volumes 201, 202 and 203 represent the air-filled space between the inner and the outer vessel walls of the cleaning tank. The coolant enters the cleaning tank in control volume 101, from where it goes through the fuel assemblies (represented by control volume 104) towards the cleaning tank head (control volume 102) and the downcomer region (control volume 103).

In Fig 3.1.1, the flow paths between the different control volumes are indicated in blue. In order to obtain a proper modeling of the transient phase, a fictive control volume has been added (control volume 105). This control volume is situated between the downcomer region and the outlet tube. The different bypass flow paths (holes and accidental bypass) inject in

this control volume. The accidental bypass has a flow area of 0.012 m<sup>2</sup>, while a total surface of 0.0083 m<sup>2</sup> has been attributed to the bypass flow through the holes at the bottom of the fuel assemblies.

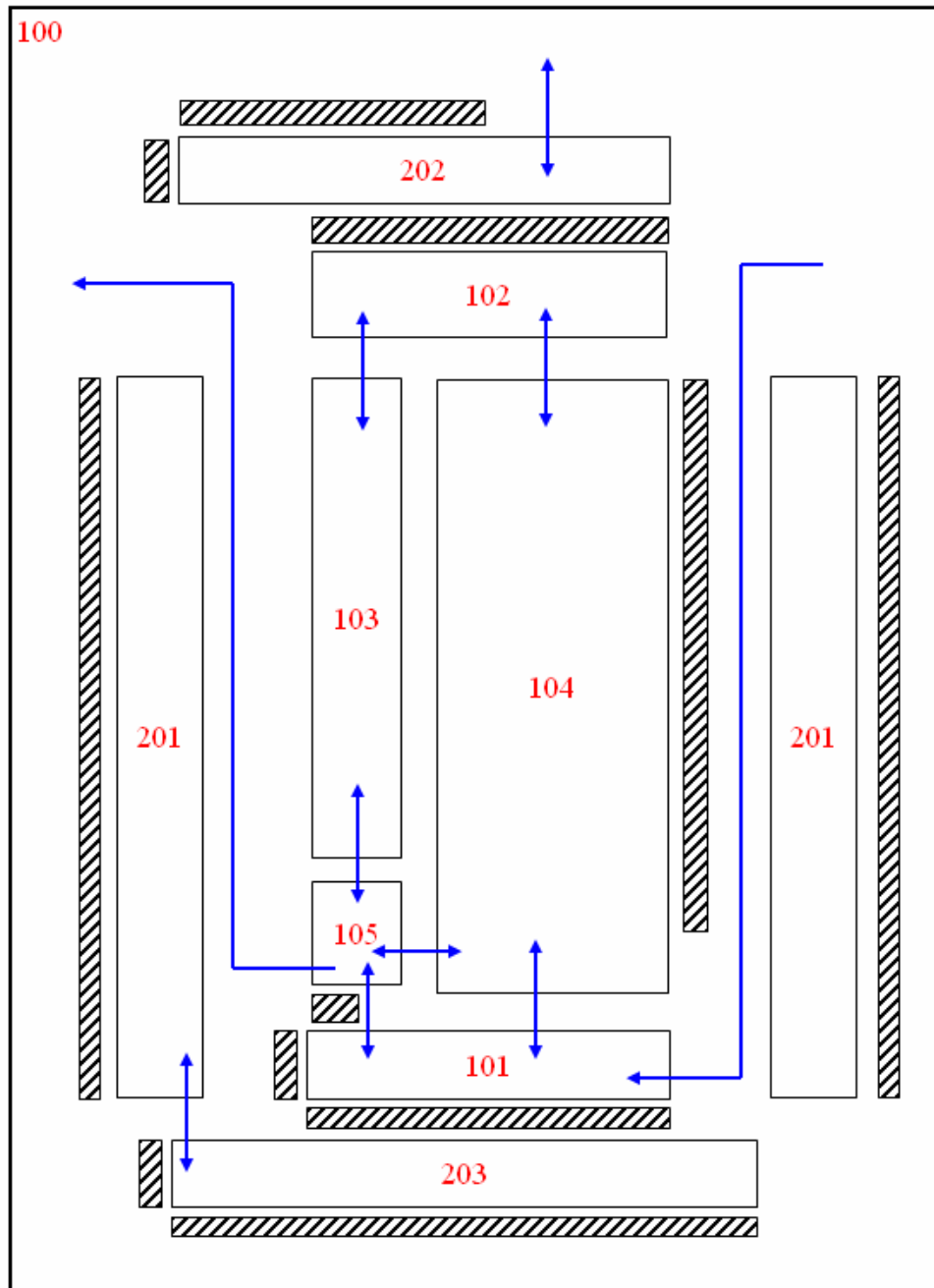


Figure 3.1.1. Schematic representation of the nodalisation scheme of the Suez-Tractebel Engineering MELCOR 1.8.5 model for the Paks Fuel cleaning tank.

### 3.1.2.2 Power distribution

Two axial zones (core and lower head zone) are defined for the core fuel assemblies. The first zone, representing the lower head, contains *three* axial levels of the fuel assemblies. *Twenty* axial levels have been modelled for the active core region. Based on the geometry in

which the fuel assemblies are placed inside the tank, the core has been divided in *three* concentric radial rings. The tank core has been modelled as a *BWR type reactor*, in order to track the contribution of the cladding and canister zirconium to hydrogen formation.

### 3.1.2.3 Axial level input

In the AEKI database, the axial power density profiles of all the assemblies, present in the cleaning tank at the moment of the incident, are given as a function of time. Since the axial power density profiles of all the fuel assemblies are similar and since the evolution in time is not significant, the axial power density profile of *fuel assembly 1 at 30 hours* is considered as representative and is implemented in the model.

Ten axial power density profiles are considered in the AEKI database. In the MELCOR 1.8.5 model, 20 axial levels are considered. The additional power levels have been obtained by linear interpolation. In Table 3.1.1, input data, required by MELCOR 1.8.5, are indicated.

	Axial level	Lowest point	Height	Corresponding HS	Rel. power dens.
	[-]	[m]	[m]	[-]	[-]
<b>Lower plenum</b>	1	0.359	0.162	10231	0
	2	0.521	0.162	10232	0
	3	0.683	0.073	10233	0
<b>Active core region</b>	4	0.756	0.1588	10211	0.3841
	5	0.9148	0.1588	10212	0.4878
	6	1.0736	0.1588	10213	0.5914
	7	1.2324	0.1588	10214	0.6951
	8	1.3912	0.1588	10215	0.8141
	9	1.55	0.1588	10216	0.9331
	10	1.7088	0.1588	10217	1.027
	11	1.8676	0.1588	10218	1.127
	12	2.0264	0.1588	10219	1.89
	13	2.1852	0.1588	10220	1.257
	14	2.344	0.1588	10221	1.293
	15	2.5028	0.1588	10222	1.329
	16	2.6616	0.1588	10223	1.333
	17	2.8204	0.1588	10224	1.337
	18	2.9792	0.1588	10225	1.303
	19	3.138	0.1588	10226	1.27
	20	3.2968	0.1588	10227	1.164
	21	3.4556	0.1588	10228	1.057
	22	3.6144	0.1588	10229	0.8373
	23	3.7732	0.1588	10230	0.6171

Table 3.1.1. MELCOR 1.8.5 axial level input.

### 3.1.2.4 Radial ring input

In Table 3.1.2, the input data for MELCOR 1.8.5 are indicated. The area of the radial rings is represented schematically in Fig. 3.1.2.

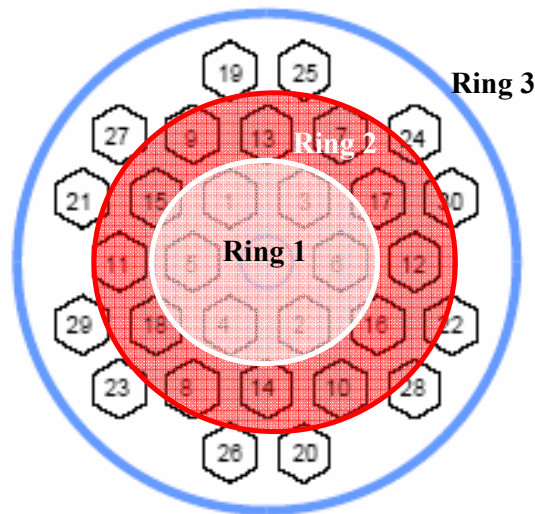


Figure 3.1.2. Schematic representation of the arrangement of the fuel assemblies in the Paks cleaning tank. The boundaries of the three concentric radial rings are indicated in the figure.

Radial ring	Cross section	Heat structure	Power per ring
[-]	[m <sup>2</sup> ]	[-]	[kW]
1	0.38	10290	42.954
2	0.65	10290	93.348
3	0.68	10290	105.336

Table 3.1.2. MELCOR 1.8.5 radial level input.

### 3.1.2.5 Inlet flow

The four inlet flow tubes have been modeled as flow paths only. Each of them has a cross section of 9.2E-3 m<sup>2</sup>. The mass flow rate has been fixed, throughout the entire calculation, and corresponds to a speed of 0.155 m/s (20,45 ton/hr). After a series of preliminary calculations, it has been chosen to set the inlet temperature to 60°C.

### 3.1.3 Chronology of main events

Event	Timing [s]
Saturation in the cleaning tank	8520
Water level drop in the cleaning tank	8520
Maximum cladding temperature exceeds 800°C	16250
Maximum cladding temperature exceeds 1200°C	20110
Start of intense Zr oxidation	16610
Failure of first fuel rod due to ballooning	-
Failure of first fuel rod before quenching	-

Table 3.1.3. Chronology of main events

### 3.1.4 Conclusions

Suez-Tractebel Engineering performed two sets of calculations with regard to the “OECD-IAEA Paks Fuel Project”. The first set (*blind* calculation) has been presented at the final project meeting. The thermal hydraulic results of this calculation are in agreement with the observations during the incident.

The second set of calculations (*open* calculation) has been performed after the final project meeting. These calculations take into account the reflections made during and after the final discussion with the other participants of the project. The *open* calculation presents not only a good agreement between the thermal hydraulic behaviour in the tank and the observations during the incident, but also shows that the degradation of the fuel assemblies follows a clear physical logic, which corresponds with the information available from the cleaning tank facility:

- (1) Start of uncover of the fuel assemblies (2h20’);
- (2) Start of fuel assembly degradation (4h35’);
- (3) Amount of core degradation (fission product releases);
- (4) Amount of core degradation (maximal cladding temperature – melting of the cladding material);
- (5) Heat transferred out of the facility with respect to the calculations performed by the University of Budapest.

It should be mentioned that certain elements of the thermal hydraulic behaviour of the TE *open* calculation are in conflict with those of other participants of the program. The main differences lay in the reduction of the water level in the downcomer, more in particular whether or not the outlet tube becomes uncovered, and the amount of heat which is evacuated out of the cleaning tank by radiation.

However, it is difficult to state which of both types of calculations reflects best the actual behaviour in the cleaning tank since only the information with regard to the fuel degradation (cladding temperature, fission product release) is available to evaluate the calculations. For both types of calculations, the behaviour of the fuel and the amount of fuel degradation are similar.

More detailed description of the Suez - Tractebel Engineering analysis is available in Appendix B/I.

## 3.2 Participant VTT

### 3.2.1 Introduction and case description

#### 3.2.1.1 Paks-2 cleaning tank incident

The fuel performance simulation began from the instant when the cooling mode of the cleaning tank was initiated and the fuel rods were being cooled by circulation of storage pool water. The cooling of the fuel assemblies was insufficient due to significant by-pass coolant flow which was formed by fuel assembly perforations and some incorrectly seated fuel assemblies, which led to increasing fuel rod cladding temperatures. After 5 hours and 10 minutes an abrupt increase in Kr-85 counts was observed. After a 9.5 hour cooling period, the underwater cleaning tank was opened, and the hot and heavily oxidised fuel rods were quenched by the cold refuelling pit water and were shattered.

### *3.2.1.2 Tools for Paks-2 cleaning tank incident analysis*

Thermal hydraulic analysis of the Paks-2 fuel cleaning tank incident was performed with the APROS-5.06 simulation code. Total of 30 fuel assemblies in the cleaning tank were divided into six groups by their decay heats.

The transient fuel behaviour during the incident was analyzed with the fuel performance code FRAPTRAN-1.3 with VTT modifications. The fuel behaviour analyses cover a representative rod from each of the groups into which the assemblies had been divided by their decay heat levels, and the time period between the start of the cleaning tank cooling mode and the instant when the cleaning tank cover was opened. The steady-state fuel performance code FRAPCON-3.3 was used to calculate the burnup dependent properties for the transient fuel performance code FRAPTRAN.

The OECD-IAEA Paks fuel project database was used for the steady-state and transient fuel behaviour calculations. The thermal boundary conditions for the transient analysis were calculated with the APROS system code. The cladding oxidation and heat generation from the metal-water reaction were calculated with FRAPTRAN by using a conservative Baker-Just oxidation correlation.

A simple perl-script set was implemented to transfer initial and boundary condition data from the OECD-IAEA Paks Fuel Project database and from the APROS calculation results. A second perl script set was implemented to transfer calculated heat generated by zirconium oxidation with FRAPTRAN back to APROS. Total of three iteration runs were performed with APROS and FRAPTRAN in turns. The goal of this iterative solution method was to achieve maximum reaction heat generation by oxidation corresponding on the decay heat of 30 FAs in the cleaning tank.

#### **3.2.1.2.1 APROS simulation model**

The main APROS simulation model parameters:

- Thermal hydraulic phenomenon modelled with 6-equation model.
- Radiation heat transfer between solid surfaces and solid surface and gas.
- The fuel assemblies were divided into three concentric rings which was taken into account in defining the viewing factors for radiation heat transfer modelling.
- Constant heat transfer coefficients were used on outer wall of the vessel (vessel wall 1280 W/m<sup>2</sup>/K, vessel cover 1450 W/m<sup>2</sup>/K) when calculating the heat losses to the storage pool.
- The total decay heat of the assemblies was 241 kW.
- The fuel rods were axially divided into 23 or 24 nodes depending on the type of the fuel assembly.
- Downcomer side of the vessel was divided into 12 nodes.
- The flow area of the perforations was 83.3 cm<sup>2</sup> and an extra by-pass area was 120 cm<sup>2</sup>.
- Centre of the cleaning tank was located 10 meters under water. The end of the outlet pipe was located at the top of the spent fuel pool.

- Inlet temperature was 30 °C and inlet mass flow was 5.8 kg/s.
- Initial cleaning tank temperature was 58 °C.

### ***3.2.1.2.2 FRAPCON and FRAPTRAN fuel performance codes***

FRAPCON is a single LWR fuel rod fuel performance code designed for steady-state calculations and to generate initial input conditions for FRAPTRAN.

The main phenomena and output parameters with FRAPCON-3 include:

- 1) radial burnup-dependent heat conduction through the fuel and cladding,
- 2) cladding elastic, thermal, creep, and plastic deformations,
- 3) fuel cladding mechanical interaction (PCMI),
- 4) fission gas release (FGR),
- 5) fuel rod internal gas pressure,
- 6) radial heat transfer between fuel and cladding,
- 7) cladding oxidation, and
- 8) heat transfer from the cladding to the coolant. The code contains necessary material properties, water properties, and heat transfer correlations.

The cladding elastic-plastic deformation model based on Finite Element (FE) approach have been implemented in FRAPCON and FRAPTRAN at VTT.

FRAPTRAN is a transient fuel performance code designed to calculate the response of a single LWR fuel rod to transient power and/or coolant conditions.

The phenomena modelled by FRAPTRAN include:

- 1) radial heat conduction,
- 2) heat transfer from cladding to coolant,
- 3) elastic-plastic cladding deformation,
- 4) cladding high temperature oxidation, and
- 5) fuel rod gas pressure.

The E110 (Zr-1%Nb) material properties and the clad rupture model for E110 clad material have been implemented in FRAPTRAN at VTT.

The standard fuel rods and the follower type fuel rods were divided in 23 and 24 axial evenly spaced nodes, respectively.

### 3.2.1.3 Initial and boundary conditions

The fuel assembly and rod design parameters the VVER-440 type fuel construction is based on the fuel design information that is provided in OECD-IAEA Fuel project database.

The LHGR profiles at the beginning of the cooling mode are presented in Figure 3.2.1. The decay heat profiles of FA groups 1-2 and 5-6 are cosine shaped while the decay heat power profiles of Group 3 and 4 are more peaked towards the upper end of the rod.

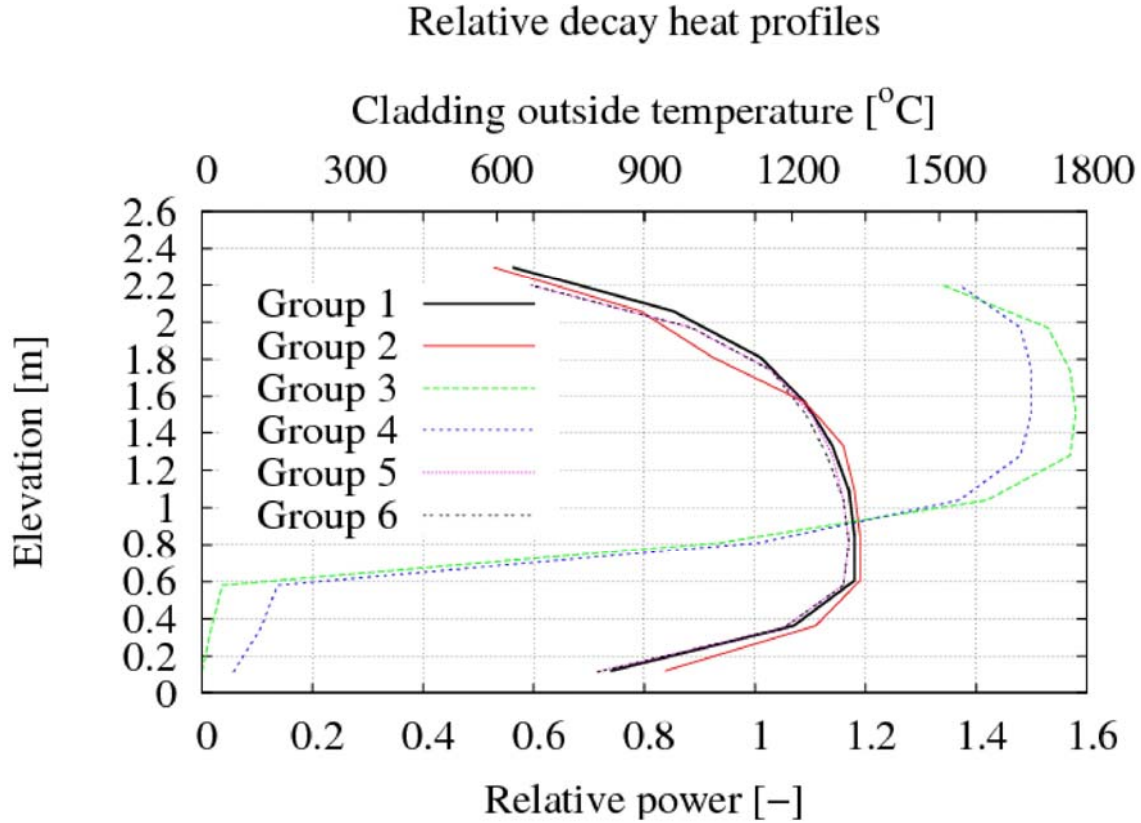


Figure 3.2.1. Relative decay heat profiles at the beginning of transient.

The fuel assemblies were divided into six groups according to their levels of decay heat. The resulting division of the fuel assemblies in six groups is given in Table 3.2.1.

Fuel assemblies	Group	Average decay heat [kW/m]
1-6	1	2.96
7-11	2	3.72
12	3	3.51
13-18	4	2.89
19-24	5	3.81
25-30	6	3.76

Table 3.2.1. Fuel assembly groups.

### 3.2.2 Calculation results

Calculated maximum fuel pellet and cladding outer surface temperatures of the FA groups are close to each other at the end of the simulation. The maximum fuel pellet and cladding outer surface temperatures during the transient are between 1866 and 2043 °C, and between 1628 and 1582 °C, respectively. The reaction energy release is highest in fuel assembly group 3 due to peaked decay heat profile and the highest clad outer surface temperature. The calculated maximum cladding temperature without oxidation modelling was 1155 °C.

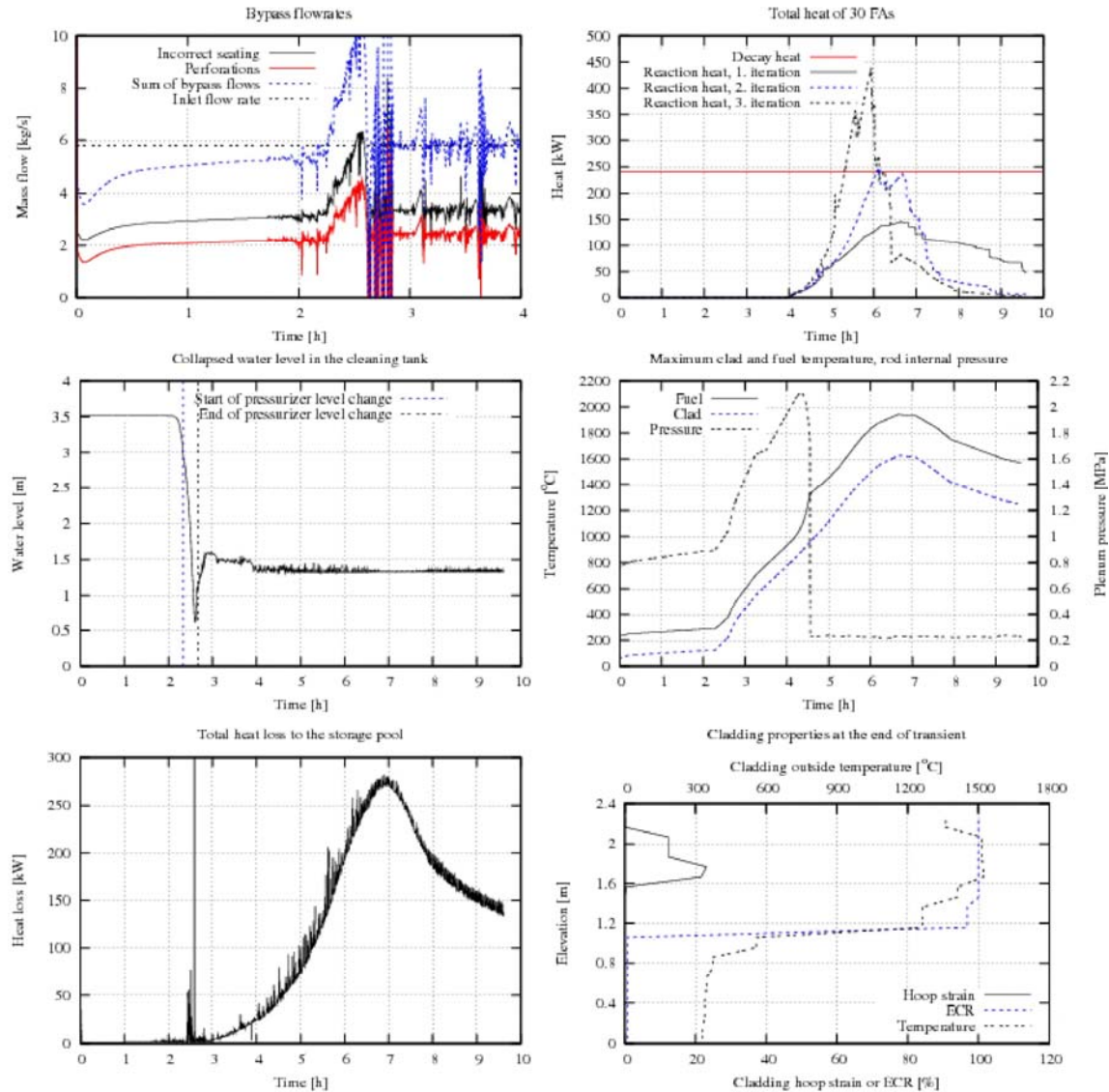


Figure 3.2.2. Thermal hydraulic and fuel behaviour calculation results.

The FRAPTRAN transient calculations suggest that the metal-coolant chemical energy produced is quite significant in the Paks-2 cleaning tank incident. The calculated chemical reaction heat is produced from oxidation of the fuel rod cladding only; the fuel assembly shroud, spacer grids etc. were not considered. FRAPTRAN calculations with the Baker-Just oxidation correlation predict that a significant chemical reaction between the zirconium cladding and steam starts after 3 h 50 min and reaches its maximum power of 441 kW at 5 hours 57 minutes into the cooling mode. The cladding burst is predicted to occur first in fuel

assembly 12 after 4h 34 min from the beginning of simulation, 36 min before the measured activity increase.

By the end of transient, 46.7 % of zirconium has been oxidised and 15.1 kg of hydrogen produced.

Time [s]	Comment
2h:1min	Saturation in the cooling tank.
2h:20min	Water level drop in the cleaning tank.
3h:50min	Start of high-temperature Zr oxidation.
4h:7min	Maximum cladding temperature exceeds 800 °C.
4h:34min	Failure of the first fuel rod due to ballooning (FA 12).
5h:5min	Failure of the last fuel rod before quenching (FAs 1-11).
5h:13min	Maximum cladding temperature exceeds 1200 °C.

Table 3.2.2. Main events of simulation in chronology order.

### 3.2.3 Conclusions

The incident in the cleaning tank of the Paks-2 NPP was analyzed with the APROS-5.06 simulation code and the FRAPTRAN-1.3 transient fuel performance code with FRAPCON-3.3 initialisation.

The voiding of the cleaning tank was well predicted by APROS. Before the voiding, it was predicted that 35 % of the coolant flow has occurred through the perforations and 55 % had flown through the by-pass formed by incorrect seating of fuel assemblies. As a result of this, only 10 % of the inlet flow cooled the fuel assemblies. Inadequate cooling led to voiding of the coolant in the cleaning tank and to overheating of the fuel rods.

Fuel failure was envisaged for all six fuel assembly groups. The cladding burst was estimated to happen at first in the fuel assembly number 12 at 4 h 34 min from the beginning of the simulation; rods in all other groups were predicted to lose their integrity within eight minutes. The cladding burst was estimated to happen 36 minutes earlier than it was detected. This result indicates that cladding temperatures and/or cladding oxidation were slightly overestimated.

The top and middle parts of the fuel rods were estimated to deform and become almost fully oxidised while the bottom parts of the assemblies would seem to remain intact. In addition, a significant amount of hydrogen is expected to be produced by zirconium oxidation.

More detailed description of the VTT analyses is available in Appendices B/II and B/III.

This research project was funded by Fortum Nuclear Services Ltd, Finland.

### 3.3 Participant GRS

The first analyses of the Paks incident with ATHLET-CD were already performed in 2003. In the frame of the OECD-IAEA Paks fuel project the data basis and code models have been successively improved as well as weaknesses and errors in the code detected and eliminated.

#### 3.3.1 Code description

The system code ATHLET-CD (Analysis of Thermal hydraulics of LEaks and Transients with Core Degradation) is designed to describe the reactor coolant system thermal hydraulic response, core damage progression, fission products and aerosol behaviour during severe accidents, to calculate the source term for containment analyses, and to evaluate accident management measures. The development and validation of ATHLET-CD are sponsored by the German Federal Ministry of Economics and Technology (BMWi)

#### 3.3.2 Files delivered for the comparison

The calculation described in this report has been finished on May 19<sup>th</sup>. The computing time of the 9 h transient was 35 h. The integral calculation covers the thermal hydraulics, the fuel behavior, and the activity release. The calculation results were post processed to create the tables to be delivered for the benchmark. According to the specification a set of 6 tables were produced:

- (1) Histories of thermal hydraulic parameters (29 variables as function of time).
- (2) Profiles of thermal hydraulic parameters by the time the maximum cladding temperature exceeds 800°C and at  $t = 32400$ s (12 variables as function of elevation).
- (3) Histories of fuel parameters (23 variables as function of time).
- (4) Profiles of fuel parameters before quenching (24 variables as function of elevation).
- (5) Histories of release from the fuel rods (5 variables as function of time).
- (6) Profiles of axial power distribution (6 variables as function of elevation).

The transient data consist of 2957 records with a time increment of approximately 10 s. The axial profiles consist of 22 records.

#### 3.3.3 Nodalisation and input model

The nodalisation scheme is presented in Fig 3.3.1. Besides the bottom and top region with inlet and air letdown, the thermal hydraulic system is modelled by 6 parallel flow channels with 24 axial nodes. Four flow channels simulate the flow within the assemblies. The surrounding fluid is modelled by two radial interconnected channels. The by-pass flows are simulated by two flow paths through the penetrations from the fixed assemblies to the surrounding fluid as well as one flow path due to incorrect seating. The cleaning tank outlet flow is modelled during the first 3 h by a pipe with constant pressure boundary condition (2.3 bar) and during the later 6 h by a controlled mass flow to limit the flow oscillations in the system. The inlet flow rate and temperature are 6 kg/s and 30 °C. The initial temperature in the tank was set to 58 °C.

Heat losses to the water pool are simulated only over the double-walled cylinder barrel (water pool temperature 30 °C). The 30 fuel assemblies are modelled by 4 representative components, each two for the fixed assemblies and for the followers. The rods and the shrouds are subdivided axially in 20 nodes with equidistant spacing of 0.122 m in the heated region and one node with 0.320 m and 0.240 m length for the lower and upper unheated part

respectively. The number of assemblies per component is 3, 6, 9, and 12 and the bundle power is 7101, 8932, 6847, and 8707 W/assembly. The total decay power is 241 kW.

### 3.3.4 Results of calculation

The mass flow through the air letdown decreases from 2.0 to 0.4 g/s over the time from 4 to 8 h. The average hydrogen generation rate is limited to 0.33 g/s, the total hydrogen generation is 4.63 kg. At the end of the calculation the maximum temperature is 1380 °C at almost stationary conditions (heat up rate 23 K/h). The temperatures of the outer most assemblies are 350 K lower, i.e. the calculated temperatures lie in the expected range.

The chronology of the main event is in the order of appearance:

Event	Timing
Beginnig of saturation in the cleaning tank	7060 s
Beginning of water level drop in the cleaning tank	8640 s
Beginning of core super heating	9140 s
Maximum cladding temperature exceeds 800 °C	14690 s
Start of intense Zr oxidation	15840 s
Rod failure in ROD2	16036 s
Rod failure in ROD3	16434 s
Rod failure in ROD1	16966 s
Rod failure in ROD4	19842 s
Maximum cladding temperature exceeds 1200 °C	21240 s

Table 3.3.1. Chronology of the main events

The timing of the water level drop is well captured by the calculation, but the release is estimated to early by 40 min.

The maximum oxide layer thicknesses are in the range of 100 to 500 µm except the cold walls of the outer most shrouds. The total relative oxidation of all claddings and shrouds is only 5.3 % due to the steam starvation in the cleaning tank.

The relative release (released mass / inventory) of fission products and of the fuel at the end of the calculation is 7.68E-3 for Xe and Cs, 6.16E-3 for I, 3.05E-4 for Te, and 8.51E-7 for U.

The end state of the simulation is depicted in figure 1. The colours indicate the temperatures (yellow > 1300 °C, red > 600 °C, blue saturation) and the void (white = 1, blue = 0) in the system. The water level is at the same height in the whole system at about 0.7 m elevation. Furthermore the ballooning of the cladding and the oxidation profile is visualized. Most oxidation layer are too thin for proper display, only in ROD3 (FOLLOW-1) the oxide layer is visible just below the maximum ballooning.

The conclusion is that the Paks incident was well predicted and the most processes were simulated adequately by the code. The estimated maximum temperatures are sensitive to the hydraulic simulation, the air letdown flow and the heat losses to the water pool.

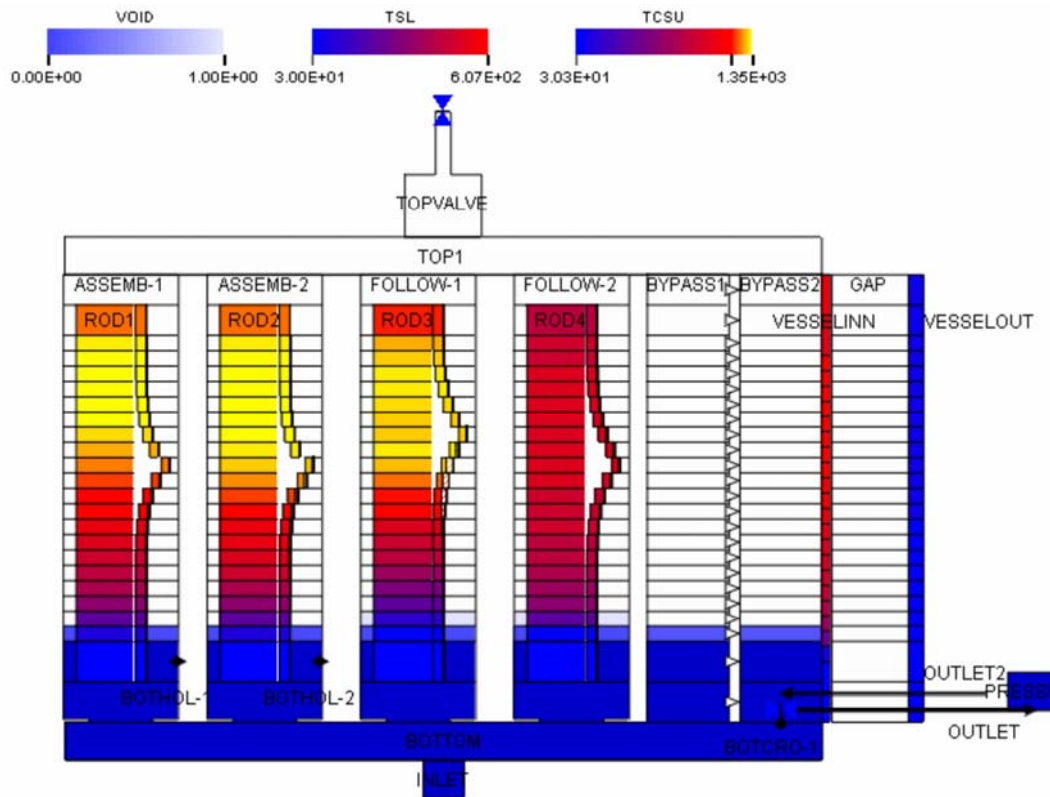


Figure 3.3.1. Nodalisation scheme and end state of simulation with ATHLET-CD.

More detailed description of the GRS analysis is available in Appendix B/IV.

### 3.4 Participant AEKI

#### 3.4.1 Thermal hydraulic analysis

#### 3.4.2 Thermal hydraulic analysis with the RELAP code

##### 3.4.2.1 Code description

The RELAP5/MOD3.3 code has been developed for best-estimate transient simulation of light water reactor coolant systems during postulated accidents. The code models the coupled behavior of the reactor coolant system and the core for loss-of-coolant accidents and operational transients such as anticipated transient without scram, loss of offsite power, loss of feedwater, and loss of flow. A generic modeling approach is used that permits simulating a variety of thermal hydraulic systems. Control system and secondary system components are included to permit modeling of plant controls, turbines, condensers, and secondary feedwater systems.

##### 3.4.2.2 Nodalisation

Two different nodalizations have been developed for the analysis. A more detailed one lumped the 30 fuel assemblies into 4 groups, but non-physical oscillations were produced by this one as soon as the upper plenum turned to two-phase conditions. Therefore a simple

nodalisation was applied, as shown by Fig. 3.4.1, where all assemblies were represented by a single flow channel. The main parts of the cleaning tank are modelled as follows:

Vol 4, Vol 6 and Vol 590 = pool water volume

Jun 5 = pump for cooling mode A

Jun 7 = pump for cooling mode B

Vol 58, Vol 60 and Vol 62 = single flow channel representing 30 fuel assemblies

Vol 570 and Vol 500 (1 –4) = upper part of tank

Vol 60 (2 – 6) = 5 nodes for active part of fuel rods (5 x 0,50 m). In the calculation presented the active part of the fuel rods was divided to 20 nodes: Vol 60 (2 – 21), i.e. 20 x 0,125 m.

Hs 100 – 106 = average heat slabs

Hs 110 – 116 = hot pins

The following by-pass areas were considered:

incorrect seating of assemblies = 120 cm<sup>2</sup>

perforation (below active part) = 84 cm<sup>2</sup>

perforation (above active part) = 84 cm<sup>2</sup>

Jun (Vol 54 - Vol 576)

Jun (Vol 58 - Vol 578)

Jun (Vol 62 - Vol 572)

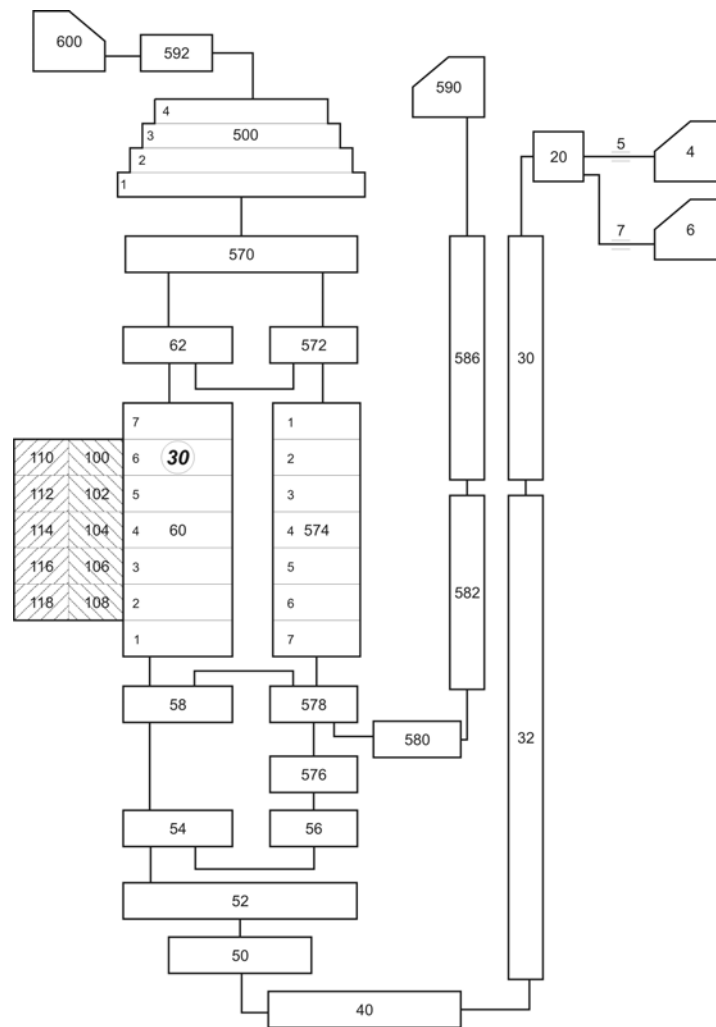


Figure 3.4.1. Nodalisation scheme for RELAP5 code

### 3.4.2.3 *Boundary conditions*

Cleaning tank inlet flow rate was imposed to represent the different cooling modes, with a 5 min. interruption in forced flow due to transition from one mode to the other:

time < -300 sec	47.20 kg/s,
-300 < time < 0 sec	0.00 kg/s
time > 0 sec	5.83 kg/s

Initial tank temperature 57 °C.

Pool temperature 30 °C.

Total fuel assembly power 241 kW.

### 3.4.2.4 *Results*

The analysis starts from stabilised conditions in the cooling mode C, with high forced flow through the tank. A 5 min. period was assumed before effective switch-over to the low flow rate of the cooling mode B was established, where flow rate to the tank was zero. In this period natural circulation was established in the tank with upward flow through the assemblies, downward in the tank and back via the perforations and by-pass area due to incorrect seating.

With the low flow rate of cooling mode B the flow rate entering the heated part of the assemblies is continuously decreasing, while the by-pass flow rate is continuously increasing. As a consequence, the coolant temperatures start to rise. Due to the rather fast decrease of the flow rate, the saturation temperature is reached at the assembly outlet already at 2830 s. In spite of that, it is not before 10560 s that significant level decrease can be observed in the cleaning tank, which is much later than the phenomenon observed during the incident, where about 2 h 20 min after change-over to cooling mode B the level of the pool rose by ~7 cm in cca. 20 min. At about 11600 s the level finally stabilises at an elevation of 1.6 m. Already before the level stabilisation fuel temperatures start to increase and by the end of the calculation the maximum temperature reaches 600 °C.

Results for the main parameters are presented in Figs. 4.1 to 4.15 as the parameter AEKI.1. (Additional figures can be found in Appendix B/V.) Due to the simplified nodalisation the inlet flow rates in Figs. 4.8-9 and 4.10-11 were estimated in the following way:

$$\text{Inlet flow rate for working assembly} = [\text{Jun}(54 - 58) - 19 * \text{Jun}(58-60)/30]/11$$

$$\text{Inlet flow rate for follower assembly} = \text{Jun}(58 - 60)/30$$

The sequence of the events can be summarised as follows:

- < -300 s 47,2 kg/s forced flow
- < 0 s natural circulation is established via the perforations and by-pass
- > 0 s 5,83 kg/s forced flow, heat-up to saturation
- 2830 s void at outlet of assemblies
- 10560 s vessel liquid level decreases
- 10730 s fuel cladding temperature increases
- 13650 s end of calculation

### 3.4.2.5 *Conclusions*

Saturated conditions are reached too early in the transient due to rather fast decrease of the fuel assembly low rate. Since elevation heads are correctly calculated in RELAP, it is assumed that this is a consequence of inappropriate friction losses in by-pass areas and /or fuel assemblies. On the other hand, the accumulation time of steam in the upper head is

overestimated that may be due to non-physical oscillations caused by transition from low to higher void fractions in the condensation models.

### 3.4.3 Thermal hydraulic analysis with the ATHLET code

In order to understand the physical processes taken place in the cleaning tank during the Paks-2 incident, in April/May 2003 a series of calculations were performed by AEKI for different batches of fuel assemblies cleaned in the tank. The thermal hydraulic analyses were performed by the ATHLET code. In what follows, the “best estimate” calculation results are presented for Batch No. 6, which is of interest for the present project.

#### 3.4.3.1 Code description

ATHLET is a one dimensional two fluid code for the thermal hydraulic analysis of reactor transients and accidents. The physical model of the code is based on the system of six integral balance equations. Application of finite volume method for spatial discretization allows a rather coarse nodalisation of modelled objects. The system of governing equations is closed by state equations, interfacial transfer conditions and constitutive equations. Non-condensable gas as well as boron dilution can be simulated by ATHLET.

#### 3.4.3.2 Nodalisation

The geometrical model included the following elements as represented by Fig. 3.4.2:

- Simplified container geometry with lower and upper plena and outlet piping. Inlet piping was only modelled by imposed pump flow rates.
- Container wall, fuel assemblies (FA) including shrouds, support plates modelled as heat structures.
- FAs grouped into 5 parallel channels with 20 axial nodes
- Tank volume outside the assemblies represented by a single channel with 20 axial nodes
- Shroud perforation of working FA at bottom and top ( $A= 7.634 \text{ cm}^2$ )

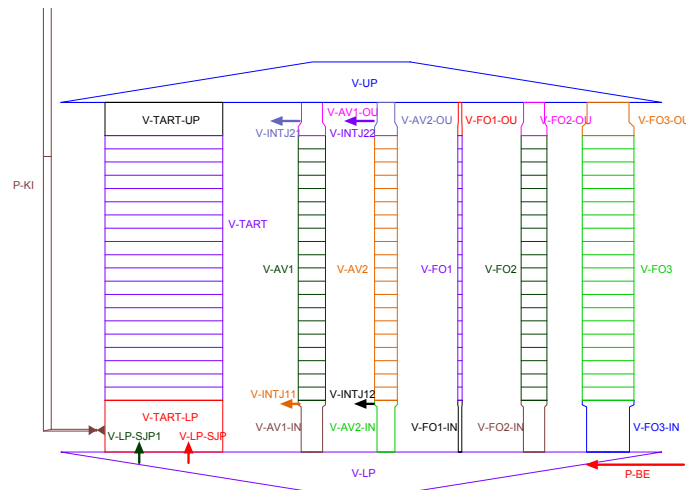


Figure 3.4.2. ATHLET nodalisation of the cleaning tank

### 3.4.3.3 *Initial and boundary conditions*

Initial and boundary conditions were selected on the basis of Batch No. 6 data:

- Total decay heat: 241 kW
- 19 follower FAs represented by 3 groups with different power
- 11 working FAs represented by 2 groups with different power
- Axial power profile: from decay heat calculations for Batch No. 6
- Pump flow rate: 170 t/h in cooling mode C and 21 t/h in cooling mode B, with instantaneous switch-over from mode C to B
- Cleaning tank initial temperature: 57°C, uniform
- Pool temperature: 30°C
- Degassing line not modelled explicitly, only constant outflow of 0.0015 kg/s assumed.
- Besides the shroud perforation of the working FAs an additional by-pass cross section due to incorrect seating of 117.5 cm<sup>2</sup> was assumed.

### 3.4.3.4 *Results*

The most important results are graphically presented in Figs. 4.1 to 4.14 as the parameter AEKI.2. Additional figures can be found in Appendix B/VI.

The mass flow rate at the inlet of the working assemblies is continuously increasing, the opposite is true for the follower ones. However, looking at the flow rates entering the heated part of the assemblies, i.e. above the elevation of the shroud perforation, all the flow rates display similar behaviour, which means that in the case of the working FAs the difference between the two flow rates exits via the shroud perforations. The flow rates of the different assemblies are slightly different due to the different power. The by-pass flow rate is continuously increasing and reaches at 10000 s almost 75 % of the total flow at the FA inlet.

As a consequence, the coolant temperatures start to rise. The saturation temperature is reached at the outlet between 5400 and 6400 s, depending on FA power. The void formation under the tank cover starts at 6500 s and by 8000 s it is completely voided. It takes about a further 1000 s that the level in the tank drops to roughly the lower 1/3 elevation of the tank. This is in good agreement with the phenomenon observed during the incident, where about 2 h 20 min after change-over to cooling mode B the level of the pool rose by ~7 cm in cca. 20 min.

A number of parametric calculations were also performed in order to assess the impact of the most important parameters: an overview is given in App. B/VI.

## 3.4.4 *Fuel behaviour calculation*

### 3.4.4.1 *Code description*

Fuel behaviour during the incident was simulated with the FRAP-T6 code. The code simulates the thermal and mechanical behaviour of one piece of fuel rod considering the heat transmission of the given subchannel. The AEKI version of the FRAP-T6 code includes special VVER models (phase transition, oxidation, burst, mechanical properties as function of oxidation) that are based on experiments with E110 type cladding. According to the

thermohydraulic calculations all coolant flowed out at the bottom of the fuel assemblies without cooling the active section.

In the FRAP-T6 calculations the coolant circulation flowrate was set to constant in the subchannel and other heat transfer methods (e.g. radiation) were not taken into account. The enthalpy of the coolant at the entry was 167 kJ/kg. The model included one fuel rod in a one-dimensional nodalisation.

The fuel assemblies with similar power histories and of the same type (follower or working) were grouped into 6 groups and only one representative assembly was calculated for each group. The average linear power, the burnup, the pressure in the fuel rod and the axial distribution were taken from the database. The calculations were made in the 10 evenly spaced axial part of the fuel rod.

#### *3.4.4.2 Results*

After the formation of steam volume in the cleaning tank the temperature of upper part of cladding exceeded 800 °C within 130 minutes. The fuel rods ballooned up and bursted, and the accumulated fission gases were released into the coolant. The burst of fuel rods occurred about 2.7 hours after steam volume formation. It is likely that this process was detected by activity detectors after 21.30 at the Paks NPP.

After bursting, the temperature of fuel rods increased and the maximum cladding temperature exceeded 1200 °C. The thickness of zirconium-oxide layer on cladding grewed quickly because of the intensive oxidation. Its local value was 300 µm, after 5-6 hour oxidation.

Time of failure of every assembly was calculated by the FRAP-T6 code and those data were used in the activity release calculations.

### **3.4.5 Calculation of activity release**

#### *3.4.5.1 Model description*

The calculational method estimates the release from the fuel rods in the percentage of isotope inventory. The method makes a distinction between release from the gap and pellet. First the gap inventory releases from the damaged fuel assemblies and then one part of the radioactive isotopes (that are located in the pellet) with different mechanisms, like fragmentation of pellet or leaching.

Parameters of the best-estimate method were derived from processing of different experimental data. This method is applied in the safety analyses of design basis accidents such as LOCA.

#### *3.4.5.2 Calculated results*

Apart from the noble gases 10 % of the total release is taken to be released in the dry phase and 90 % is released after the rupture is recovered. All the noble gas release is taken to occur in the dry phase.

The calculations of activity releases were performed for every assembly. The fuel assemblies with similar power histories and of the same type (follower or working) were grouped into 6

groups. In the next table and figure it could be seen that good agreement was found between calculated and measured activities.

In case of volatile isotopes good agreement was found between the measured activity release and results of calculations. The most significant difference appeared for non-volatile elements.

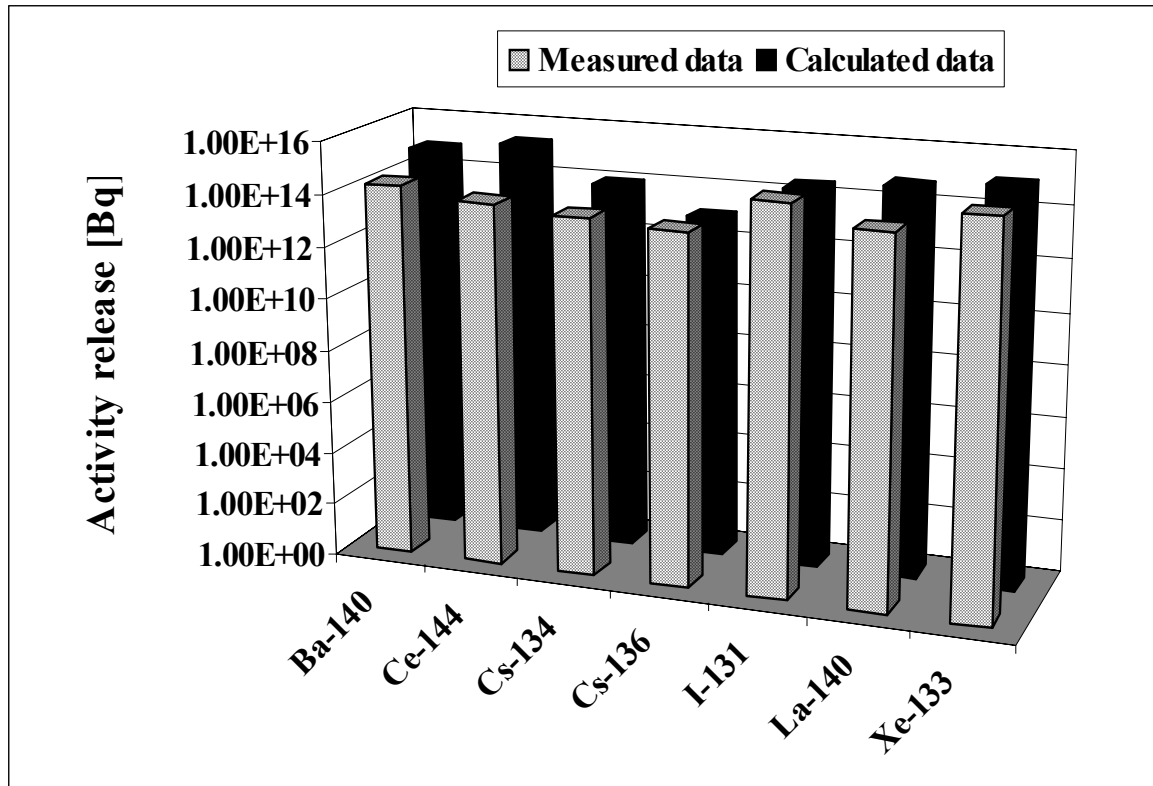


Figure 3.4.3. Comparison of measured and activity data

### 3.4.6 Summary of calculated results

thermal hydraulic calculation	RELAP5	ATHLET
saturation in the cleaning tank	2830 s	5400 s
water level drop in the cleaning tank	10560 s	8000 s
fuel behaviour calculation	FRAP-T6	
maximum cladding temperature exceeds 800°C	15800 s	
maximum cladding temperature exceeds 1200°C	17720 s	
start of intense Zr oxidation	17000 s	
failure of the first fuel rod due to ballooning	18850 s	
failure of the last fuel rod before quenching	20010 s	

Table 3.4.1. Calculated times of main events

More detailed description of the AEKI analyses is available in Appendices B/V, B/VI, B/VII and B/VIII.

### **3.5 Participant BME NTI**

On 10-11<sup>th</sup> of April, 2003 a serious incident caused heavy damage of 30 fuel assemblies in a cleaning tank which was installed into the refuelling pit of the 2<sup>nd</sup> unit of the Paks NPP. The incident was investigated by several scientific institutes and with different analytical and numerical methods and tools. Among other methods, the early stage of the incident when one-phase flow was in progress was investigated with 3D CFD calculations in 2003 in the BME NTI. In the same institute newer 3D CFD calculations were performed on this stage of the serious incident in the framework of the OECD-IAEA Paks-2 Fuel Project in 2007. Robust meshing, detailed geometry and the best known real parameters were built into the model. By modifying the model's geometry the effects of displacements of one or two working fuel assemblies were also investigated.

#### ***3.5.1 The 3D CFD models of the cleaning tank***

The 3D CFD model of the cleaning tank contained 11 working and 19 follower fuel assemblies. The assemblies were modelled as hexagonal prisms with a coaxial cylinder cut out from it. The cylinders' cross section was equal with the assemblies' flow cross section. The 12 perforations on the bottom part of the working assemblies were replaced by 6 perforations of 13 mm in diameter per each assembly. The 12 perforations on the top part were replaced by 2 perforations. The leg parts of the working assemblies were modelled in a detailed manner.

Three different versions of the model were developed. In the W11\_F19\_DIS1 and W11\_F19\_DIS2 model versions displacements of one and two working fuel assemblies were taken into account such a way that apertures have been opened at the corresponding assemblies' very bottom end. The cross section of the apertures was 2030 mm<sup>2</sup>. The W11\_F19\_DIS0 model version did not contained any displacements.

The 4.1 million control volumes mesh contained unstructured tetrahedral mesh with hexahedral core combined with extruded pyramid elements.

#### ***3.5.2 Boundary conditions, parameters of the model***

For all calculations the laminar flow model was used. The buoyancy was taken into account with the Boussinesq-approximation. All walls were modelled as free-slip walls.

The fuel assemblies were divided into six groups by its decay heat power profile. The decay heat power density profile inside the FAs' models was given as point slope functions. The data set for the heat power profiles was given on the basis of the OECD-IAEA Paks-2 project's database. Different volumetric quadratic resistance values were set inside the working and follower fuel assemblies based on literature data.

The inlet parameters were constant static pressure and 36 °C inlet temperature. The outlet setting was constant mass flow rate of 5.555 kg/s. All calculations were run as transient calculations of 8,000 seconds. The time-step was set to be 2.5 s. The sensitivity for the time stepping was investigated. The aim of the runs was investigating the one-phase thermal hydraulic processes during the "B" operational mode which started at 16:40, 10<sup>th</sup> of April, 2003.

### 3.5.3 Calculational results

The calculations for the different model versions gave qualitatively very similar results. These characteristics are summarized in the following bullets and the most important numerical results are summarized in Figure 3.5.1.

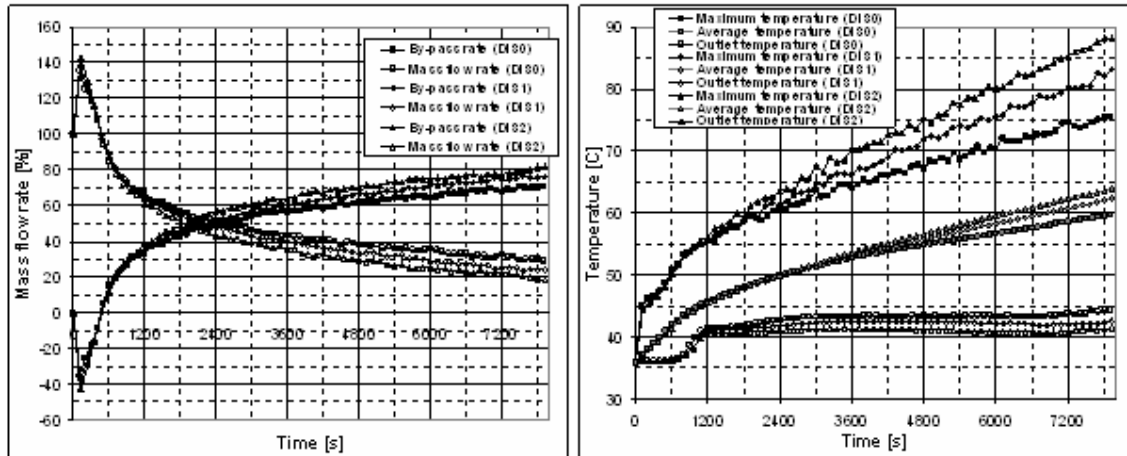


Figure 3.5.1. Left side: By-pass rate through the working FAs' bottom perforations and the displacement orifices and mass flow rate through the active parts  
Right side: Maximum temperature values, whole flow domain volume average temperatures and mass flow weighted temperature averages for the outlet

- (1) The temperature stratification developed from the very beginning. After 1200 seconds such temperature fields developed that it kept its characteristics for the further part of the transients: The tank outlet temperatures froze at about 41-44 °C temperature values which means that the decay heat power was not removed from the cleaning tank for any of the calculations since the differences between inlet and outlet temperatures were less than 10,5°C. After 1200-1800 s, the temperatures increased with similar rates in time in the flow domain at different levels above the level of the working FAs' bottom perforations.
- (2) At 1800-2400 s, the sum by-pass flow become higher than the net flow through the FAs' active parts and increased further. At 8000 s, it reached 70% in case of the W11\_F19\_DIS0 calculation, 75% for the W11\_F19\_DIS1 calculation and 81% in case of the W11\_F19\_DIS2 calculation.
- (3) The calculations show that the maximum temperature did not reach the saturation temperature even after 8000 s. On the basis of trend line fitting it can be stated that the increasing of the maximum temperatures had a rate of about 3.4 and 4.6 K/1000 s after 1200 s for the different model versions. *With these rates the saturation temperature (~120 °C) would have reached after 22900, 17400 and 14700 s for the W11\_F19\_DIS0-DIS1-DIS2 calculations respectively.*
- (4) On the other hand, it has to be emphasized that the initial temperature of the cleaning

tank which was valid at 16:40, 10<sup>th</sup> of April, 2003 is unknown. The results' characteristic and the temperature values presented in Figure 3.5.1 refers to that independently from the initial temperature, a similar stratified temperature field could be developed after a while. It is likely that in case the initial temperature had been higher, the saturation temperature would have been reached earlier.

From the above explained details, the following most important conclusions may be drawn:

- The calculations showed that even with or without any fuel assembly displacements the temperature stratification could have been developed and blocked the flow through the fuel assemblies and the saturation temperature could have been reached after enough long period of time.
- On the other hand, by taking into account the fact that the maximum temperature reached the saturation within 8400 s during the incident, the results point out that beside the working fuel assemblies' bottom perforations more by-pass area was present in the bottom part of the cleaning tank.

More detailed description of the BME NTI analysis is available in Appendix B/IX.

### **3.6 Participant VEIKI**

Calculations performed with the MELCOR 1.8.5. version on IBM PC using two different models of MELCOR the PWR and BWR model.

#### ***3.6.1 MELCOR PWR and BWR models of the cleaning tank***

##### PWR Model

The parts included into the MELCOR modelling scope for the cleaning tank are given in Figure 3.6.1.

The system was modelled with a total of 49 control volumes. The surge tank was connected to the cleaning tank at the top of the upper plenum. 11 fixed FA have been considered with 12 holes (each with d=9mm) at the bottom and 12 holes at the top. The 19 follower FA were without holes. The geometry of fixed FA and followers were considered to be the same using the fixed FA as base.

Heat losses from the inner vessel to the vacuum gap between the inner and outer vessel has been modelled. Subsequently the outer vessel communicated the heat to the pool of shaft No.1. Inner vessel wall assumed to be core boundary HS was calculated with radiation heat transfer taken into account through the vacuum gap between the two vessels. The flow-paths connecting the control volumes are also summarised in Figure 3.6.1.

Degraded core calculations were performed by the COR package. The decay power has been specified as a value valid 13 days after the shutdown. MELCOR calculated it as 258.2 kW.

The core (Figure 3.6.2) has been modelled with 6 radial rings (ring1 is empty representing the central hole) and 21 axial levels in the core. The fuel assemblies were divided into 5 groups and placed into rings 2-6. (Ring1 was empty).

The COR 6 radial rings and 21 axial levels have been grouped into several control volumes as of Fig 3.6.1. The power distribution is given in Figure 3.6.3. Initial conditions were the following:

- Pool temperature 30 °C
- Tank coolant temperature 57 °C
- Fuel assembly temperatures Coolant+1-2 °C
- Pump flow rate 22 t/h

Ring1	Ring2	Ring3	Ring4	Ring5	Ring6
Central Hole	Fixed FA 1-6	Fixed FA 7-11 Follower 12	Followers 13-18	Followers 19-24	Followers 25-30

Table 3.6.1. Distribution of assemblies in radial rings of the model

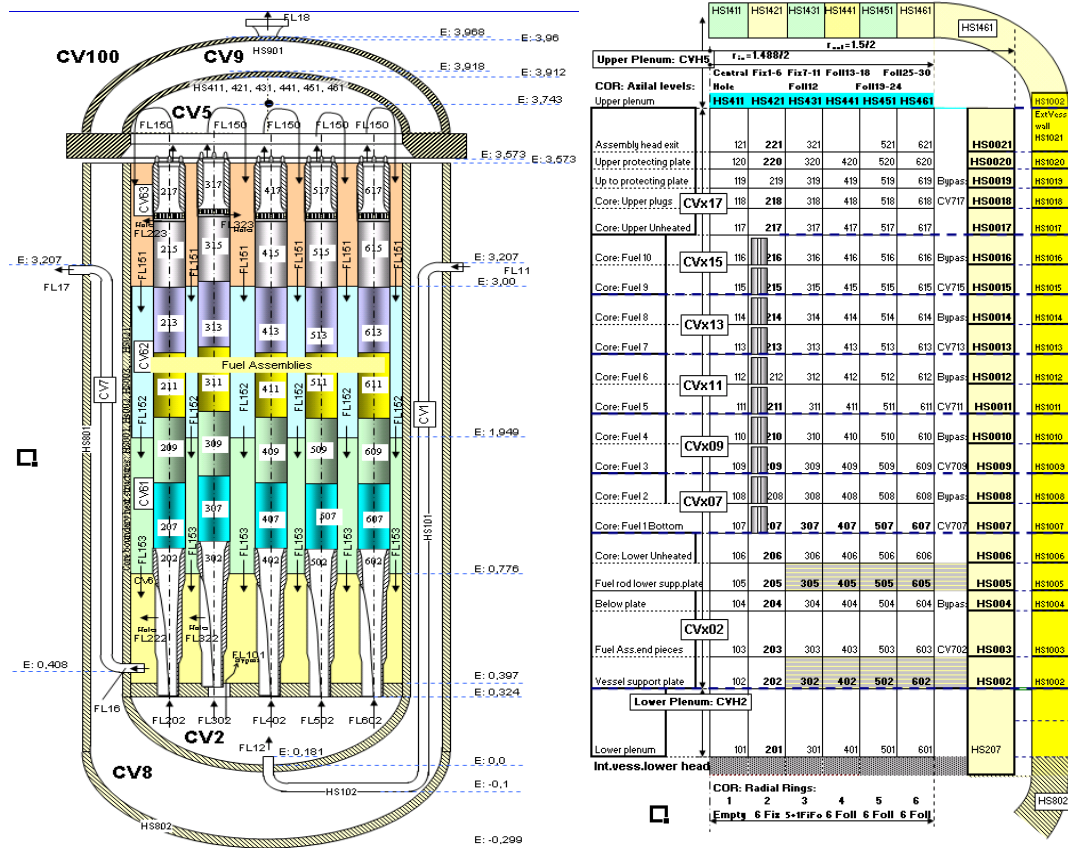


Figure 3.6.1. MELCOR 1.8.5 tank PWR nodalization

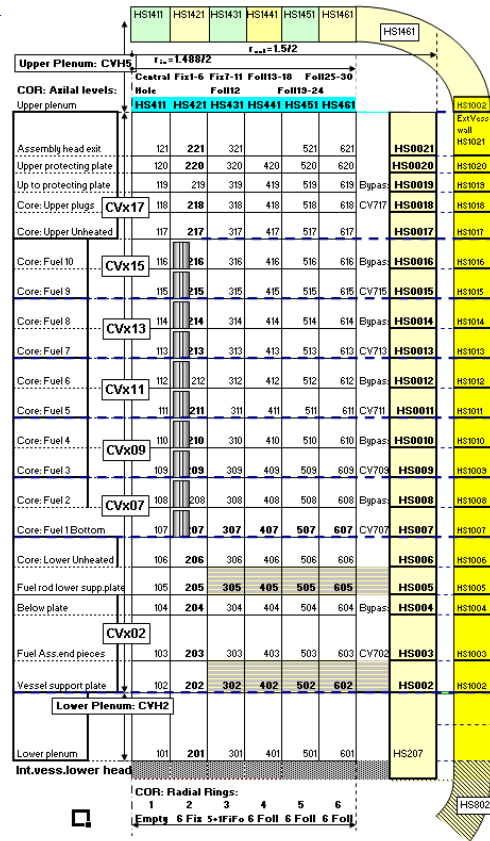


Figure 3.6.2. MELCOR 1.8.5 core BWR nodalization

## BWR Model

The MELCOR BWR model – different from PWR model mainly by the presence of by-pass CVs - can model the channel boxes of the VVER-440/213. It allows to simulate heat transfer to space outside of the fuel assemblies modelled as by-pass region of a BWR core. In this way it was possible to avoid the modelling of the oxidation of VVER-440 Zr channel boxes by a double surface area.

The space outside of the fuel assemblies (by-pass) has been divided along the vertical in the same way as the CVs along the core axial levels.

Opposite to the PWR model where the fuel-containing outer-most core ring (No6) was transferring heat to internal vessel wall simulated as core wall in the BWR model space outside of the fuel assemblies (by-pass) transferred heat the to wall of the inner vessel modelled as core wall. (However core wall still receives radiative heat from the outermost core ring.) These by-pass CVs also communicated with the space inside the fuel assemblies by heat conduction via the assembly walls (channel boxes).

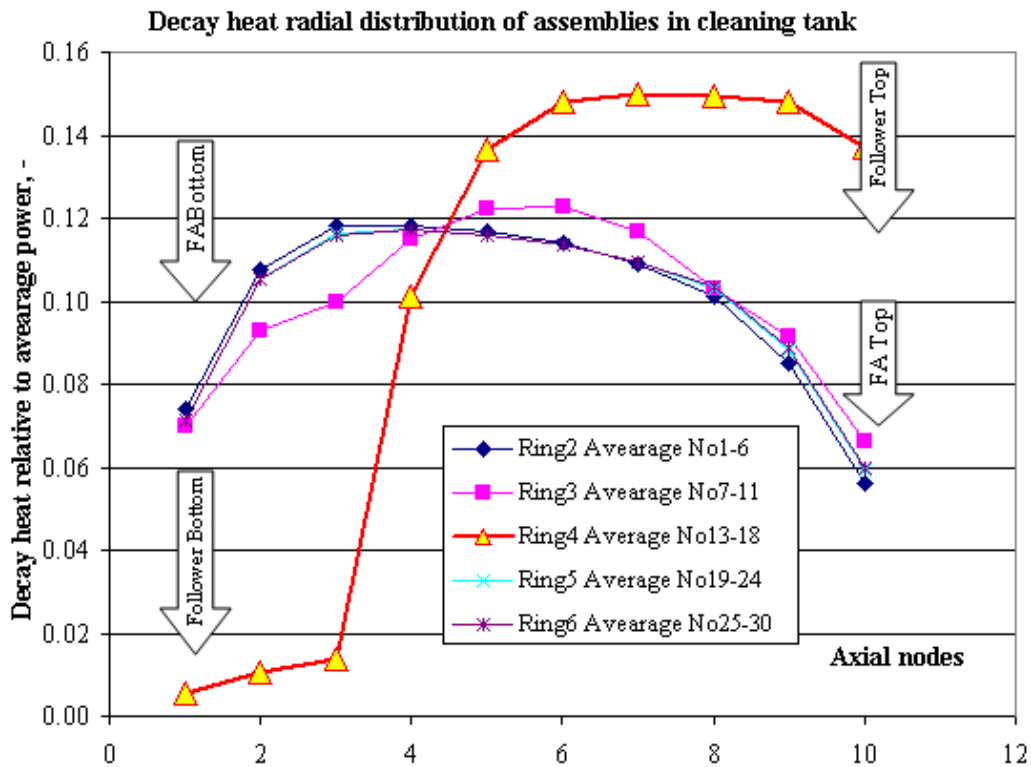


Figure 3.6.3. Radial and axial distribution of FA decay power in the Paks-2 cleaning tank.

### 3.6.2 Safe envelope of operation

Simple hand calculations were done to identify the safe margins of inlet flow-rates at assembly bottom without and with steam generation. The results show that about 12% of nominal flow-rate would have been enough to remove the decay heat without boiling and an even smaller flow if the vent line could remove the steam generated to avoid level depression and uncover.

Calculating the time needed to fill the upper plenum by steam and plotting it vs. steady state flow for heat removal with steam generation one can obtain the time range for accident development (Figure 3.6.4). Figure 3.6.4 shows a very steep change around 12% of nominal flow. This figure also contains the flow-rates experienced with MELCOR before the strong two-phase flow, which shows that some channels are generating steam and some are not both in MELCOR and in simple hand calculations. The figure shows that uncover by release of dissolved gases is not a real danger.

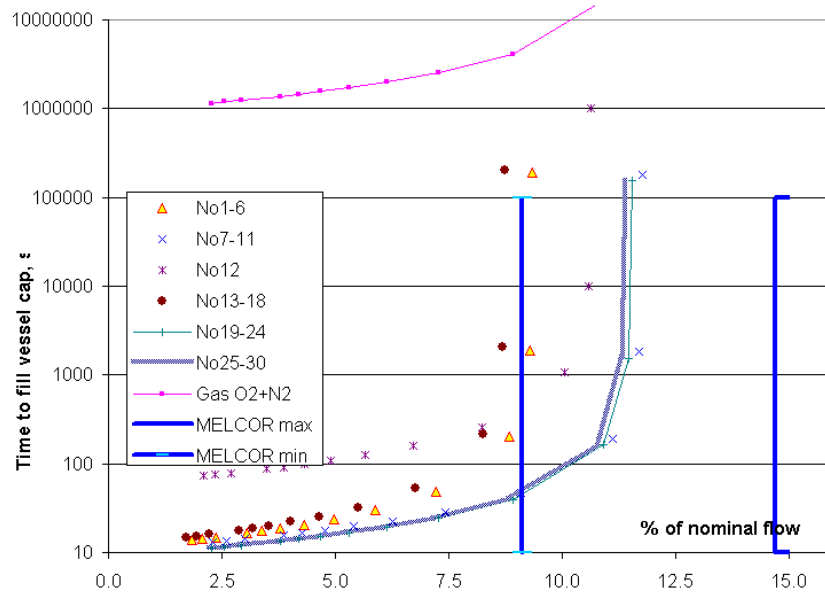


Figure 3.6.4. Time needed to fill the upper plenum (vessel cap) by steam vs. relative flow-rate ensuring steady-state heat removal with steam generation from groups of FA of Paks-2 cleaning tank. (Relative to nominal flow to group assuming 22 t/h for the whole vessel.)

### 3.6.3 Transient calculations

If vent line was suddenly open at moderate steam generation rate, most of the steam got discharged from the tank and the FA were re-flooded. However if vent line was open all the time then strong water level depression was experienced. The final calculations were done with vent line closed.

Ring No. 3 was assumed to be miss-positioned (area=0,0120m<sup>2</sup>) and inlet flow area to ring 3 (lowermost CV = FA unheated end tail containing the bottom holes ) has been reduced by the same amount.

The calculation was started from  $t = 0$  s which corresponded to switching to low flow-rate pump – operation “AMDA C”. The timing of the main events is shown in Table 3.6.2. The observed water temperature exiting the tank was about 37 C, which was reproduced by the calculations well.

The results were sensitive to size a vacuum (0.01 bar in BWR model) between the two tanks and surface emissivity (0.8 in BWR model) of the vessel walls. These influenced first of all the radiative heat loss to water pool in shaft No1 at later stages. However the heat-up times did not change too much because radiation starts to be important only at elevated temperatures. More detailed description of the VEIKI analysis is available in Appendix B/X.

Vent line closed PWR: Run9nA BWR: Run H	<i>Accident phase</i>	Mark	Time, s PWR model	Time, s BWR model	Time, s Observed
<b><i>Initial heat-up</i></b>					
Initiating event			0.0		0.0
Core starts to boil	<b><i>Boil-off</i></b> Ring4 elev. 415	<b>B</b>	5600	7190	NA
<b><i>Core heat-up</i></b>					
Core uncover	<u>Ring3-4</u>	<b>U</b>	9600	9800	8400
Core exit temp. above 550 C	<u>Ring4</u>	<b>S</b>	15921	15706	
<b><i>Core damage</i></b>					
Start of Zr-H <sub>2</sub> O reaction	<u>Ring4</u>	<b>Z</b>	17804	17664	
Gap release	<u>Ring4</u>		17977	17999	
	<u>Ring3</u>		22123	21711	18600-24600
	<u>Ring5</u>		21030	23600	(1)
	<u>Ring6</u>			23141	
Molten Zr (T>1825 C)			Not reached	19901	

(1) 18600-24600s corresponds to time interval of April 10, 16:40-23:30h

Table 3.6.2. Comparison of calculated and observed events using MELCOR PWR and BWR models.

### 3.6.4 Conclusions

Based on several calculations with different MELCOR models (PWR and BWR) it can be concluded that MELCOR reproduced the incident phenomenon well, and the experience can be utilized in plant calculations. There is no big difference between the MELCOR PWR and BWR models results in term of accident progression and activity release. However the MELCOR BWR physical model describes the heat transfer and oxidation phenomena of fuel assembly channel boxes special for this case better.

A coarse nodalisation in the core could not achieve conditions when steam generation started for the present case with low heat generation.

Calculations were done with the vent line closed. Some studies were also done with vent line on the tank open. Preliminary results suggest, that some core damage might have happened even in case of vent line open. However lack of precise data prevents us from drawing strong conclusions on this case.

### 3.7 Participant KI/IRSN

The presented results of the Paks-2 cleaning tank incident simulation with ICARE/CATHARE code are obtained in the frame of technical collaboration between RRC “Kurchatov Institute” (Russia) and IRSN (France), and should be regarded as a common RRC KI and IRSN contribution to OECD-IAEA Paks fuel project.

This work was carried out in accordance with recommendations from OECD-IAEA Paks fuel project meetings and input transient and modelling parameters are set following current database of Paks incident. An analysis of the calculation results is done accounting the requirements for the participants of the project.

### **3.7.1 Code description**

The ICARE/CATHARE code, developed in IRSN (France), is devoted to calculate in detailed mechanistic way core degradation during severe accidents in LWRs. Both parts of the code, ICARE2 and CATHARE, were developed separately as for analyses of wide range of high temperature core phenomena as for realistic simulations of thermal hydraulics in different reactor components. Recent wide validation of coupled ICARE/CATHARE code against numerous integral experiments and SFD reactor scenarios showed its applicability and high prediction power, in particular, to VVER reactors and VVER type experimental facilities.

The first part of the current work included simulation of thermal hydraulic phase of the incident using CATHARE2 V1.3L\_1 code. The second part concerned phenomena during SFD phase, which appeared after dryout of the tank, heat-up and the high temperature evolution of the fuel assemblies. The SFD phase was simulated using the updated version of the ICARE/CATHARE code with ICARE2 V3.2 code version.

### **3.7.2 Thermal hydraulic phase of the transient**

It was assumed that 3 of 30 fuel assemblies have additional flow by-pass at their entry. This by-pass is formed due to incorrect positioning of these assemblies on the support plate of the tank. Cross-flow area of the by-pass 120 cm<sup>2</sup> was chosen in accordance with decisions of the 1st Meeting on OECD-IAEA Paks fuel project. Moreover ordinary by-pass due to perforation in the lower part of 11 fixed assemblies was taken into account. Geometry and hydraulic resistance values of the fuel assemblies were reproduced in the input data.

Water inlet mass flow 5.5 kg/s with temperature about 30°C was supplied with a pump to the tank from the cooling pond to cool the fuel assemblies.

The code predicted that major part of the water, supplied into the tank in the cooling mode, was lost through the by-pass and the perforation. Only 10-20% of supplied water took part in the cooling process. It led to insufficient cooling of the fuel assemblies and their gradual heat-up. The temperatures reached the values leading to water boiling ~2 hr after the moment of flow reduction at the beginning of cooling mode. Assembly dry-out began at ~2 hr 20 min and continued ~20 min. Water level stabilization was predicted at elevation ~0.7 m, timing of steam void formation and final level position correlated with known plant data.

An uncertainty analysis was performed to estimate the variation range of physical parameters at the beginning of SFD phase. Four series of variant calculations were carried out, including by-pass flow area, gas relief pipe flow capacity and decay heat power. It was shown that duration of the period from inlet flow reduction until the onset of the assemblies' dry-out varied in wide range (from 6% to 15%) due to these parameter uncertainties. Pressure loss coefficients of the assemblies located in the tank were found to be less important parameters for the incident simulation.

All known events and parameters of initial (thermal hydraulic) phase of the cleaning tank incident were successfully reproduced in CATHARE2 calculation. The results of this calculation formed initial and boundary conditions for subsequent ICARE2 calculations.

### **3.7.3 SFD phase of the transient**

According to Paks database all 30 assemblies inside cleaning tank are divided on 6 groups, basing on burn up history and type of the assembly:

1. Fix assemblies 1-6 (burn up 10.9 MW day/kgU, power 7.159 KW);

2. Fix assemblies	7-11	(burn up 27.0 MW day/kgU, power 9.006 KW);
3. Follower	12	(burn up 9.2 MW day/kgU, power 8.154 KW);
4. Followers	13-18	(burn up 21.3 MW day/kgU, power 6.694 KW);
5. Followers	19-24	(burn up 13.9 MW day/kgU, power 8.837 KW);
6. Followers	25-30	(burn up 13.7 MW day/kgU, power 8.719 KW).

Total decay power at time of incident was 241 KW.

Axial meshing in ICARE2 simulation included 20 nodes along heated region of the fuel rods. A nodalization scheme with 3 parallel channels was used. Additionally, recently developed best-fitted correlations for Zr+1%Nb alloy oxidation have been applied.

The first characteristic event of SFD phase appeared at 14360 second, when maximum cladding temperature exceeds 800 °C. The assembly of the 3<sup>rd</sup> group (single assembly № 12) first reaches this temperature that totally corresponds to the peculiarities of the local decay power, which according to Paks database is the highest for this assembly at the same elevation. Later increase of radiation heat transfer smoothes this dependence and hottest zone is shifted to central region of the cleaning tank. The assemblies of the 1st group (assemblies № 1-6) first reach temperature of 1200 °C at time 19700 s.

According to simulation results maximum fuel rod temperatures does not exceed 1500 °C, which is realized approximately after 24000 seconds of the transient. Our analyses show that growth of maximum temperatures is limited by oxygen starvation. The temperature between fuel and cladding generally is rather small and differs by 5-10 °C.

The evolution of internal fuel rod pressure, which is obtained during the simulation, indicates that first failure of fuel rod occurred at  $\approx$  16700 second in the central assembly. The latest failure occurs about 500 seconds later on the periphery. It should be noted that these results should be regarded only as a preliminary ones, as they were obtained with application of mechanical behaviour model CREEP, which was developed for Zircaloy claddings.

The analyses of evolution of oxidation state of the assemblies show that total extent of Zr oxidation is not very high increasing to approximately 15% at the end of the transient. At the same time local oxidation of the fuel rod cladding appears to be substantial (about 80%) at narrow region in central part of the cleaning tank.

Specific Zr oxidation behaviour of the regarded transient is realized in simulation of hydrogen release. Following the computation the entire transient can be subdivided in three periods. Firstly, when time is less than 20000 s, simulated temperatures are relatively low with no limitations on oxygen supply. Afterwards the hydrogen release rate is limited by oxygen starvation and blanketing and remained constant. At the end of the transient the primary Zr in major part of hot zone is converted into  $\alpha$ -Zr(O) and total hydrogen release rate decreased. Total hydrogen release reaches in this simulation the value about 11.5 kg .

Axial distribution of simulated external diameter of fuel rods at the instant before quenching and zirconia layer thickness at the same instant correlates one with another. Therefore it can be supposed that 25% of cladding radial increase during ballooning led to subsequent increase in Zr oxidation rate and is one of the reasons of heavy oxidation at these elevations. The comparison of simulation results for different assembly groups shows certain dependence on radial position of the group. Namely, the central group (number 1 in the database list) is simulated with highest temperatures and oxide scale thickness, while these values decrease from the center to the periphery. The latter effect is mainly the consequence of substantial role of radiation transfer inside the cleaning tank.

A current analysis is based on recently developed by NSI RRC KI best-fitted correlations for Zr+1%Nb oxidation, which were obtained from results of several experimental groups. The difference between this kinetic and previously used VNIINM one (so-called Sokolov correlations) falls mainly in the temperature regions  $T > 1500$  °C and  $T < 1300$  °C, where best-fitted correlations predicts higher rate of oxygen mass gain. Here the results, obtained with both sets, are compared for Paks incident scenario. The comparison shows that maximum temperatures in variant simulation are lower and are reached at later instants than in base case.

Generally, simulations of current studies confirmed behaviour of accident scenario with respect to the uncertainties of the models and incident settings, which was outlined as a result of previous investigations.

Further examinations are foreseen (outside of the OECD-IAEA Paks fuel project) with the improved modelling of mechanical properties of Zr+1%Nb alloys. An update of CREEP module of the ICARE2 code with mechanical properties of Zr1%Nb claddings is foreseen in the nearest future with application to Paks incident at the second half of 2007 year. This work will be performed in the frame of technical collaboration between RRC “Kurchatov Institute” and IRSN.

More detailed description of the KI/IRSN analysis is available in Appendix B/XI.

### **3.8 Participant IVS**

Analysis was performed using the integral code ASTEC (Accident Source Term Evaluation Code), version V1.3 rev0.

#### **3.8.1 Code description**

The ASTEC V1 series has been developed jointly by IRSN and GRS since 1998 with the aim to get a fast running code for the simulation of the total sequences of severe accidents in LWR from the initiating event up to the possible fission product release to the environment. The code version V1.3 rev0 was released in December 2006. The integral code ASTEC consists of several modules. Only several of them were used in the analysis of Paks cleaning tank accident:

- CESAR for RCS two-phase thermal hydraulics during the front-end phase and the degradation phase;
- DIVA for core degradation including late phase phenomena (molten pool, corium slump to lower head, corium in lower head) and vessel failure;
- ELSA for release of FP from fuel rods and debris and of materials from control rods, using a semi-empirical approach;
- SOPHAEROS for FP vapour and aerosol transport in RCS;

In typical reactor applications the ASTEC modules are working in coupled mode exchanging the relevant data through common database. The front-end thermal hydraulic phase of the accident is calculated by CESAR module. When the core heat-up takes place, the CESAR thermal hydraulics in the downcomer, lower plenum and core is replaced by DIVA module and only rest of system is henceforth analyzed by CESAR module. Pre-defined basic configuration of the core and lower part of reactor vessel, which represents arrangement of typical PWR, is assumed in DIVA. Typically, the core region is split into arbitrary number of

radial rings and axial layers. The same axial power profile has to be considered in all rings. Contrary to DIVA the CESAR nodalisation is very flexible and thus applicable to “arbitrary” thermal hydraulic systems. All above mentioned points imply certain limitations in modelling of Paks cleaning tank arrangement. The two most important are as follows:

- 1) Uniform axial power profile has to be considered in all fuel assemblies (at least during core heat-up and degradation phase).
- 2) After start of DIVA module (i.e. after start of core heat-up and replacement of CESAR core nodalisation by DIVA nodalisation), it was not possible to model direct by-pass from the lower holes of fuel assemblies to outlet nozzle from cleaning tank.

To cope with this, two successive calculations were performed:

- CESAR stand alone up to start of fuel heat-up (analysis focused on precise modelling of the front-end thermal hydraulics of the cleaning tank);
- All modules in coupled mode since the beginning of the fuel heat-up (450 °C); the original fine CESAR nodalisation was replaced by simplified one and proper inlet/outlet boundary conditions (analysis focused on fuel degradation).

### 3.8.2 Nodalisation scheme

The 30 fuel assemblies were split into 5 groups (6 assemblies in each group) based on their location from the centre of cleaning tank:

1<sup>st</sup> (central) ring: assemblies No. 1 to 6,

2<sup>nd</sup> ring: assemblies No. 7 to 12,

3<sup>rd</sup> ring: assemblies No. 13 to 18,

4<sup>th</sup> ring: assemblies No. 19 to 25,

5<sup>th</sup> (outer) ring: assemblies No. 26 to 30.

The burnup of fuel assemblies within one group was relatively close each to other. The exception was assembly N<sup>o</sup> 12 in 2<sup>nd</sup> group. Average power within each group was proportional to average burnup. This defines radial power distribution in 5 parallel core channels (CESAR) and in 5 core rings, respectively. The total “core” power was 241 kW.

ring No.	1	2	3	4	5
average power of one FA [W]	7159	9006	6694	8837	8719

Table 3.8.1. Radial power distribution (from centre to outer part)

Uniform axial distribution was used for both, CESAR and DIVA modules. This distribution represents an average calculated from all fuel assemblies.

Only simplified approach was used in modelling of fission product release and transport. Generic data were used for initial FP inventory instead of specific and the same inventory was considered in all fuel assemblies. Individual isotopes were not modelled, only elements.

axial mesh	1	2	3	4	5	6	7	8	9	10
relative power	6.372 $10^{-2}$	9.126 $10^{-2}$	1.001 $10^{-1}$	1.151 $10^{-1}$	1.200 $10^{-1}$	1.199 $10^{-1}$	1.159 $10^{-1}$	1.081 $10^{-1}$	9.575 $10^{-2}$	7.028 $10^{-2}$

Table 3.8.2. Axial power distribution (from bottom to top)

### 3.8.2.1 CESAR nodalisation

Main features of CESAR nodalisation are as follows:

- Core (heated volume) represents only part inside fuel shrouds;
- By-pass represents part outside shrouds;
- 5 parallel core channels modelled;
- 14 axial nodes used in total (2 lower, 2 upper and 10 heated nodes containing fuel);
- Lower head with BC (representing inlet from cooling pump) and water inlet to fuel assemblies;
- Upper head – outputs from fuel assemblies and by-pass; degassing line on the top was modelled too;
- 10 horizontal junctions (holes in the shrouds, improperly positioned FA was not considered);
- Heat transfer through shrouds modelled;
- Outlet pipe and pressure BC.

### 3.8.2.2 DIVA nodalisation

- Basic components: Lower plenum, core (5 radial rings, 19 axial meshes – 15 of them heated) and by-pass;
- Urbanic-Heidrick model was used for cladding oxidation;
- DIVA is not able to model forced circulation cooling of lower part of tank (i.e. direct by-pass through lower holes to outlet from tank; “once through” model have to be used instead;
- Because of once-through model, the inlet BC was chosen to keep constant water level ~ 1 m from the bottom of cleaning tank (i.e. applied inlet flow rate was chosen just to compensate water boil off from flooded part of FAs; real inlet flow rate was higher due to direct flow by-pass through the lower holes of FAs to outlet nozzle from cleaning tank. Heat losses from the tank walls were artificially increased to compensate this effect.

### 3.8.3 Main results

Overall system behaviour was reasonably well predicted by ASTEC code. In total 4.68 kg of hydrogen was produced during the analysis. Maximum cladding oxidation in central part of upper, uncovered core region reached 100%. Burst of cladding occurred in all rings except of outermost one. Maximum cladding temperature during the accident was lower than 1400 °C. More detailed description of the IVS analysis is available in Appendix B/XII.

Event	Time [s]
Transition from cleaning to cooling regime (16:40 h. real time)	0
Local saturation in the fuel assembly	~ 9 500
Increase of PRZ water level 7 cm	10 700 – 12 100
Max. cladding temperature 450 °C (start of DIVA module)	14 014
Max. cladding temperature 800 °C	17 872
Failure of the 1 <sup>st</sup> fuel rod due to ballooning	19 311
Start of intense Zr oxidation (production > 2 g/s)	22 000
Failure of the last fuel rod before quenching*	22 019
Max. cladding temperature 1200 °C	24 930
End of analysis	34 410

Table 3.8.3. *Chronology of main events in analysis*

\* the fuel assemblies in outer ring remained intact

### 3.9 Participant VUJE

#### 3.9.1 Description of the input model

The RELAP5/Mod3.2.2 code was used for thermal hydraulic analyses of Paks incident. The code has been developed for the analyses of light water reactor coolant systems during transients and postulated accidents. More detailed code description is listed in Appendix B.

Calculation model of cleaning tank with 30 pieces of fuel assemblies was developed. Nodalisation of the model is shown in Fig. 3.9.1.

The model is composed from interconnected simple volumes. Coolant inflow into tank is realized by connection no.30. Type of this connection is ‘TMDPJUN’. Volume under fuel assemblies is represented by one ‘BRANCH’ type volume ( no.31).

Fuel assemblies are lumped into 6 groups according to [2]. Each group of fuel assemblies is modelled by ‘PIPE’ type component (volumes 1 - 6). These volumes are split in axial direction onto 13 sections. Fuel part of assemblies is divided onto 10 axial sections. These fuel sections are represented by heat structures 1001 - 1006. In each group of fuel assemblies, decay heat and axial profile of decay heat is defined according to [2].

Volume of cleaning tank above fuel assemblies is modelled by single volume no.34. Component no.35, connected into upper part of volume no. 34, represents tank relief valve. This valve opens when tank pressure exceeds 0.25 MPa.

Coolant flows from tank through volume no. 38 (‘PIPE’ type) into ‘TMDPVOL’ component no.40, where the constant pressure is set (boundary condition). Tank heat losses are modelled by heat structures no. 1020 and 1021.

More detailed description of the input model is presented in the Appendix B.

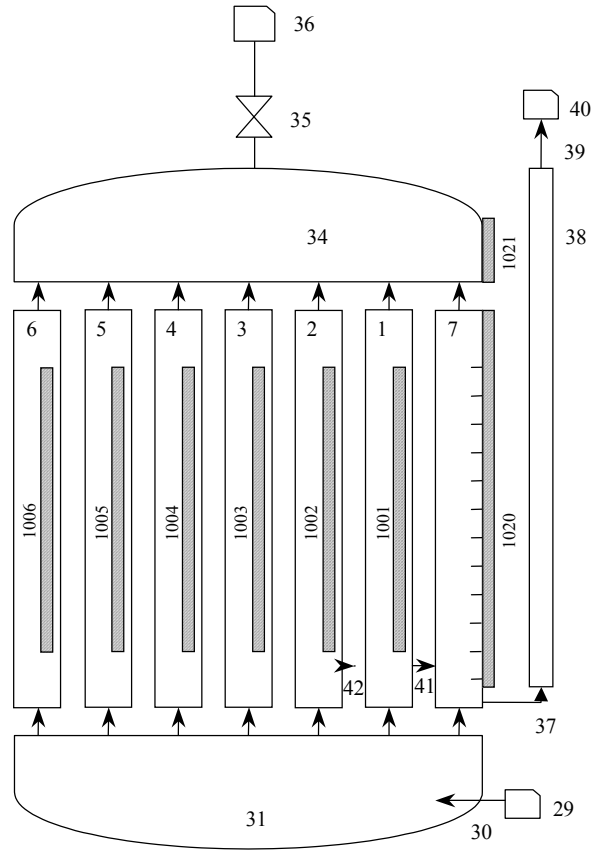


Figure 3.9.1. Nodalisation of cleaning tank

### 3.9.2 Initial and boundary conditions

Initial and boundary conditions for analysed cases were set in order to reach as good agreement with the real conditions during incident as possible.

In this chapter the reference case is showed. Initial and boundary conditions for this case were set as follows:

Parameter	Value
By-pass flow area	120 cm <sup>2</sup>
Decay power of assemblies No. 1 - 6	42.952 kW
Decay power of assemblies No. 7 - 11	45.028 kW
Decay power of assembly No. 12	8.154 kW
Decay power of assemblies No. 13 - 18	40.164 kW
Decay power of assemblies No. 19 - 24	53.021 kW
Decay power of assemblies No. 25 - 30	52.312 kW
Total decay power	241.7 kW
Initial coolant temperature in container	56 °C

Initial container pressure	0.23 MPa
External pool temperature	30 °C
Temperature of inlet coolant	30 °C
Inlet mass flow	21 t/h

Table 3.9.1. Main parameters of the VUJE calculation

Axial profile of decay heat distribution for each assembly group was defined according to [2]. Graphical form of axial profile of decay heat distribution is presented in Appendix B/XIII.

### 3.9.3 Description of results

Process analysis begins at the moment of start of the intermediate cooling with coolant mass flow through tank of 21 t/h. Due to the lower flow rate of the intermediate cooling pump, the by-pass flow through the perforations in the assembly shroud and at the bottom of incorrectly seated assemblies became much more significant, than it was during the cleaning operation with high flow rate. Up to 90 % of water added into cleaning tank flows through these perforations and through the by-pass. Cooling of fuel assemblies is not sufficient and heating up of the water leads to saturation state at the top of the cleaning tank at the 4500 s.

Event	Time [s]
Start of cooling mode (mass flow 21 t/h)	0
Saturation temperature in the cleaning tank	4500
Start of water level drop in the cleaning tank	7260
Air letdown valve opening	9440
Maximum cladding temperature exceeds 800°C	13900
Start of intensive Zr oxidation	16400
Maximum cladding temperature exceeds 1200°C	20600
Maximum cladding temperature (1470 °C in assembly no.12)	29700
End of calculation	36000

Table 3.9.2 Chronological sequence of important events

Water level in tank begins to decrease after 2 hours since start of intermediate cooling regime. Water level is stabilised at level 1.8 m from lower plate. This decreased water level leads to the temperature increase of the fuel assemblies. Due to its highest and peaked axial decay heat profile, maximum cladding temperature 1470 °C is found in assembly 12 at time 29700 s. The air letdown valve opens at 9440 s, when tank pressure exceeds 0.25 MPa. Flow rate through this valve is approximately 5 g/s.

Chronological sequence of important events is presented in Table 3.9.2. The results in graphical form are presented in Appendix B/XIII.

### References to Chapter 3.9

- [1] RELAP5/MOD3.2.2 Manuals, NUREG/CR-5535-Vol. I.-VII.

- [2] E. Szabó, Z. Hózer, Database for the OECD-IAEA Paks Fuel project, AEKI-FRL-2006-408-01/02-M2, Budapest, September 2006

### **3.10 Participant USNRC**

This summary report describes the analysis of the Paks event using the MELCOR severe accident analysis code. The Paks event was a fuel degradation accident in a cleaning tank in the spent fuel pool of the reactor at the Hungarian Paks Nuclear Power Station. In the event, 30 assemblies in the cleaning tank overheated due to inadequate heat removal.

#### **3.10.1 Code description**

A MELCOR model was developed to represent the inner cleaning tank, the outer tank, the 30 assemblies within the tank, and the surrounding pool. The specified boundary conditions for the model included the tank inlet flow rate, the assembly decay heat, the hydrostatic pressure at the tank exit and degassing line, and the operation of the hydraulic lid locking system of cleaning tank. It was assumed that a 0.01 m<sup>2</sup> leakage hole opened at 9.5 hours when the tank lid was unlocked. Some of the inlet flow leaked around misaligned assemblies at the base plate of the inner tank (i.e., FL-101) and by-passed the fuel assemblies. The leakage area was specified to be 120 cm<sup>2</sup> as agreed at the second workshop. The leakage was due to incorrect seating of the assemblies into the lower support plate. The perforations at the top and bottom of the shroud of the standard assemblies were also modelled as leakage paths.

At the top of the inner tank, there was a 10 mm OD degassing line. In normal operation, the degassing line is full of water. It was assumed that water within the degassing line precluded vapour flow until the inner tank steam bubble was established and the tank was starting to pressurize. From the Paks database, the degassing line resistance corresponded to a length of 15 m and its elevation change was 13.1 m. The MELCOR model was subdivided into 5 rings to represent the 30 assemblies.

The MELCOR CORSOR-Booth fission product release model was used and the volatile specie release coefficients were modified to match measurements from recent French experiments. The vapour pressure, compound form, and initial inventory default inputs were modified to represent Cs<sub>2</sub>MoO<sub>4</sub> and CsI as the dominant compounds for the cesium and iodine releases. The initial fission product inventory in the gap between the fuel and cladding was estimated to be <0.1%, based on the calculated released fission product gas.

#### **3.10.2 Thermal hydraulic Response**

The accident simulation was started when the system was configured to a single submersible pump (i.e., the conditions at 4:40 pm on April 10, 2003) and was terminated 0.5 hours after the tank lid was unlocked, which flooded the tank (i.e., 10 hours). The inlet flow to the cleaning tank was initially 5.69 kg/s and 30°C. From the previous operation, the water temperature in the tank was 57°C (330 K).

Following the shift to the low-flow submersible pump and the storage pool as the water source, relatively cold water (30°C) was introduced into the initially warm tank (57°C). 65% (i.e., the initial maximum) of the cold water flowed upward into the assemblies and was approximately evenly distributed across the 30 assemblies. The calculation assumed that some of the water leaked through the gap between baseplate holes and the assemblies (initially ~25% of the tank inlet flow) and some leaked through the perforations on the

standard assembly inlet nozzles (initially ~10% of the tank inlet flow). The cold water cooled the bottom of the assemblies and increased the hydrostatic pressure drop through those pathways relative to the leakage pathways. Hence, the calculated leakage flow across the baseplate and through the standard assembly perforations steadily increased while the assembly flow decreased. As the accident progressed, the calculated assembly flow dropped to 12% of the inlet flow by 1.7 hours while the leakage flow increased to 88% (52% across the baseplate and 36% through the perforations in the standard assemblies).

As a result of the flow reduction into the assemblies, the calculated fluid temperature at the upper portion of the assemblies steadily increased towards saturation conditions. At 1.97 hours into the simulation, the water at the exit of Assembly 12 started to boil. By 2.44 hours, all the assemblies were boiling. As steam exited the assemblies, it created a steam bubble, which filled the top of the tank and depressed the water level in the tank and in the assemblies. One of the few measurements available during the accident was the primary circuit pressurizer level, which was hydraulically connected to the storage pool with the cleaning tank. At 2.6 hours into the accident (7:20 pm on April 10, 2003), the pressurizer tank showed a 70 mm water level increase (i.e., an undiagnosed indication of water displacement from the cleaning tank). The timing of the calculated drop in the cleaning tank water level closely corresponded to the measured increase in the pressurizer tank level.

The calculated level response shows an initial level depression to 1.2 m followed by a recovery to 1.4 m (i.e., measured from the bottom plate). Although the rate of steam production exceeded the degassing flow, condensation of steam against the relatively cool inner tank wall reversed the level trend. After 3.2 hours, non-condensable hydrogen from the zirconium-steam oxidation reaction started to replace steam in the upper tank. The water level remained at 1.4 m until 9.5 hours when the hydraulic latch on the lid was opened.

At a water level of 1.4 m, the top 60% of the fuel was uncovered. The steam flow due to boiling below the 1.4 m water level was inadequate to cool the fuel. The top portions of all the assemblies heated from 2.5 hours to 9.5 hours. Due to thermal radiative heat transfer, there was a temperature gradient from the assemblies closest to the inner tank wall (#19 -#30) versus the assemblies at the center of the tank (#1 - #6). The peak temperatures of the assemblies in the middle ring (#7 through #18) lied between the inner and outer rings of fuel assemblies.

The peak cladding temperature was calculated to be 1743 K, which occurred in Ring 1 (Assemblies 1 through 6) just prior to the tank reflood. The corresponding peak temperatures calculated for Rings 2 through 5 were 1540 K, 1672 K, 1667 K, and 1403 K, respectively. The temperature response of the fuel was a complex function of the magnitude of the decay heat and oxidation powers, the axial power profile, the magnitude of steam generation below the water level in each assembly to drive oxidation, the radiative exchange to surrounding assemblies or the tank wall, and the convective heat removal rate. The radiative heat losses to the tank wall had a significant impact of the peak temperatures. For example, the heat losses to the tank wall exceeded the decay power of the assemblies in Ring 5 after 6.1 hr. However, the fuel temperatures in Ring 5 continued to increase due to radiative heating from the assemblies in the inner rings. Because the assemblies in Ring 1 were the furthest from the tank wall, they reached the highest temperature. In the middle ring of assemblies, Rings 3 and 4 had higher decay heat power in the region above the water level and therefore reached a higher temperature than the assemblies in Ring 2. Although Ring 3 (Assembly 12) had the highest decay power above the water level and initially heated the fastest, radiative exchange

to the surrounding assemblies and low steam production below the water level (i.e., for continued oxidation) limited its peak temperature to below Ring 1.

### ***3.10.3 Fission Product Release***

The first failure of the fuel cladding and release of the gap fission products was calculated to occur at 4.0 hr in Assembly 12. The other rods subsequently failed from 4.2 hr to 4.9 hr. The thermally driven fission product releases continued following the rod failures in each group of assemblies. After about 6 hr, the release increased more rapidly. Approximately half of the volatile xenon, cesium, and iodine releases occurred in the last 1.5 hours (i.e., between 8 hr to 9.5 hr).

The calculated releases were 1.1% of the noble gases, 1.1% of the cesium, 0.8% of the iodine, 0.02% of the barium, and 0.03% of the cerium and lanthanum. The data from the measurements of 8 representative nuclides were integrated for the following time periods after the accident: 1 day, 3 days, 7 days, 14 days, and 2 years. In general, the comparisons of the MELCOR results to the 14-day integrated tank measurements were relatively good. The temperature profile from the inner assemblies to the outer assemblies meant the calculated fission product releases were higher in Ring 1 versus Ring 5. The overall calculated and measured results show that approximately 1% of the volatile inventory (i.e., the noble gases, cesium, and iodine) was released during the high temperature portion of the accident, which is in good agreement with the 14-day data. The measured time-evolving release of some nuclides raises some uncertainty in the comparison of MELCOR to some nuclides (i.e., what is attributed to the delayed transport from the tank from the high temperature accident versus continued low-temperature dissolution release). The comparison of the calculated and 14-day barium release data suggests higher releases than calculated. The cerium and lanthanum release models had good agreement with the 14-day integrated data.

More detailed description of the USNRC analysis is available in Appendix B/XIV.

Event	Calculated Timing	Measured or Estimated Timing	
Assembly 12 reaches saturation near the assembly outlet	1.72 hours	n/a	
Water level starts to drop in the cleaning tank	2.36 hours	2.33 - 2.66 hours	
Water level stops decreasing	2.67 hours		
Peak cladding temperature exceeds 800°C	3.69 hours	n/a	
Hydrogen production >2.5 g/s	4.8 hours		
Zr oxidation shows signs of steam limiting	>4.8 hours		
First fuel rod failures (Assembly 12)	4.00 hours		
Second fuel rod failures (Assemblies 13-18)	4.17 hours	5.22 hours (9:53 pm) (First rad. alarm)	
Third rod failures (Assemblies 1-6)	4.31 hours		
Fourth rod failures (Assemblies 7-11)	4.39 hours		
Last fuel rod failures (Assemblies 19-30)	4.94 hours		
Gap + thermal noble gas release is >0.1%	4.94 hours		← Note A
Hydrogen production >3 g/s	5.10 hours		n/a
Peak cladding temperature exceeds 1200°C	5.23 hours		
Start of quench	9.50 hours	9.50 hours	

Table 3.10.1. Chronology of Main Events

Notes:

- A. The gap releases in the calculation were assumed to be small (<0.1%) based on fuel behaviour calculations in the Paks database. The calculated releases did not exceed 0.1% of the initial inventory until 4.94 hours, which is in better agreement with the timing of the first alarm measurement than the first gap release.

#### 4 COMPARISON OF CALCULATED RESULTS

The results of the calculations were provided by eleven organisations from eight countries for this final report. Some organisations carried out all three types of calculations (thermal hydraulics, fuel behaviour and activity release), while other organisations focused their work on one or two selected calculation type.

The name of analysts, the codes and the type of performed calculations are summarised in Table 4.1.

Country Organization	Analyst	Code	Calculations		
			Thermal hydraulics	Fuel behaviour	Activity release
Belgium TRACTEBEL	Jarne Verpoorten	MELCOR 1.8.5	+	+	+
Finland VTT	Pasi Junninen	APROS	+		
	Kari Pietarinen	FRAPCON-3 FRAPTRAN		+	
Germany GRS	Klaus Trambauer	ATHLET-CD	+	+	+
Hungary AEKI	László Pernecky	RELAP 5 mod 3.3	+		
	István Trosztel	ATHLET	+		
	Attila Molnár	FRAP-T6		+	
	Emese Szabó	EU LOCA model			+
Hungary BME NTI	Gábor Légrádi	CFX	+		
Hungary VEIKI	Gábor L. Horváth	MELCOR 1.8.5	+	+	+
Russian Federation/ France KI/IRSN	Yuri Zvonarev	ICARE2 V3.2 / CATHARE2 V1.3L_1	+	+	
Slovak Republic IVS	Peter Matejovic	ASTEC	+	+	
Slovak Republic VUJE	Martin Fogel	RELAP 5	+		
United States of America US NRC	Kenneth Charles Wagner	MELCOR	+	+	+

Table 4.1. Summary of performed calculations

The calculated time of the main events as provided by the participants are summarised in Tables 4.2 and 4.3. Participant BME NTI is not listed in the tables, for their calculation

covered the initial single-phase period of the event and the analysis did not reach saturation in the cleaning tank that was the first event requested to report. Plots of selected parameters are shown in chapter 4.4.

	TRAC-TEBEL	VTT	GRS	AEKI.1	AEKI.2
saturation in the cleaning tank (s)	8520	7260	7060	2830	5400
water level drop in the cleaning tank (s)	8520	8400	8640	10560	8000
maximum cladding temperature exceeds 800°C (s)	16250	13800	14690	15800	
maximum cladding temperature exceeds 1200°C (s)	20110	18780	21240	17720	
start of intense Zr oxidation (s)	16610	14820	15840	17000	
failure of the first fuel rod due to ballooning (s)	-	16440	16036	18850	
failure of the last fuel rod before quenching (s)	-	18300	19842	20010	
maximum cladding temperature (°C)	1400	1628	1381	1152	
total Zr oxidation (%)	12	46.7*	4.6	4.1	
final hydrogen production (kg)	13	15.1	4.63	3	

Table 4.2. Calculated time of main events and some integral parameters by participants SUEZ - TRACTEBEL ENGINEERING, VTT, GRS and AEKI

AEKI.1 and AEKI.2 correspond to thermal hydraulic calculations by RELAP and ATHLET codes respectively.

\*Only the zirconium of rod cladding was considered in VTT calculations.

	VEIKI	KI/IRSN	IVS	VUJE	USNRC
saturation in the cleaning tank (s)	5600	7200	9500	4500	6192
water level drop in the cleaning tank (s)	9600	9600	12100	7260	9612
maximum cladding temperature exceeds 800°C (s)	17500	14360	17872	13900	13284
maximum cladding temperature exceeds 1200°C (s)	18688	19700	24930	20600	18828
start of intense Zr oxidation (s)	17804	18000	22000	16400	17280
failure of the first fuel rod due to ballooning (s)	17977	16700	19311	-	14400
failure of the last fuel rod before quenching (s)	21030	17200	22019	-	17784
maximum cladding temperature (°C)	1895	1471	1350	1440	1470
total Zr oxidation (%)	-	12.6	10.9	-	11.0
final hydrogen production (kg)	-	11.5	4.68	-	7.79

Table 4.3. Calculated time of main events and some integral parameters by participants VEIKI, KI/IRSN, IVS, VUJE, USNRC

## 4.1 Thermal hydraulics

In the first part of the incident – until a fairly stable steam volume in the upper part of the cleaning tank is formed – the course of the incident is determined by thermal hydraulic effects. The main thermal hydraulic phenomena in this period are the following:

- Distribution of the tank inlet flow rate among the fuel assemblies, shroud perforations and by-pass due to incorrectly seated assemblies.
- Change in the above flow distributions with heat-up of the coolant inside the assemblies and in the down-flow part of the cleaning tank.
- Steam formation in the upper sections of the assemblies and its accumulation in the tank upper head.
- Flow stagnation in the fuel assemblies and decrease of the tank level.
- Stabilization of the tank level.

A large variety of codes has been used by the 11 participants. MELCOR and RELAP5 were the most widely used ones: with 3 and 2 participants, respectively. One user evaluated the thermal hydraulic part with the ATHLET and APROS code, respectively, and the CFX CFD code was also applied for the first part of the incident. All other users applied tools with severe accident capabilities: ATHLET-CD, ICARE/CATHARE, ASTEC.

The modelling approach applied by the participants differed in the number of groups the 30 fuel assemblies were distributed to. The most widely used grouping consisted of 5 or 6 groups, based on type (working or follower) and on similar power of the assemblies, but 4, 3 and 1 groups were also applied by GRS, Suez - Tractebel Engineering and AEKI in its RELAP5 analysis, respectively. The draw-back – especially of the two last calculations – is that the difference in the inlet flow rate of working and follower assemblies cannot be captured, but the overall behaviour in the first phase can be fairly well predicted even by these simple models, since the flow rates in the heated part of the different assemblies are very similar.

Most of the participants divided the heated part of the fuel channels to about 20 axial nodes: in an earlier parametric study performed by the ATHLET code it was demonstrated that this is sufficient for convergence. In some cases only 10 axial nodes were applied that might impact the accuracy of the results.

In order to assess the thermal hydraulic phenomena listed above Figs. 4.1 to 4.14 are of interest from the comparison plots.

The coolant outlet flow rate from the tank is shown in Fig. 4.1. As it can be expected, in the first period, until steam formation, it corresponds to the inlet flow rate that was used as a boundary condition in the analyses. The flow rate increase due to substantial steam formation around 8000-10000 s is shown by all calculations.

The tank outlet temperature (Fig. 4.2) varies in the early phase between 35 and 40 °C – the value depends on the amount of by-pass flow calculated by the different participants. The only exception is one calculation, which applied an inlet temperature of 60°C. Again, the effect of steam production is visible in each of the results, although the resulting temperature peak differs strongly.

The initial system pressure (Fig. 4.3) shows large variation, which is due to the different approach chosen in the calculations to impose this boundary condition. All analyses show pressure increase, when steam is produced in the tank that must be related to the increased pressure drop between the highest point of the tank outlet tube (where most calculations used a pressure boundary condition) and the tank upper plenum due to the increased flow rate in two-phase conditions.

Figures 4.5 and 4.6 display the outlet temperatures of assemblies 1-6 and 12, respectively, i.e. those of working and follower assemblies. The figures show considerable differences among the participants during the heat-up phase to saturation, which can be explained mainly by the fact that the flow rates along the heated parts are rather different. (To some extent differences in assembly group powers and fuel heat capacities may be the cause as well.)

Figure 4.11 shows that there is a factor 3 difference among the calculated inlet flow rates to the follower assembly, but all the calculations predict correctly the decreasing trend of the flow rate during the subcooled period, which is the result of the continuously changing elevation head balance between the regions inside and outside the assemblies. Similar differences can be seen at the inlet of the working assemblies, as shown by Figs. 4.8 and 4.9, although neglecting the two extreme results, the flow rates are closer. Most of the flow rate entering the working assemblies exits via the shroud perforations at the bottom, as shown by Figs. 4.13 and 4.14. Here again, the tendency of all the calculations is correct, indicating an increased loss of the coolant via the perforations with time. An important amount of the inlet flow to the cleaning tank passes through the assumed by-pass due to incorrect seating, as evidenced by Fig. 4.12. The trend here is similar to that of the perforation, i.e. the flow rate by-passing the assemblies is increasing with time. It is interesting to note that there is a sort of compensation between these two by-pass flows: when in a given calculation the perforation flow rate is low, the baseplate by-pass is high.

For the differences in the calculated flow rates the following reasons can be suspected: different by-pass areas and loss-coefficients used by the participants, but also the models of friction losses in the laminar-turbulent transition region may be responsible. In spite of the relatively large differences in different flow rates it can be said that – in view of the very delicate balance between elevation head losses and laminar flow friction losses – the range of the results is acceptable.

Tables 4.2 and 4.3 summarize the times to saturation in the different calculations: the dispersion is rather important, ranging from 2830 to 9500 s, even if most of the cases put it around 7000 s. It should be mentioned that most flow rates, but especially those through the heated part (Fig. 4.9) show strong oscillation when saturation conditions are reached at the fuel assembly outlet.

The calculated levels of the cleaning tank are compared in Fig. 4.4 and in Tables 4.2 and 4.3. These indicate that the analyses predict the level decrease due to steam accumulation in the upper head with an uncertainty range of 5000 s, although most of the calculations predict it between 8000 and 10000 s.

## **4.2 Fuel behaviour**

Fuel behaviour calculations have been carried out with the MELCOR, ICARE2, ATHLET-CD, ASTEC, FRAPTRAN and FRAP-T6 codes. The initial state of the fuel rods at the

beginning of the incident was defined using the results of TRANSURANUS and FRAPCON-3 analyses.

After the formation of steam volume and low water level in the cleaning tank the fuel rod temperatures started rapid increase. The initial heat-up rate in the dry phase was similar in most of the calculations (about 0,1 °C/s). In 2-3 hours after the beginning of dry phase the maximum fuel temperatures in most of the calculations reached 1000 °C. The further increase of temperature was much slower (Figs. 4.19, 4.20 and 4.21). There were two typical temperature histories for the high temperature phase (above 1000 °C) of the event:

- Some calculations produced a temperature plateau and the maximum temperature seemed to converge to a given value. Obviously in these analyses some kind of equilibrium was reached between the internal heat sources (decay heat and heat zirconium oxidation) and heat removal from the cleaning tank (losses to the surrounding water as shown in Fig. 4.16, coolant circulation by the pump, gas and steam release through the air letdown valve).
- Some other calculations indicated peak in the temperature histories and showed decreasing values in the last phase of the incident. The peak values can be associated with the period of very intense zirconium oxidation.

The calculated cladding temperatures were close to the fuel temperatures, for the thermal power in the rods two weeks after reactor shutdown was very low: the average linear power was 0.26 W/cm. The maximum cladding temperatures reached 800 °C between 14000-18000 s and 1200 °C between 19000-25000 s. The typical value of maximum cladding temperature was between 1200-1400 °C, but some calculations showed even higher temperatures close to the melting point of zirconium (Figs. 4.22, 4.23 and 4.24).

The maximum cladding temperatures were received not for the same fuel assemblies by different participants. Basically two cases can be identified for the location of maximum temperature: the fuel assemblies with maximum power or fuel assemblies in the centre of the cleaning tank. It can be explained by the following considerations:

- The power of fuel assemblies was not the same but varied between 7 and 9 kW. Furthermore there were significant differences between the axial power distributions, since the normal working assemblies had cosine shaped profile and the follower assemblies had local peak in the upper section of the fuel rods. The nodalisation schemes developed by the participants included different groups of assemblies with different powers and power profiles.
- Some numerical models represented the fuel assemblies in form of parallel channels without any connections between them. Some other calculations specified thermal connections between the channels or used a ring structure for the simulation of the position of fuel rods.

The calculated axial profile of temperature distribution in the fuel rods was also influenced by the above factors. In most of the calculations the maximum temperature was reached in the upper-middle part of the rods. The bottom part of the rods had cladding temperature close to the temperature of cooling water. The shape of the temperature profile usually was similar to the power profile applied in the modelling of the given group of fuels rods. Comparing the temperature profiles at the moment when 800 °C cladding temperature was reached large

differences (200-300 °C) can be found e.g. for the central fuel assemblies that can be explained by the applied radial profiles (Figs. 4.17 and 4.18).

The fuel rod internal pressure showed increasing trend until the burst of fuel rods (Figs. 4.24). Some calculations captured well the short period when the intense plastic deformation resulted in pressure increase before the cladding integrity was lost. The failure of the first fuel rod was indicated by the participants between 14000 and 19000 s. It is in very good agreement with the observation of first noble gas activity release that was detected at 18600 s (21.50 real time) during the Paks-2 incident. The calculations confirmed that the first activity release from the cleaning tank was the result of plastic deformation and burst of fuel rods.

The fuel rod internal pressure at the moment of burst was typically between 12 and 20 bars. The simulation of cladding plastic deformation was carried out with Zircaloy-4 models by some participants and with VVER specific (E110 cladding) correlations by other participants. However the most significant effect on the calculated failure pressure had the initial pressure of the fuel rods (Figs. 4.24).

The ballooning and burst of fuel rods continued after the failure of the first rod. Most of the calculations indicated the failure of all fuel rods in the 30 assembly. The last rods failed usually within one hour after the burst of first rod (Tables 4.2 and 4.3). According to the results of some calculations several fuel rods remained intact until the opening of the cleaning tank. The calculated fuel rod external diameters (Fig. 4.29) indicated that the neighbour rods could touch each other and it could significantly reduce the flow area in the assembly. The deformation in some cases was overestimated, since the single rod models were not able to take into account the effect of neighbour rods on the maximum deformation.

The intense zirconium oxidation started at about 15000 s in most of the calculations (Tables 4.2 and 4.3). The simulation of zirconium oxidation in several calculations covered not only the fuel rod cladding, but the shroud of the assemblies as well. The maximum cladding oxidation at the end of the incident reached 100 % in one calculation and varied between 10-80 % in the other analyses (Fig. 4.25). The calculated shroud oxidation was between 20-90 % (Fig. 4.26). The profile of oxide layer thickness showed maximum in the upper-middle part of the rods, the typical value was between 100-600  $\mu\text{m}$  (Figs. 4.30 and 4.31). The typical value of total oxidation of zirconium components at the end of calculation was between 4-12% (Fig. 4.27). Only one calculation showed considerably higher (47 %) oxidation value. The corresponding mass of produced hydrogen was between 3 and 15 kg (Tables 4.2 and 4.3). The average value of hydrogen production was less than one g/s (Fig. 4.28). The large scatter in the calculated degree of zirconium oxidation can be explained by several factors:

- The temperature histories (Figs. 4.21, 4.22 and 4.23) and temperature profiles (Figs. 4.17 and 4.18) had obviously very important effect on the oxidation process. However it must be mentioned that the maximum temperatures and maximum degree of oxidation were produced in different calculations.
- The oxidation process was influenced by the availability of steam. Since the release of produced hydrogen was limited through air letdown valve (Fig. 4.15), the accumulation of hydrogen in the cleaning tank could reduce the access of steam to zirconium surface and suppress the oxidation process.
- The calculation of oxidation kinetics was carried out with different correlations. Models with conservative correlations (e.g. Baker-Just) produced much more

oxidation than some other models with realistic VVER specific models (e.g. AEKI correlation).

- In some calculations only the oxidation of cladding was taken into account and the oxidation of Zr shroud was not considered.

The quenching of hot fuel rods was simulated only by one calculation. Quenching did not lead to temperature or hydrogen production peaks in the calculations (Figs. 4.21, 4.22 and 4.23), because the zirconium surfaces were heavily oxidised in the dry period of the incident and because the temperature of cladding and shrouds were too low for melt formation and subsequent strong escalation.

The opening of the cleaning tank at the end of the incident was simulated only from thermal point of view. The applied codes did not have detailed models for the simulation of the fragmentation of fuel assemblies due to thermal and mechanical stresses. The hydrogen uptake of zirconium probably played very important role in the embrittlement of fuel assemblies, but the hydrogen uptake and its effect on the mechanical strength of cladding can not be simulated by the currently available fuel behaviour codes.

### 4.3 Activity release

Activity release simulations have been carried out with the MELCOR and ATHLET-CD codes and one series of hand calculations was performed using the EU model for calculating the releases and consequences of a large LOCA model.

Most of the calculations produced data not for isotopes, but for elements or groups of elements. The calculated release rates in those cases were multiplied by the isotope inventory of 30 assemblies to receive the requested activity release values.

The beginning of activity release from the fuel rods corresponded to the first fuel failures due to ballooning and burst. The good capture of timing of fuel failure was already discussed in chapter 4.2. The further activity release was related to the increase of number of failed fuel and to the increase of fuel temperatures.

The main observation for some important elements can be summarised as follows:

- Noble gas release calculations were compared to activity measurements in the chimney of the reactor hall. The transport time between the cleaning tank and the chimney can be estimated as less than one hour considering the ventilation system of the reactor hall. Some calculations were close to the measured values, but there were calculations showing much higher release from the fuel, too. The estimated relative release from measured data was 1.19% for  $^{133}\text{Xe}$  (Fig. 4.32).
- Iodine release was generally slightly underestimated by the calculations. However the values were close to the measured value that was 1.41 % for  $^{131}\text{I}$  isotope. The measured value was determined from coolant activity measurements considering the first two weeks after the incident. Two calculations produced data with about one order above and below the measured relative release (Fig. 4.33).
- Cesium release was slightly overestimated by all calculations (Fig. 4.34). The measured values were 0.74 % and 0.53 % for  $^{134}\text{Cs}$  and  $^{137}\text{Cs}$  isotopes, respectively.

- Tellurium ( $^{132}\text{Te}$ , Fig. 4.35) and cerium ( $^{141}\text{Ce}$ , Fig. 4.36) releases were well reproduced by some of the participants. The release of actinides ( $^{242}\text{Cm}$ ) was overestimated by all calculations (Fig. 4.37).

The scope of activity release calculations was limited to the release from fuel and did not include the transport of radioactive isotopes in the spent fuel storage pool or in the reactor hall.

#### 4.4 Plots of selected parameters

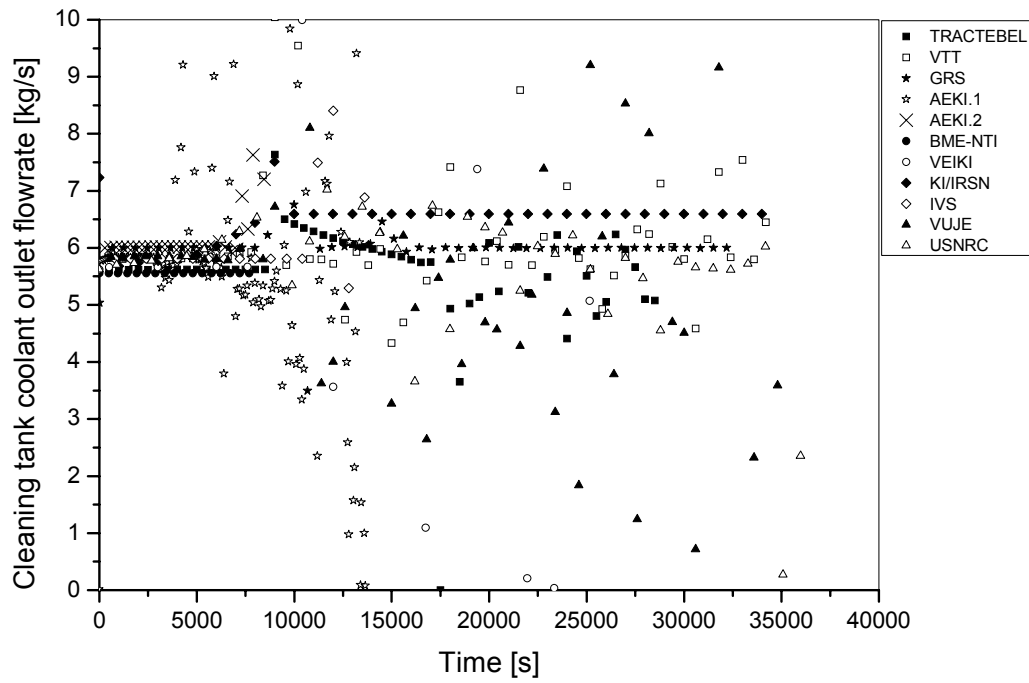


Figure 4.1. Cleaning tank coolant outlet flowrate

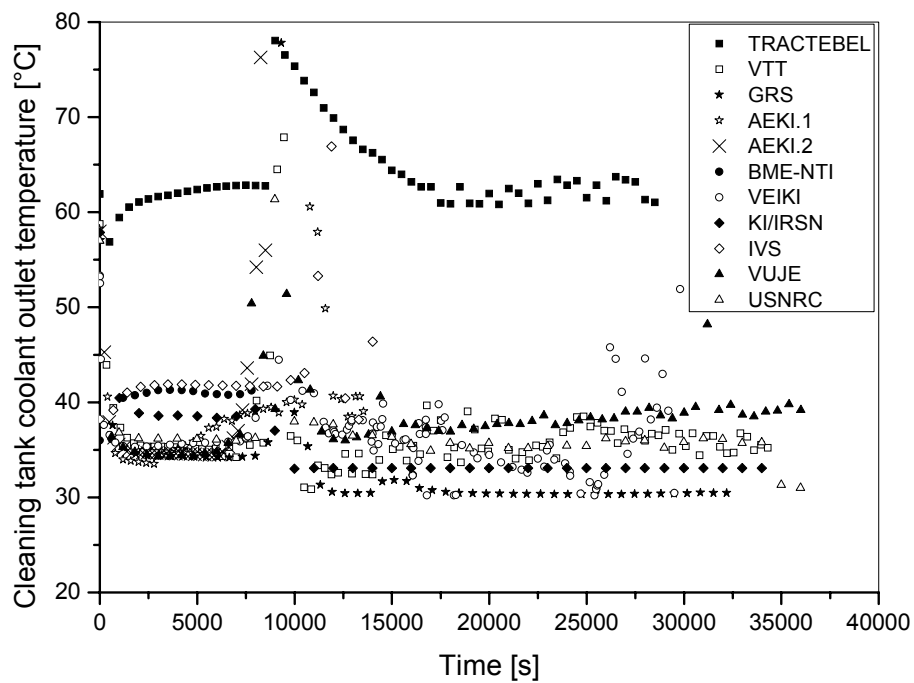


Figure 4.2. Cleaning tank coolant outlet temperature

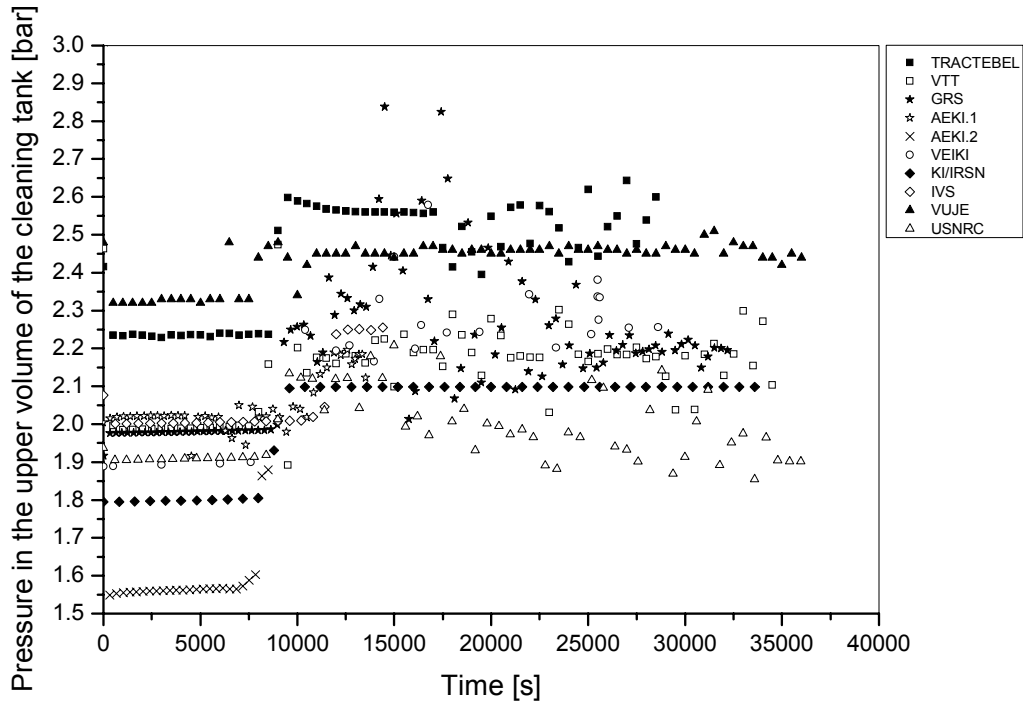


Figure 4.3. Pressure in the upper volume of the cleaning tank

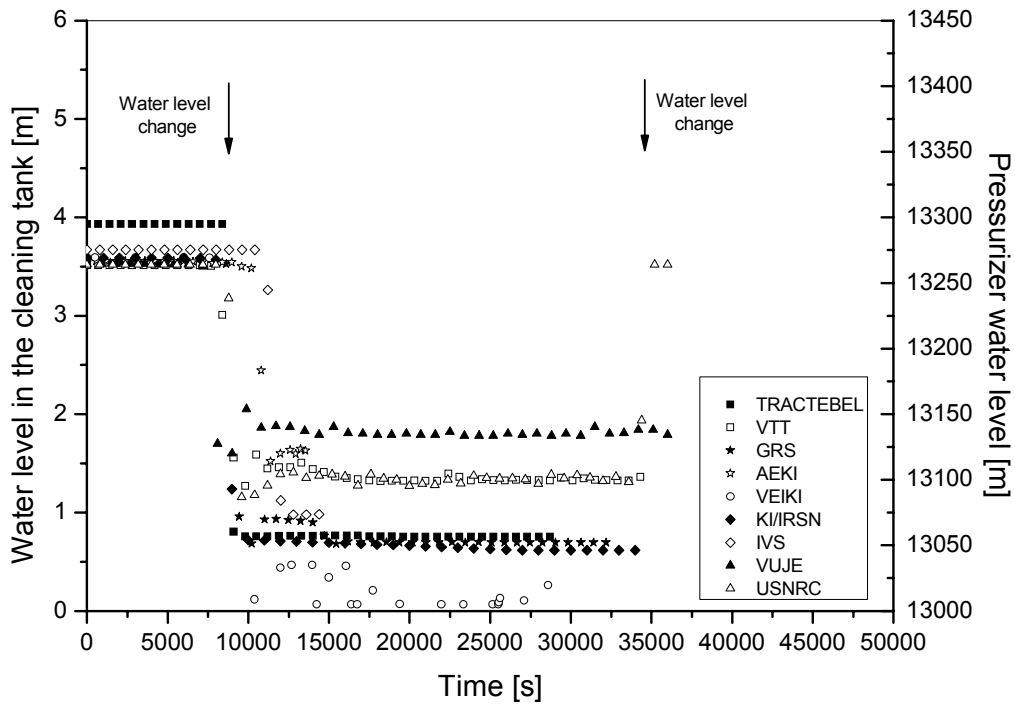


Figure 4.4. Water level in the cleaning tank

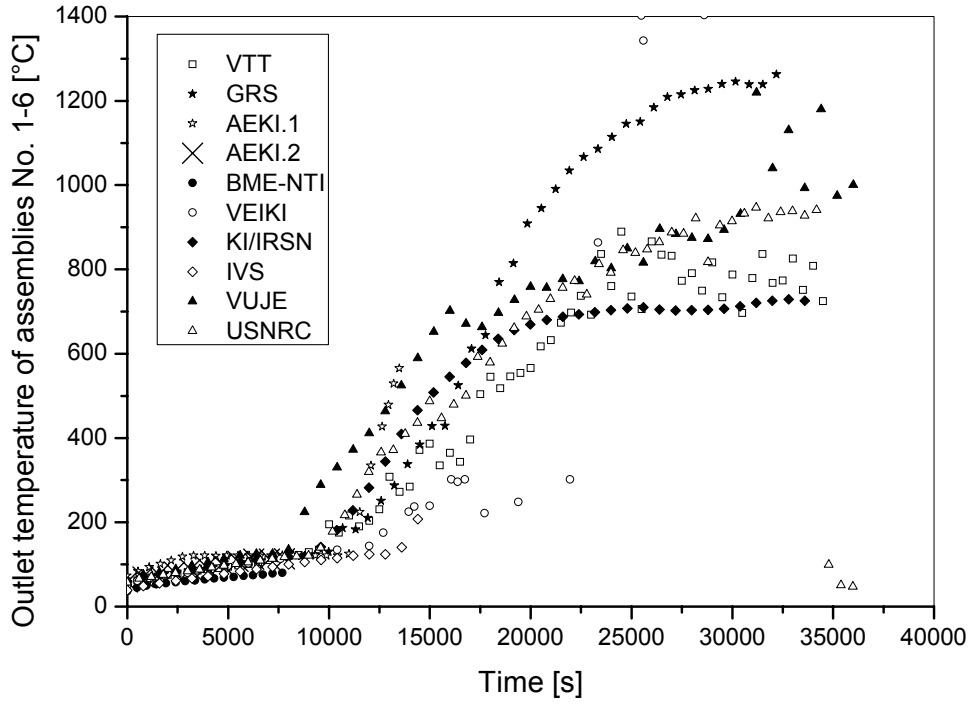


Figure 4.5. Outlet temperature of assemblies No. 1-6

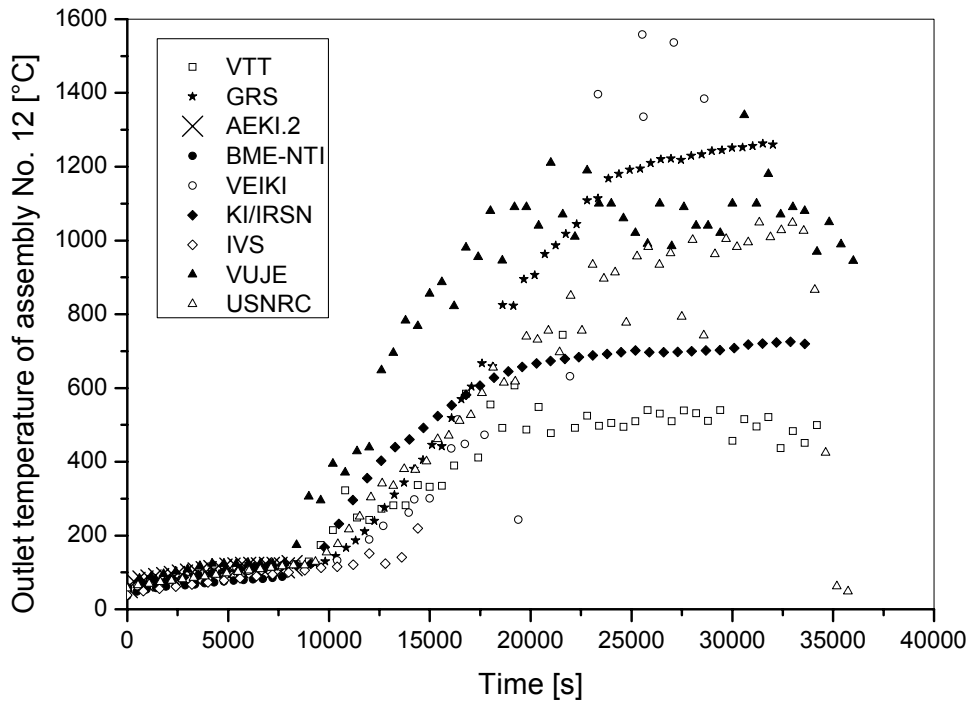


Figure 4.6. Outlet temperature of assembly No. 12

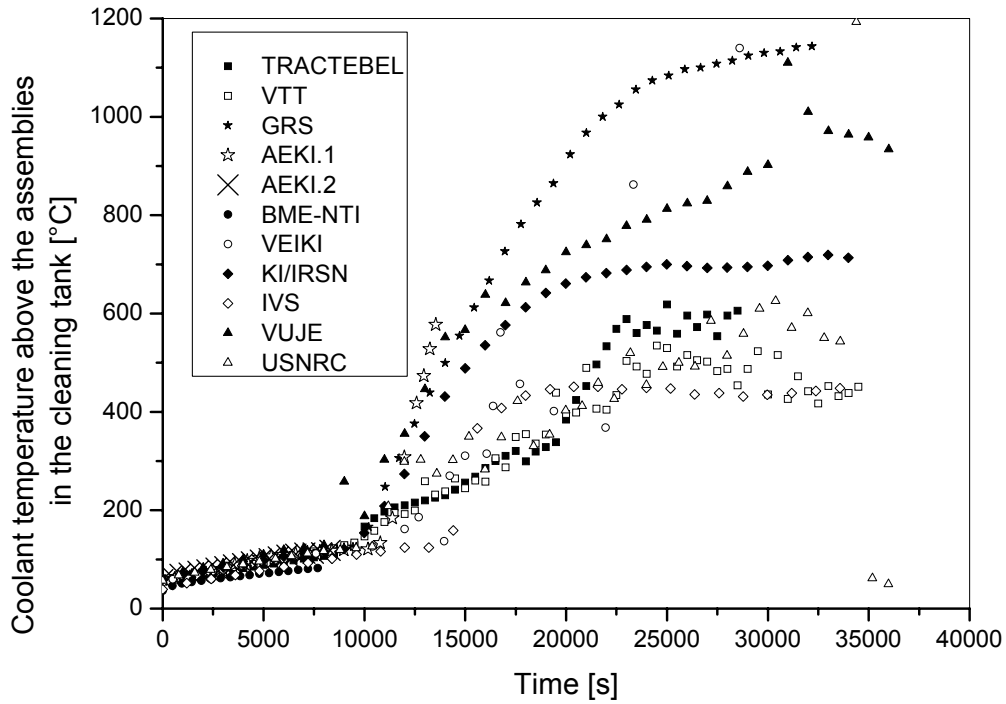


Figure 4.7. Coolant temperature above the assemblies in the cleaning tank

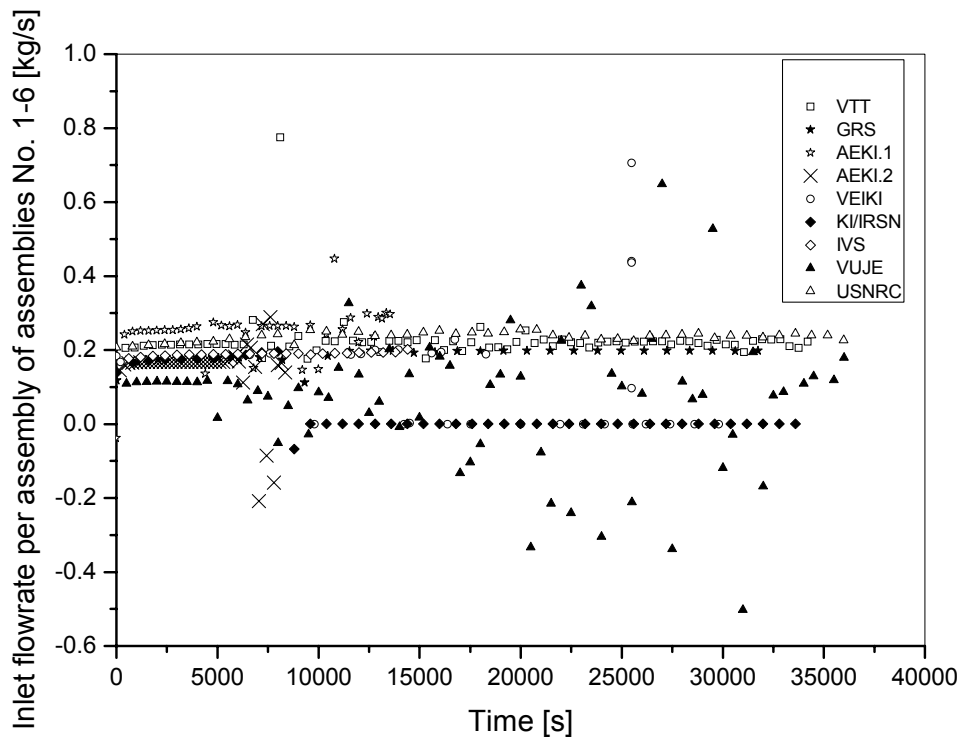


Figure 4.8. Inlet flowrate per assembly of assemblies No. 1-6

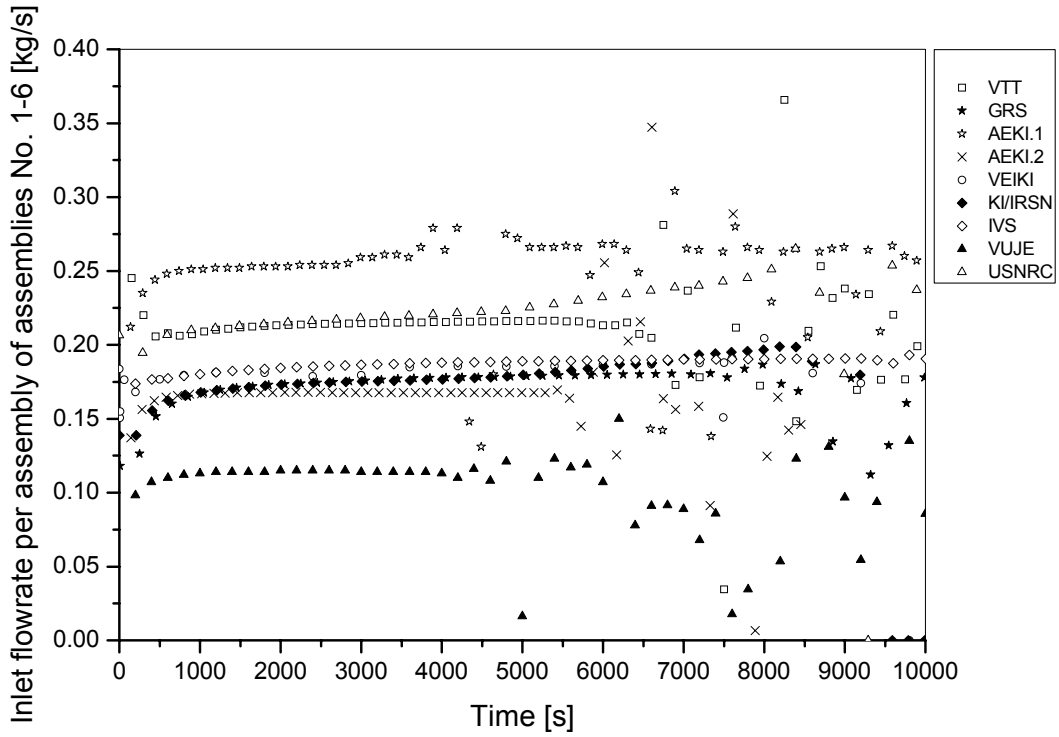


Figure 4.9. Inlet flowrate per assembly of assemblies No. 1-6 (first 10000 s)

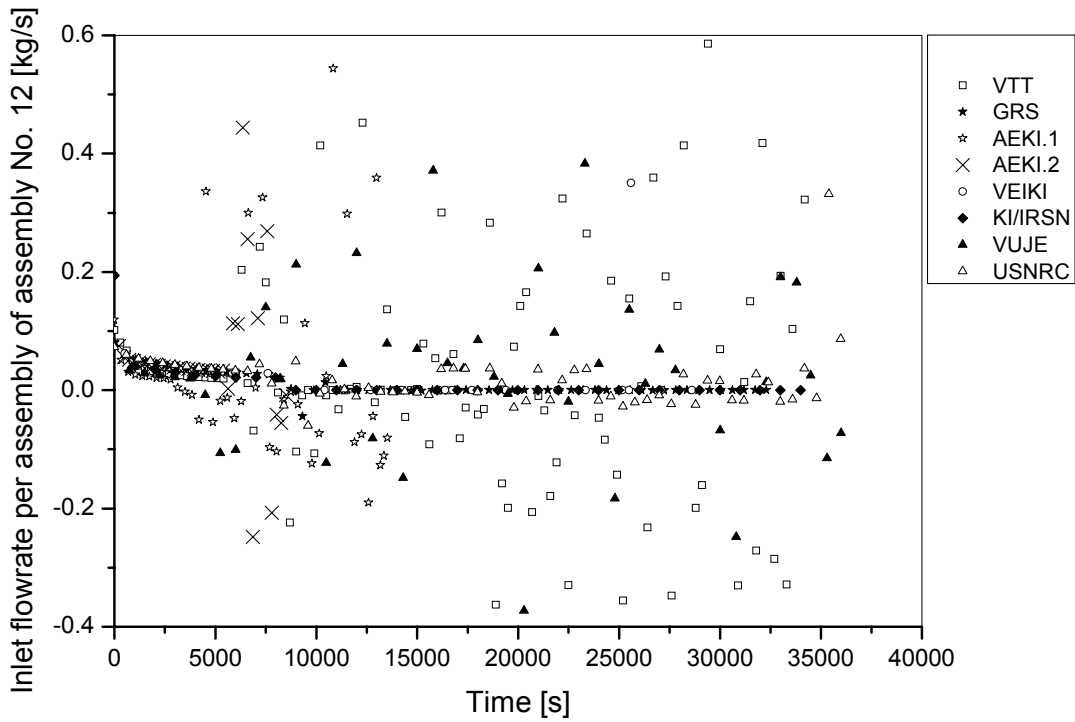


Figure 4.10. Inlet flowrate per assembly of assembly No. 12

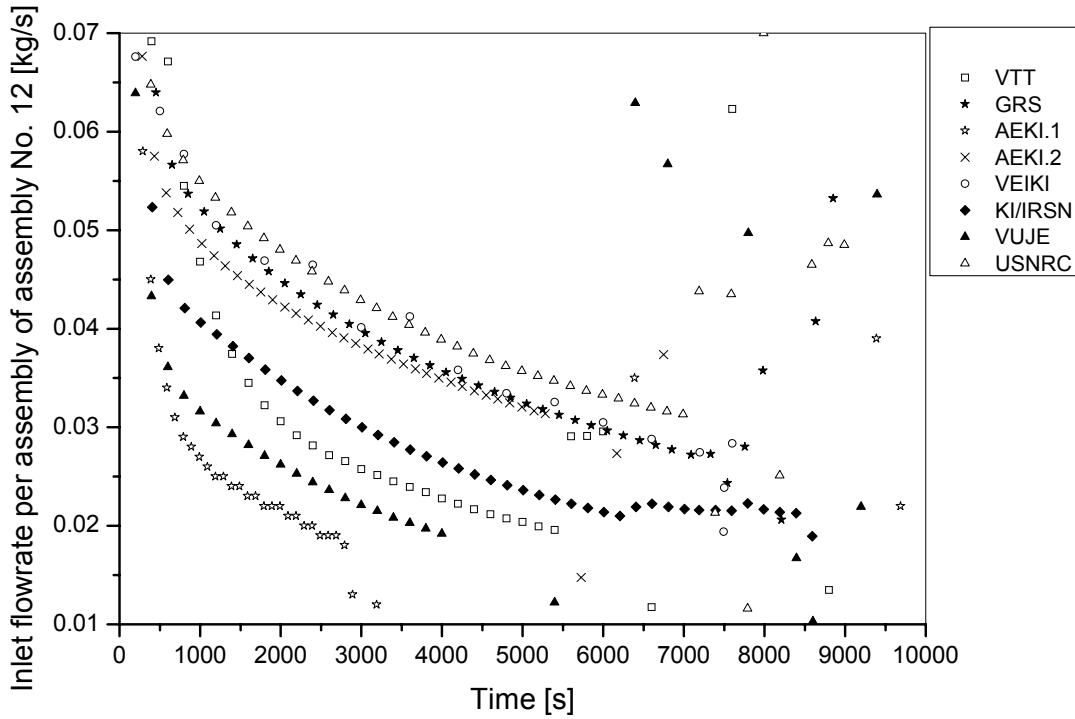


Figure 4.11. Inlet flowrate per assembly of assembly No. 12 (first 10000 s)

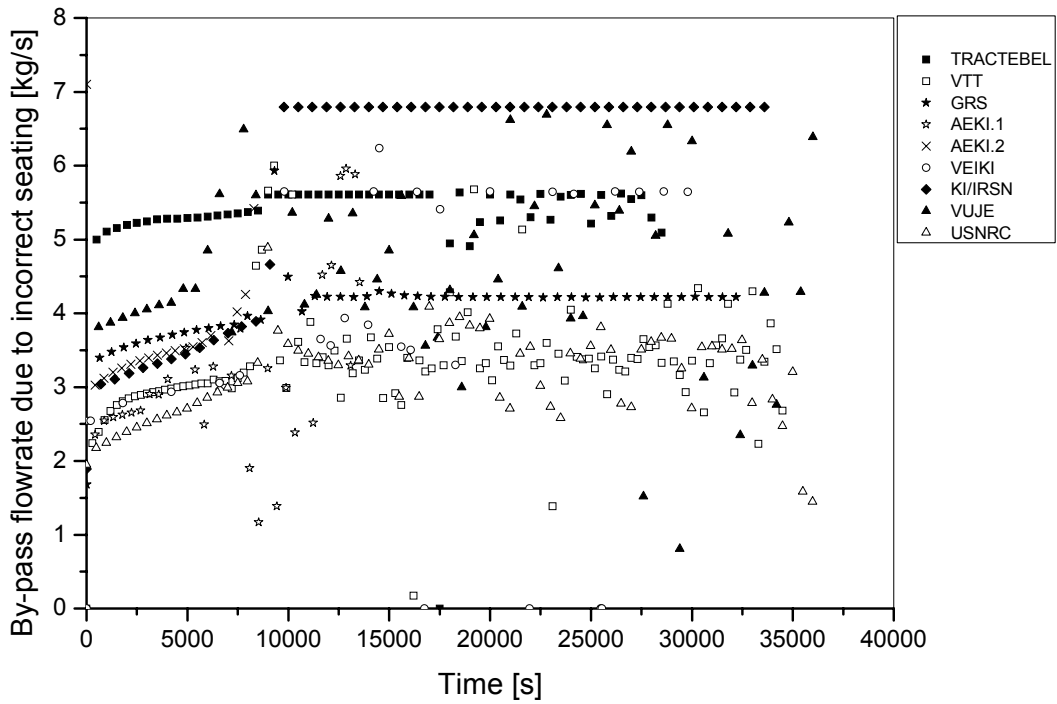


Figure 4.12. By-pass flowrate due to incorrect seating

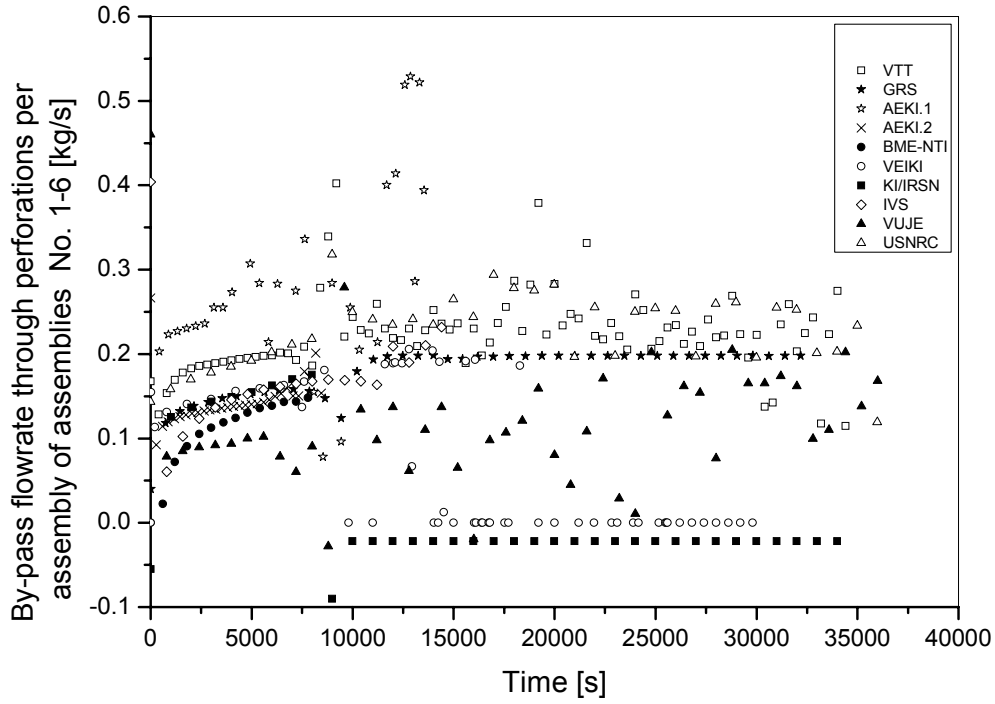


Figure 4.13. By-pass flowrate through perforations per assembly of assemblies No. 1-6

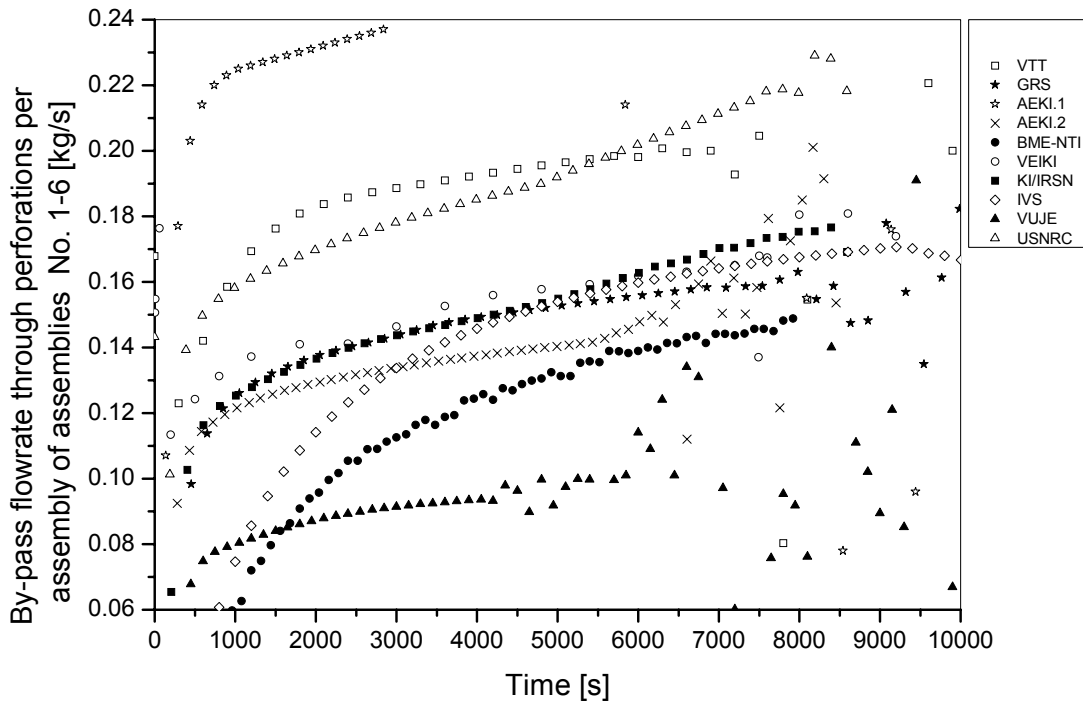


Figure 4.14. By-pass flowrate through perforations per assembly of assemblies No. 1-6 (first 10000 s)

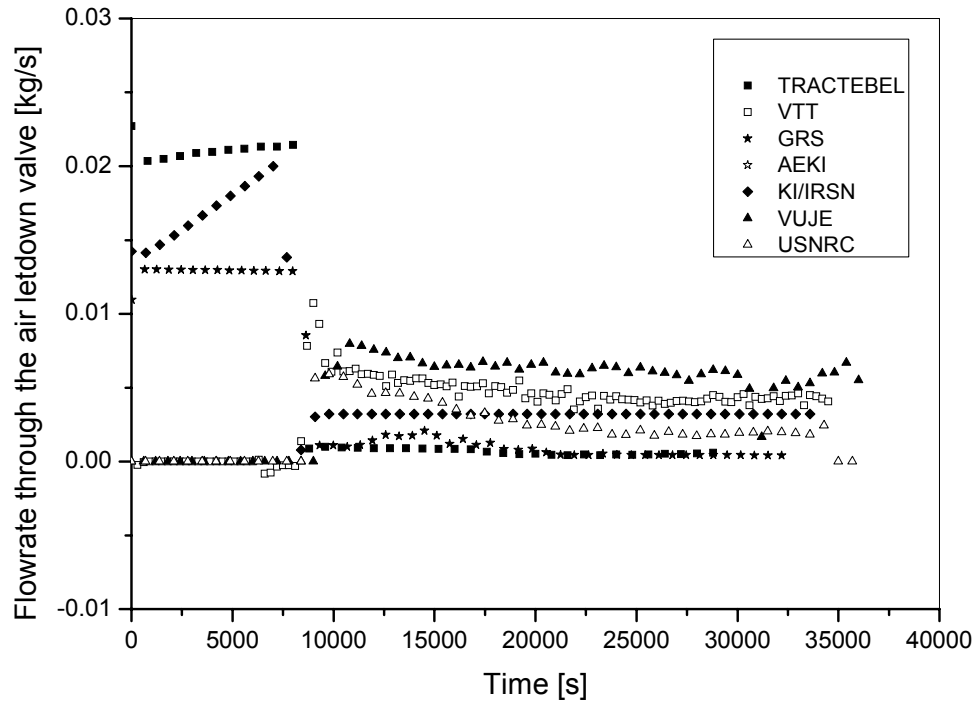


Figure 4.15. Flowrate through the air letdown valve

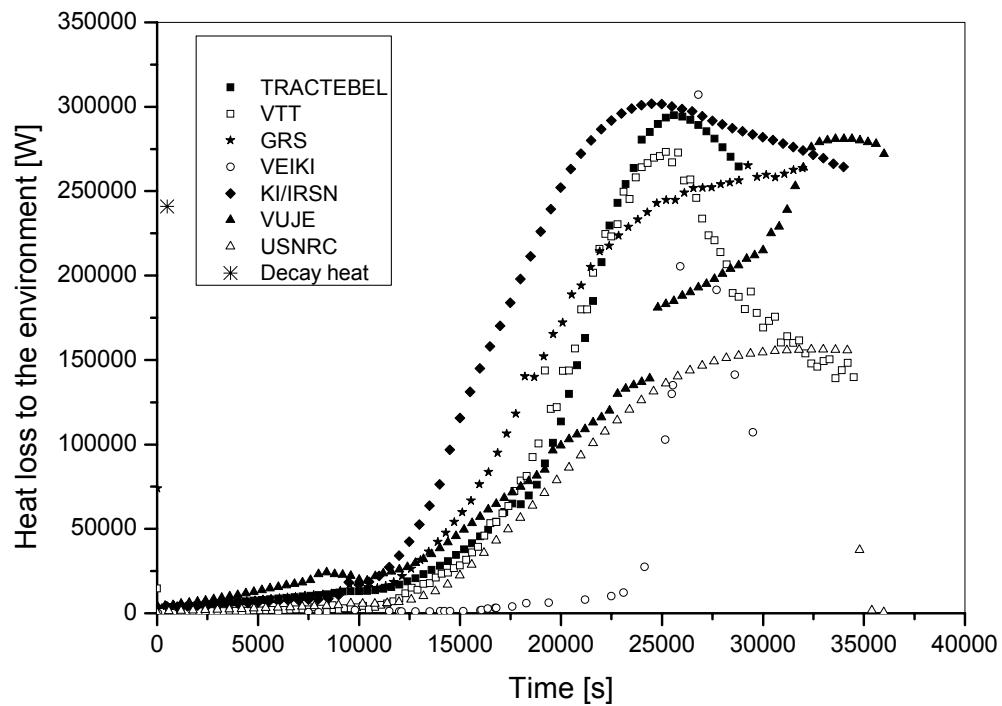


Figure 4.16. Heat loss to the environment

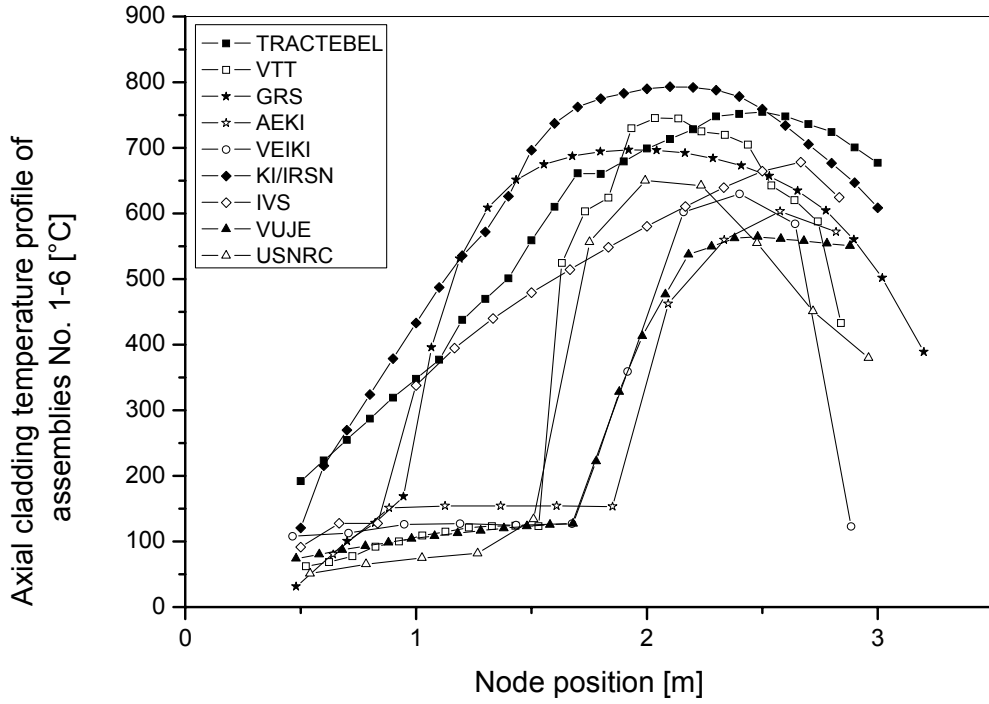


Figure 4.17. Axial cladding temperature profile of assemblies No. 1-6

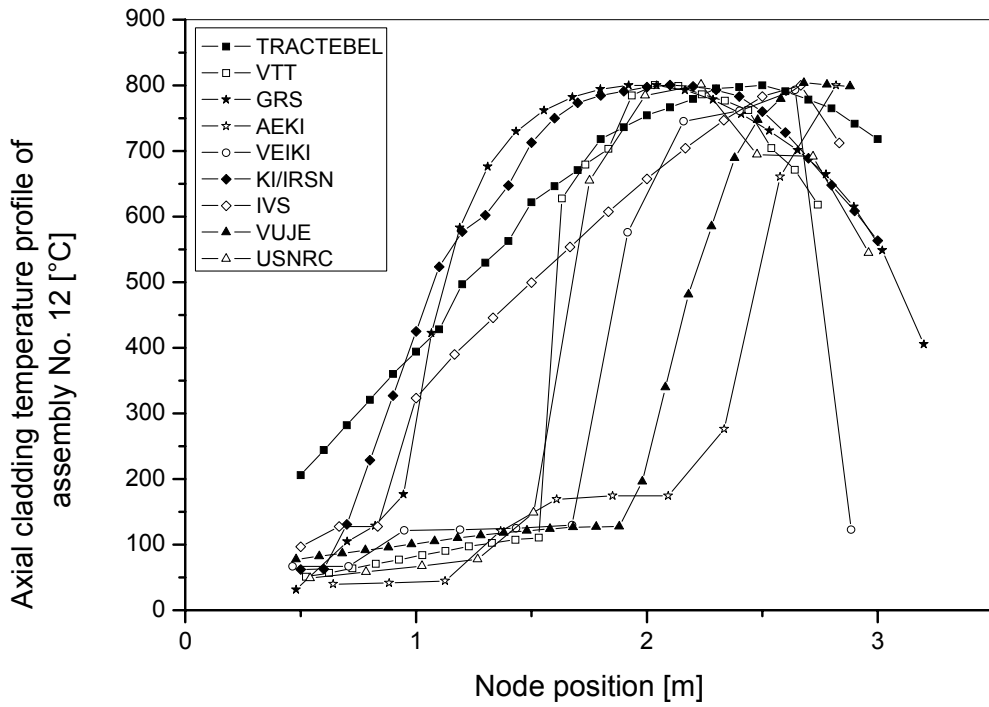


Figure 4.18. Axial cladding temperature profile of assembly No. 12

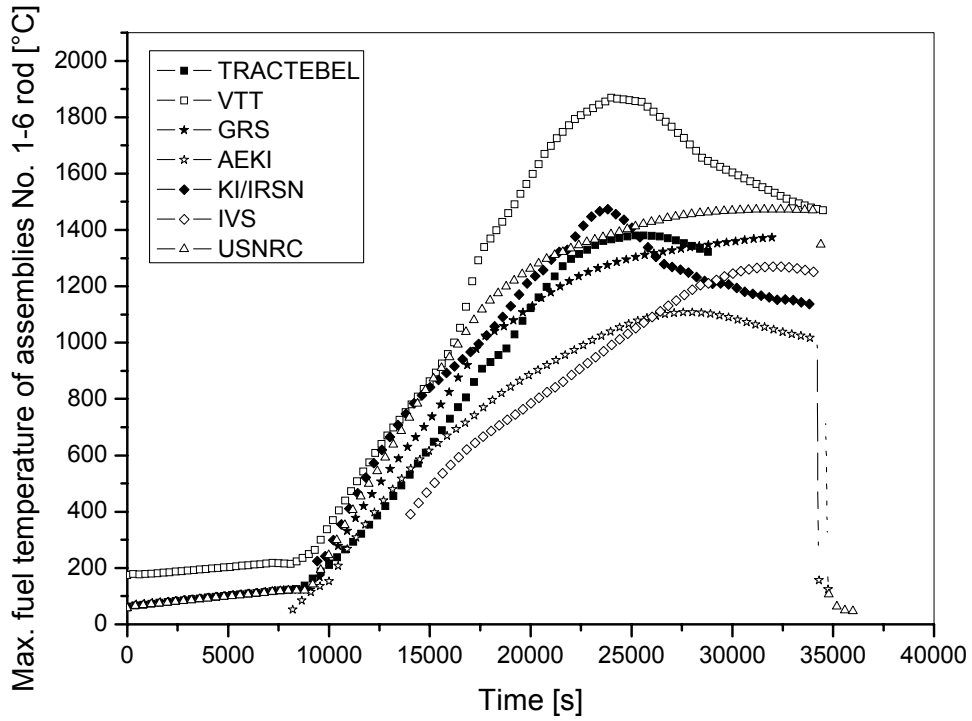


Figure 4.19. Max. fuel temperature of assemblies No. 1-6 rod

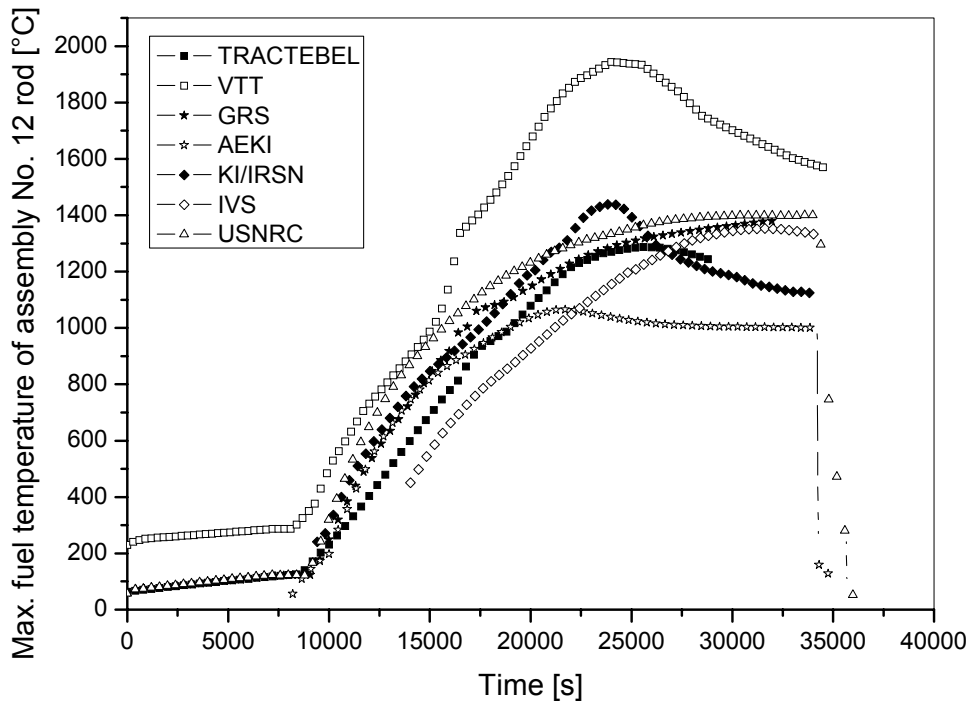


Figure 4.20. Max. fuel temperature of assembly No. 12 rod

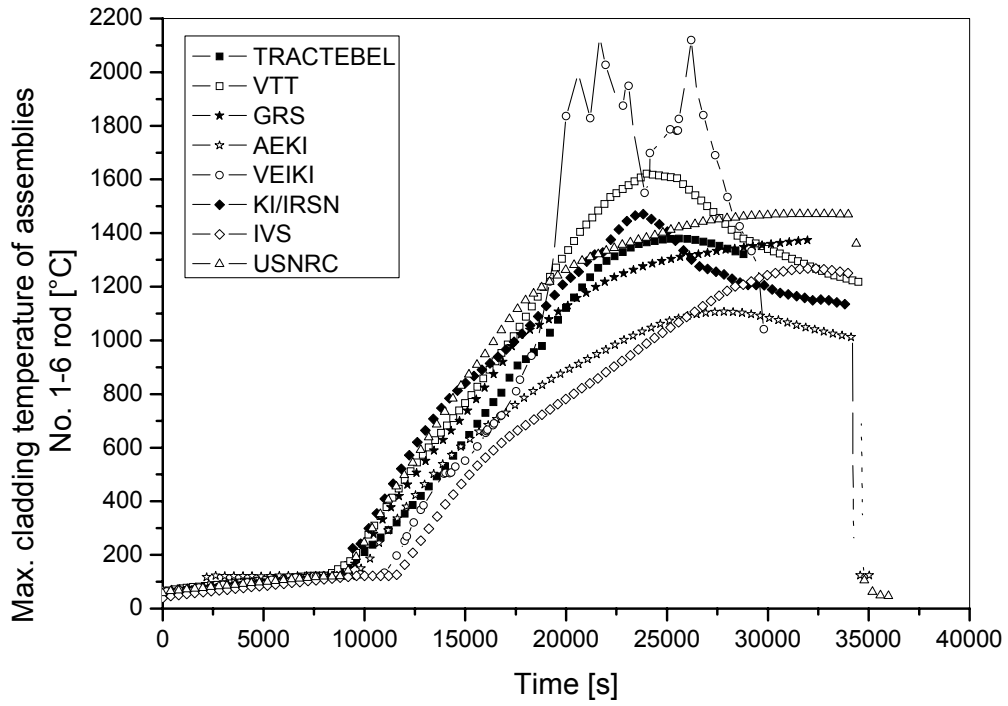


Figure 4.21. Max. cladding temperature of assemblies No. 1-6 rod

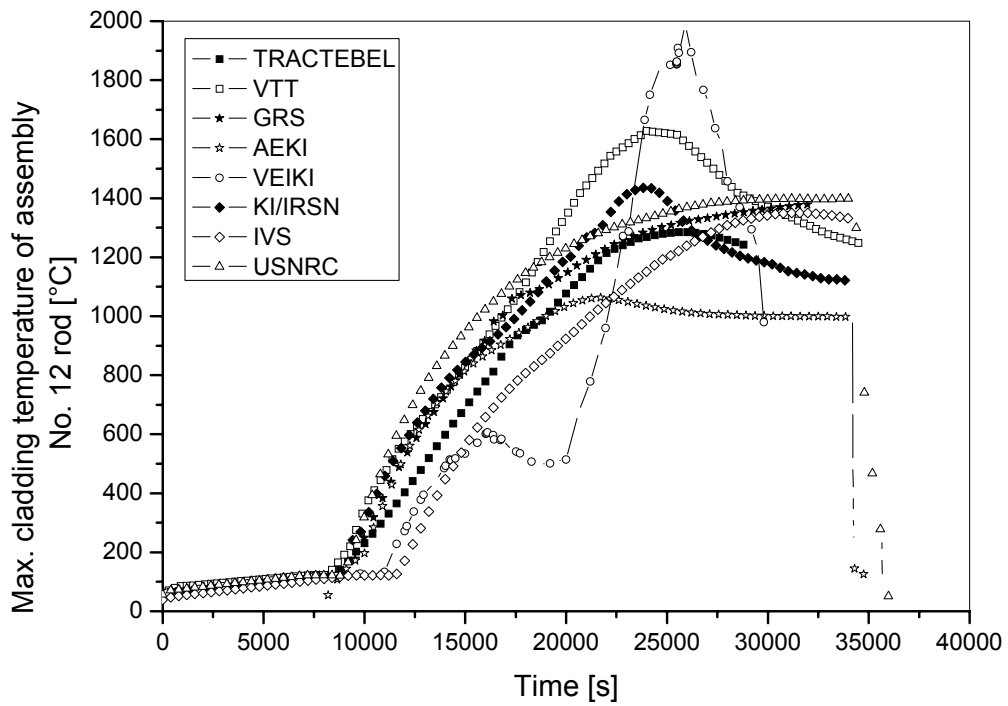


Figure 4.22. Max. cladding temperature of assembly No. 12 rod

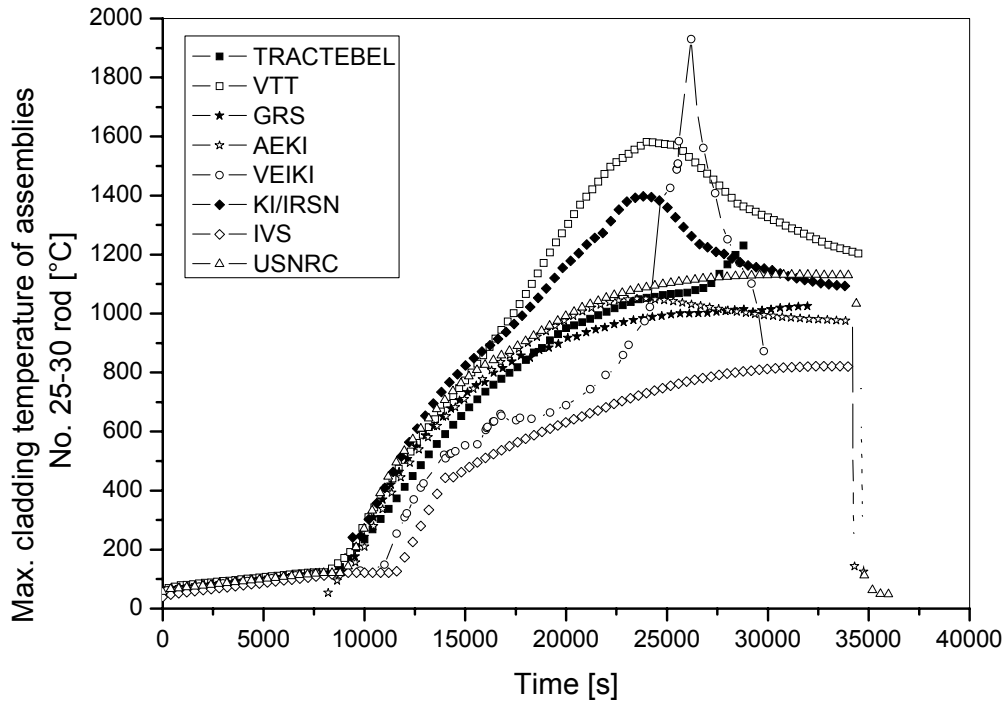


Figure 4.23. Max. cladding temperature of assemblies No. 25-30 rod

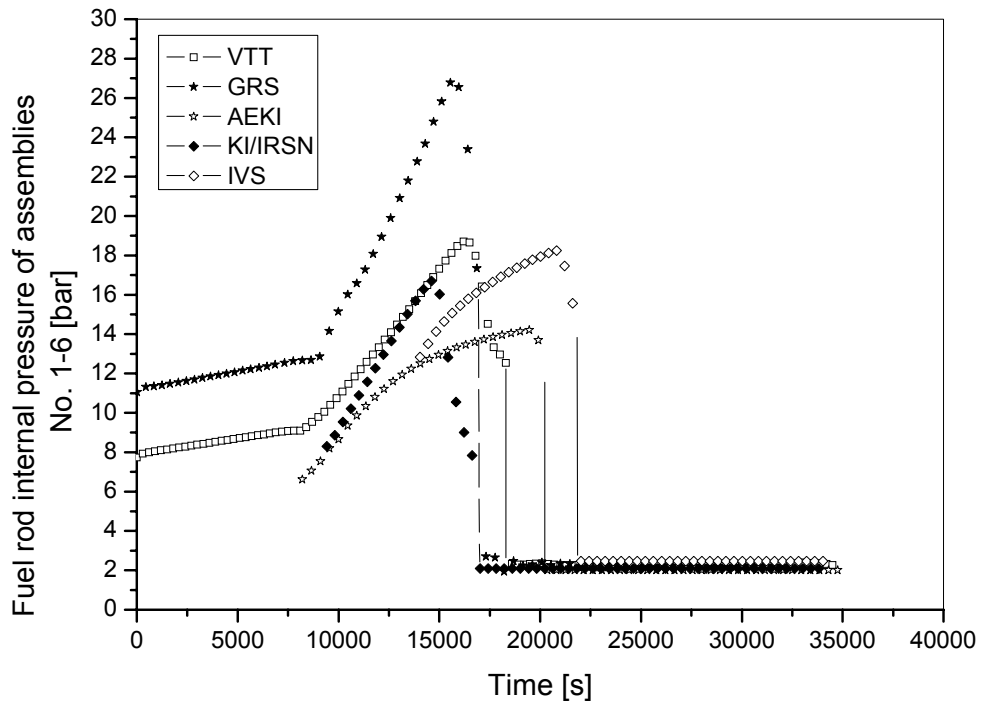


Figure 4.24. Fuel rod internal pressure of assembly No. 1-6

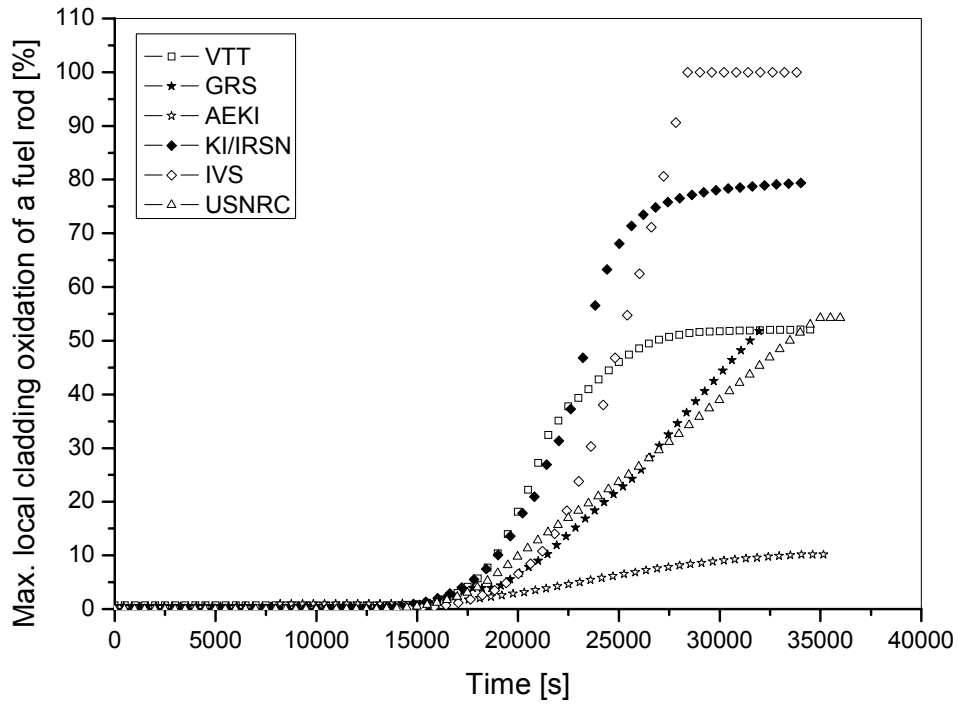


Figure 4.25. Max. local cladding oxidation of a fuel rod

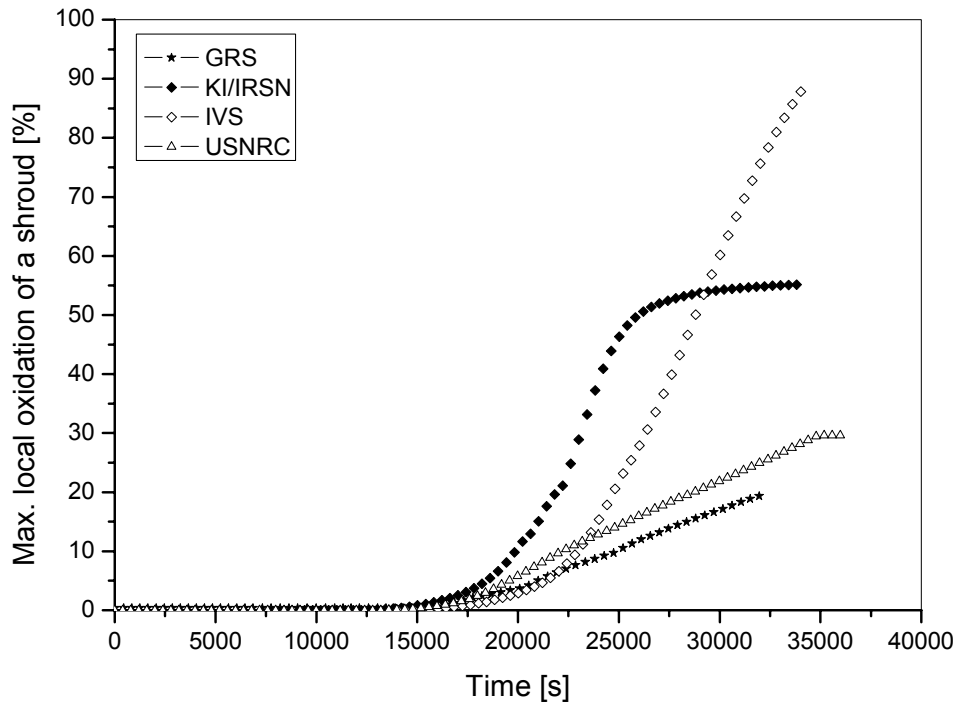


Figure 4.26. Max. local oxidation of a shroud

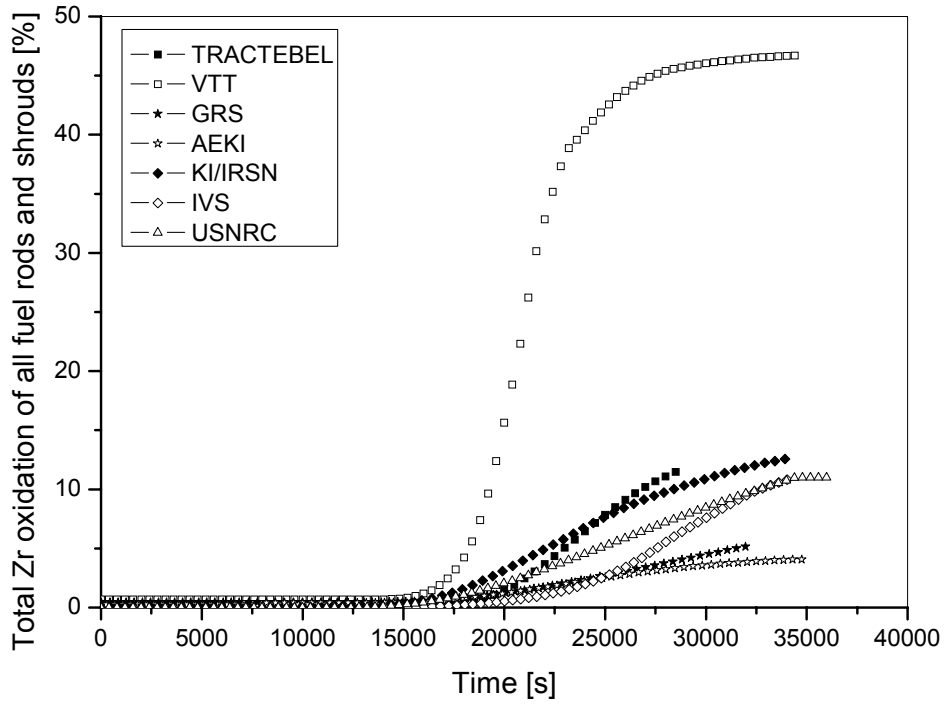


Figure 4.27. Total Zr oxidation of all fuel rods and shrouds

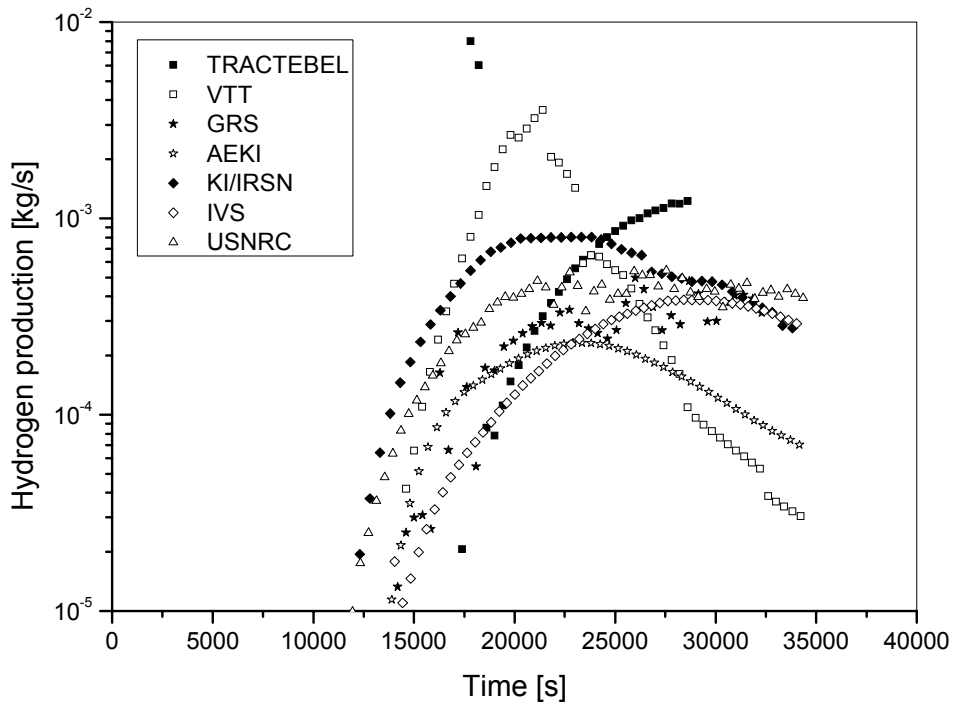


Figure 4.28. Hydrogen production rate

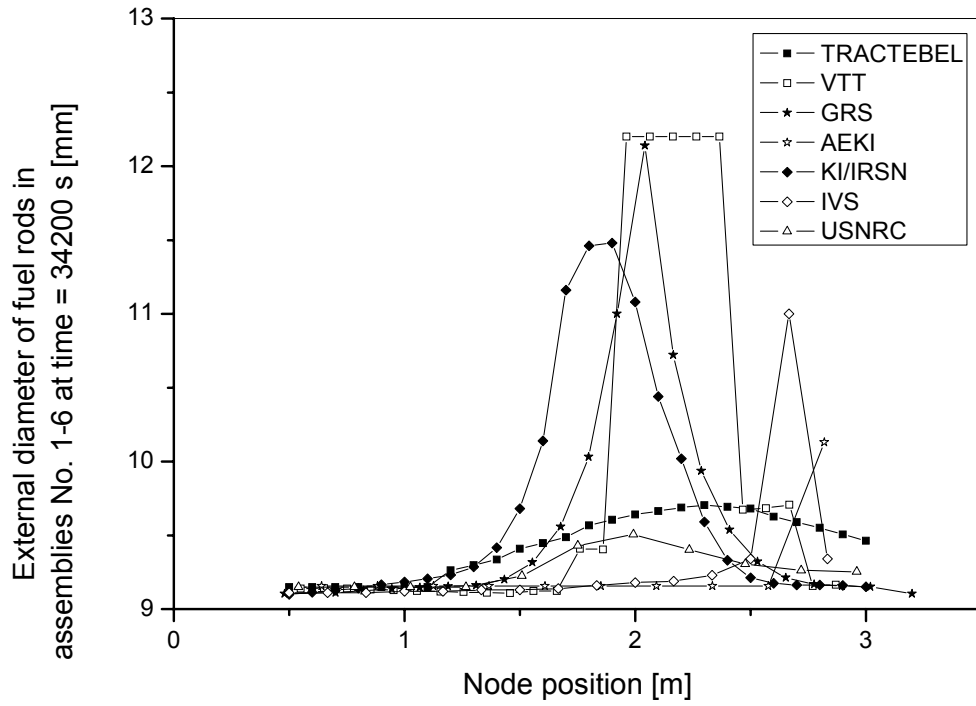


Figure 4.29. External diameter of fuel rods in assemblies No. 1-6 at time = 34200 s

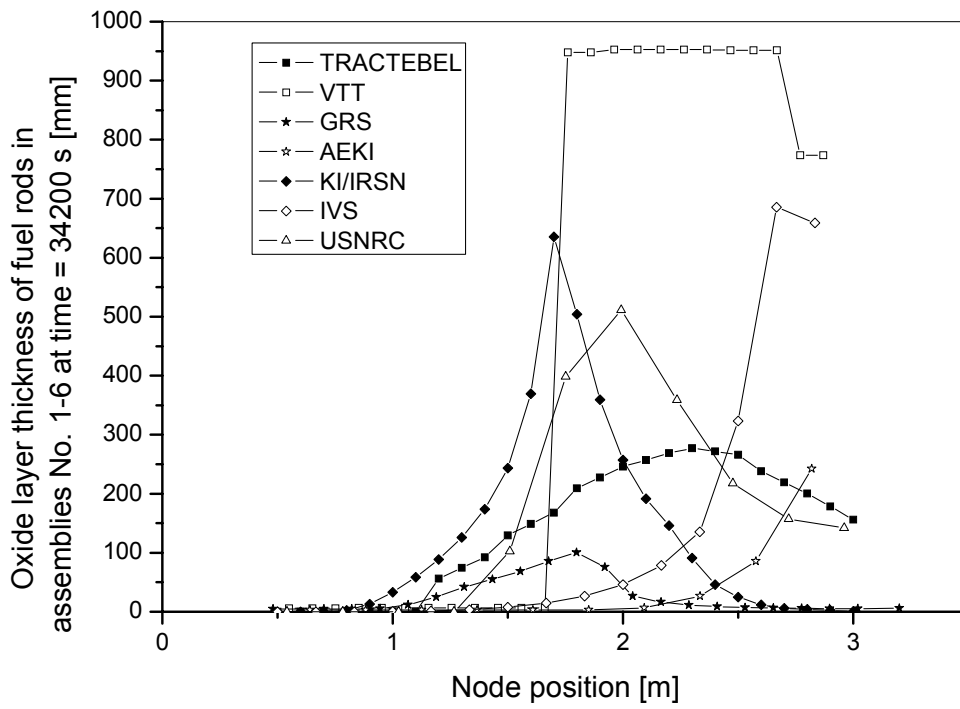


Figure 4.30. Oxide layer thickness of fuel rods in assemblies No. 1-6 at time = 34200 s

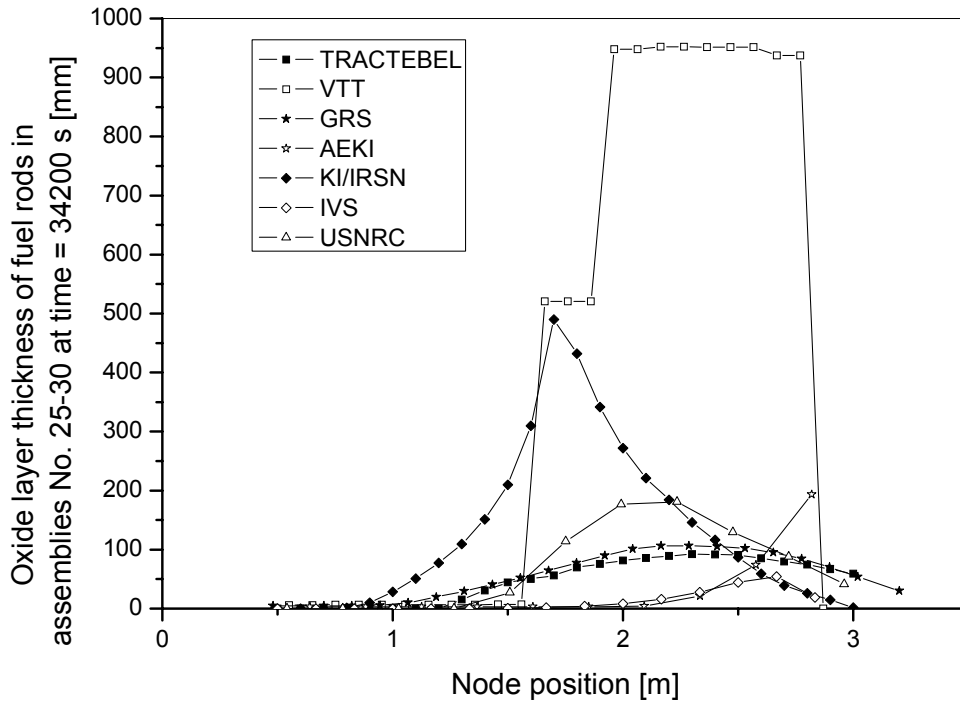


Figure 4.31. Oxide layer thickness of fuel rods in assemblies No. 25-30 at time = 34200 s

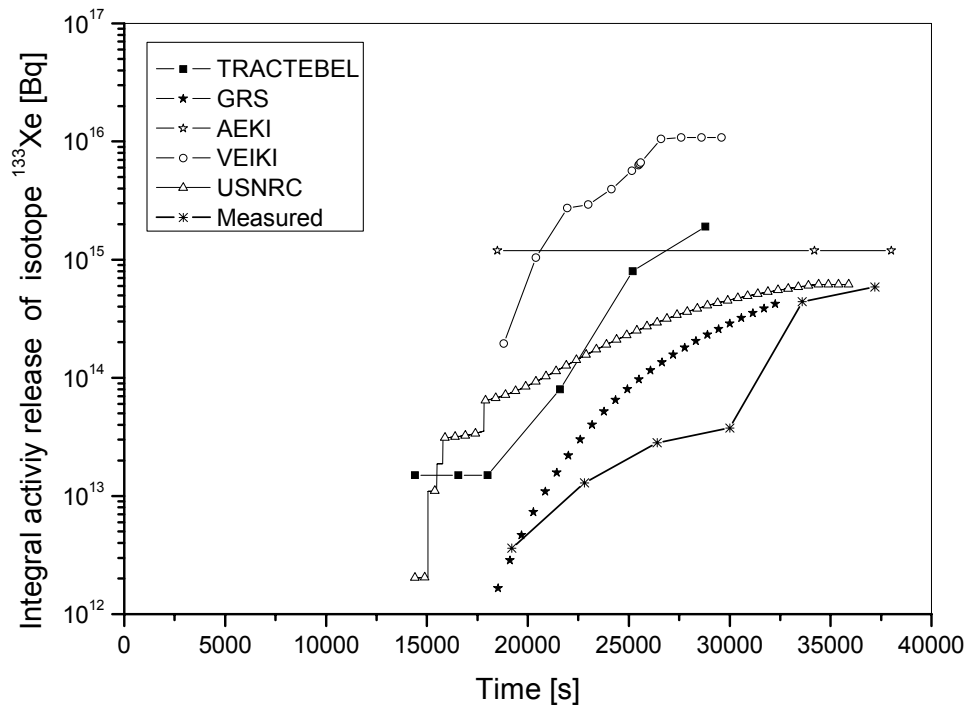


Figure 4.32. Integral activity release of isotope  $^{133}\text{Xe}$

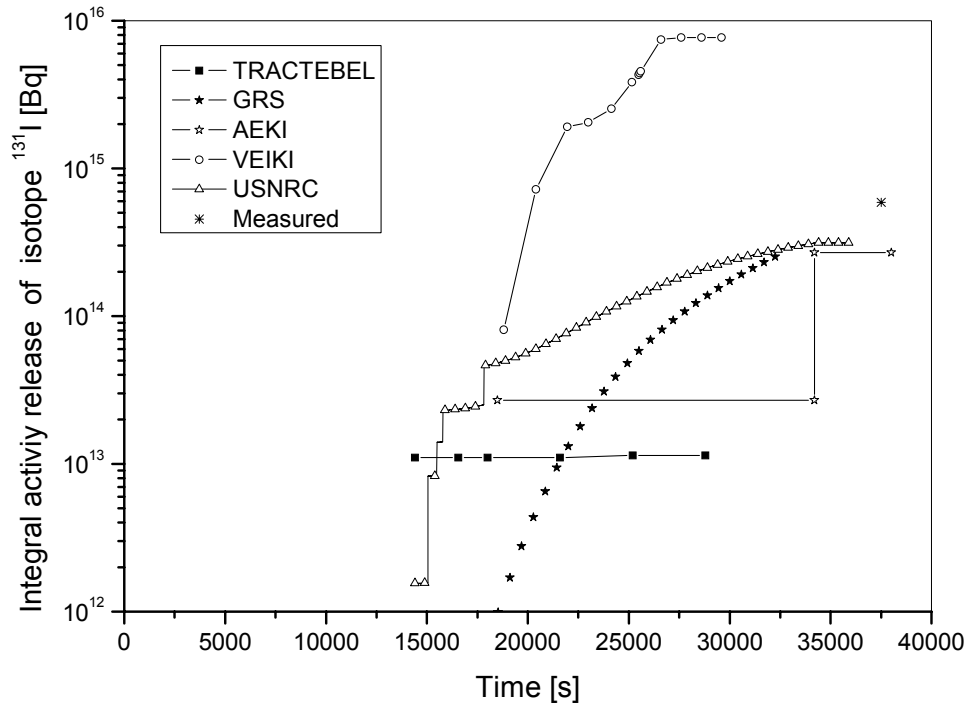


Figure 4.33. Integral activity release of isotope  $^{131}\text{I}$

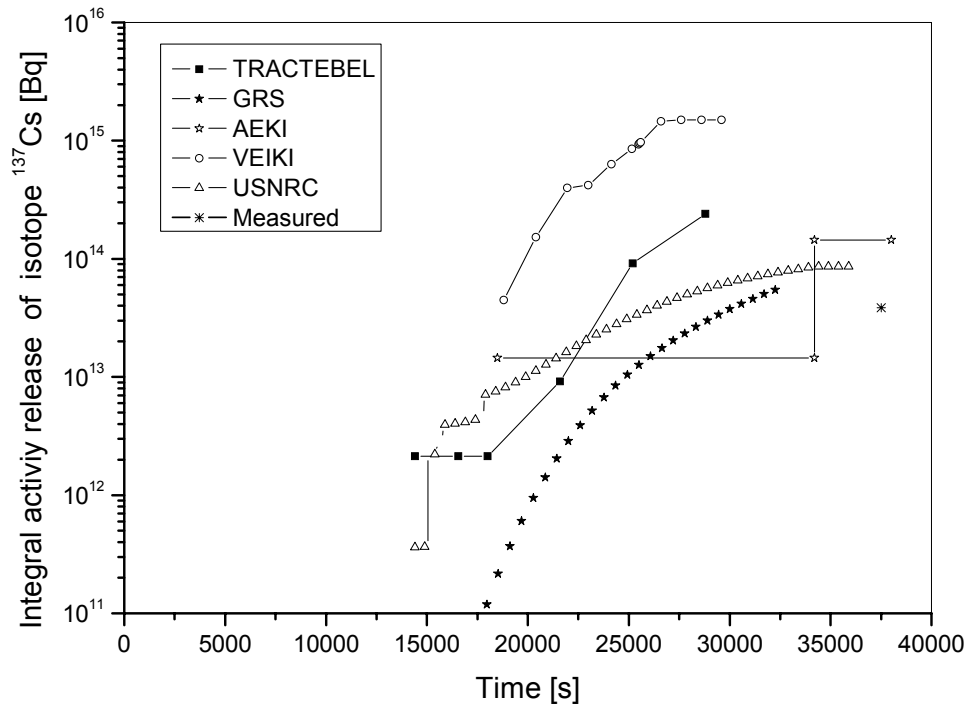


Figure 4.34. Integral activity release of isotope  $^{137}\text{Cs}$

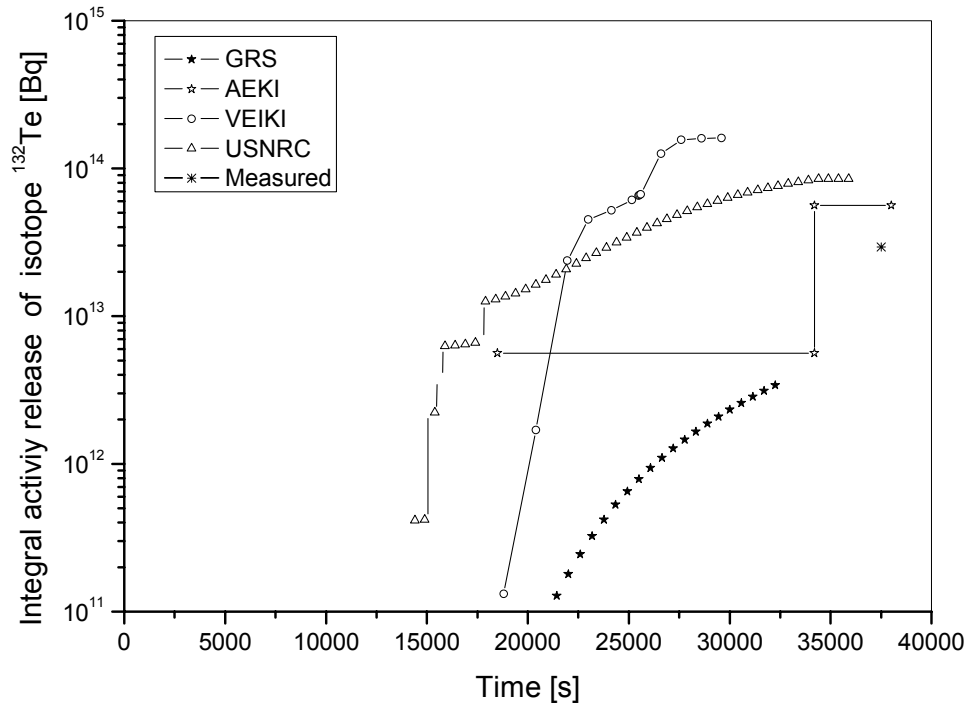


Figure 4.35. Integral activity release of isotope  $^{132}\text{Te}$

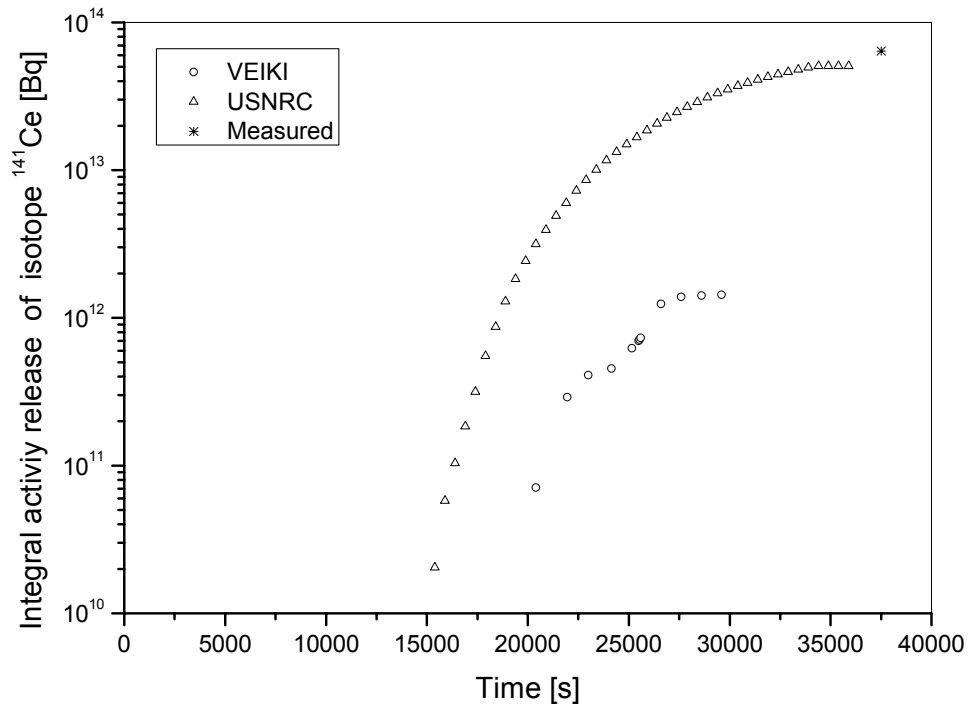


Figure 4.36. Integral activity release of isotope  $^{141}\text{Ce}$

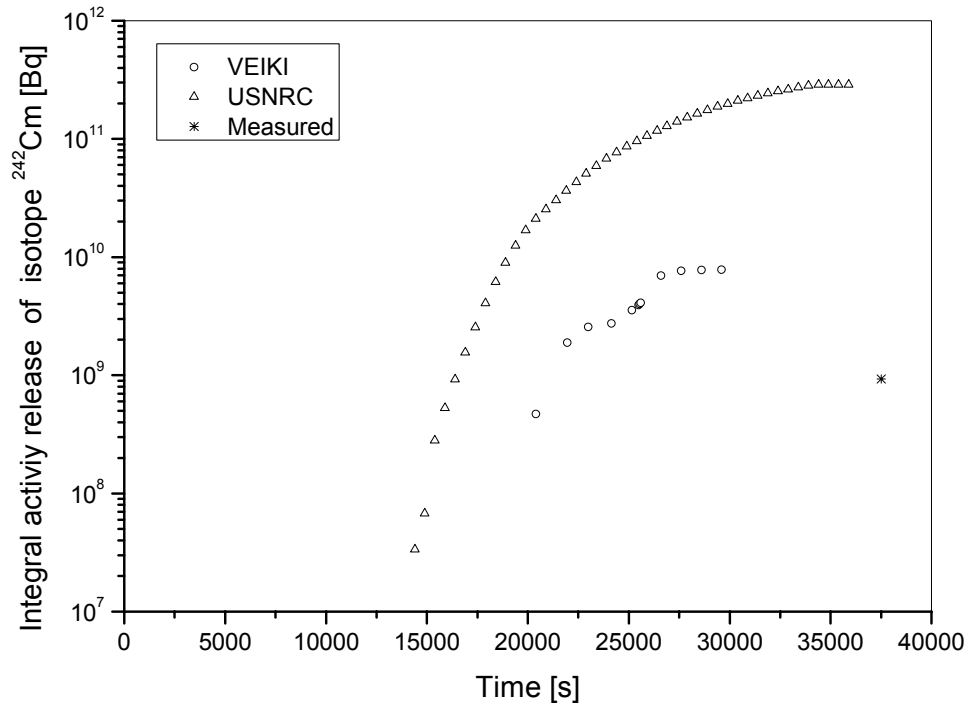


Figure 4.37. Integral activity release of isotope  $^{242}\text{Cm}$

## 5 RECOMMENDATIONS

The OECD-IAEA Paks Fuel Project was a valuable international program that was actively supported by 9 member states. Phase 1 included a thorough development of a comprehensive database to provide input data for severe accident analysis calculations. In support of the project, numerous simulations of the thermal hydraulic response, the fuel behaviour, and the fission product source term were performed by the participants. The three workshops provided an excellent forum to exchange ideas, to discuss the progression of events and key phenomena in the incident, and to assess the capabilities of various accident analysis codes. It is recommended that future programs used to investigate nuclear incidents include these effective features.

AEKI has performed an experimental simulation of the Paks-2 cleaning tank incident in the Core Degradation Experiment (CODEX) facility. The experiments in the CODEX facility simulated the whole scenario of the incident using electrically heated fuel rods. The test conditions were selected in such a way that several unknown parameters of the incident were covered. The final state of the fuel rods showed many similarities with the conditions observed after a severe core damage incident at a nuclear power plant. Hence, it is probable that the thermal conditions and chemical reactions were also similar in the tests and in the incident. Since the initial and boundary conditions were well controlled in the experiments, it is recommended that follow-on CODEX calculations be performed by the participants and presented at a future working group meeting.

The damaged Paks fuel has been removed from the cleaning tank and is stored in special containers in the spent fuel storage pool of the Paks NPP. The NPP intends to send all damaged fuel to Russia for reprocessing. Phase 2 was intended to cover a hot cell examination of the damaged fuel. At present, there is no funding or program to perform Phase 2. The following benefits were envisioned from the Phase 2 program.

- The damaged Paks fuel represents actual irradiated nuclear fuel from a power reactor that endured severe damage. Most of our current knowledge on the behaviour of fuel under severe accident conditions is based on small-scale experiments which use electrical heating. The examination of the Paks fuel could confirm or enhance the understanding of ballooning, oxidation, hydrogen uptake, and change of mechanical properties under severe accident conditions.
- The similarities between the Paks-2 event and a large break loss-of-coolant accident (LOCA) include high temperature oxidation in steam and quench by cold water. However, the differences are significant. These include the distance between assemblies, low decay heat (2 weeks after shutdown), very long oxidation time, stagnant steam volume, and hydrogen-rich atmosphere. In addition, the Paks fuel has a very sharp transition zone. The bottom of the fuel was under water and the top was heavily oxidized. Between those regions, there is a transition zone where varying levels of fuel damage exist. There is uncertainty when the fuel will fail under heavily oxidized conditions. An examination of the transition zone in the Paks fuel would provide data on the fuel cladding strength and integrity as function of oxidation under beyond design basis conditions.
- Many severe accident analysis codes do not model the mechanical integrity of oxidized fuel during a reflooding event. It is believed that the Paks fuel was extensively damaged

during the reflood of the cleaning tank. A characterization of the cladding strength at the assembly failure locations as described in the previous bullet could lead to more realistic thermo-mechanical failure models for the severe accident computer codes.

The removal of the fuel from the Paks cleaning tank was videotaped. Any further characterization of the event should include a review of the videotapes to further quantify the physical damage state. The review should include any observations on the axial, radial, and azimuthal damage patterns (e.g. for insights into heat loss and heat-up behaviour), a best estimate level depression, qualitative observations on the material strength and behaviour when cutting the debris for removal, a description of the debris on the baseplate and lower vessel head (e.g., whole pellets, size of oxidized cladding flakes), and a description of pictures of rod ballooning or other damage insights where views were possible. It is recommended to use the videotapes for the further evaluation of the state of the damaged Paks-2 fuel.

The database of the OECD-IAEA Paks Fuel Project includes valuable measured data on the activity release from damaged fuel under wet storage conditions. The use of such data was beyond the scope of the project, since the numerical analyses focused on the simulation of the incident. It is recommended that this part of the database be used in other (e.g. water chemistry, leaching of fuel, long term waste disposal) projects in the future.

## 6 CONCLUSIONS

The original objectives of the OECD-IAEA Paks Fuel Project were successfully met. The basic information that was necessary for the simulation of Paks-2 incident had been collected. Numerical analyses based on a common database were carried out with sophisticated models using codes that are used in the evaluation of the safety of nuclear power plants. The simulations covered thermal hydraulics, fuel behaviour and activity release aspects of the Paks-2 incident.

The calculations captured well some events as e.g.

- the time and speed of water level change in the cleaning tank and in the surrounding pools,
- the time of first fuel failures that very probably took place as a result of ballooning and burst of fuel rods at high temperature,
- the rate of released activity from the fuel.

The numerical analysis improved the understanding of Paks-2 event and helped to precise some unknown parameters of the incident as e.g.

- the by-pass flow at low flowrate amounted to 75-90 % of the inlet flowrate that led to the formation of steam volume,
- the maximum temperature in the tank was between 1200-1400 °C,
- the degree of zirconium oxidation reached 4-12 %,
- the mass of produced hydrogen was between 3 and 13 kg.

The OECD-IAEA Paks Fuel Project improved the current knowledge on fuel behaviour under accident conditions and recommended some further actions for research in this area.

## ABBREVIATIONS

AEKI	Hungarian Academy of Sciences KFKI Atomic Energy Research Institute
AMDA	Automatic Mobile Decontaminating Instrument
CFD	Computerized Fluid Dynamics
CSNI	Committee on the Safety of Nuclear Installations
FA	Fuel Assembly
FE	Finite Element
FGR	Fission Gas Release
FP	Fission Product
GRS	Gesellschaft für Anlagen- und Reaktorsicherheit mbH
INES	Incident on the International Nuclear Event Scale
IRSN	Nuclear Safety and Radioprotection Institute
ISP	International Standard Problem
KI	Russian Research Centre “Kurchatov Institute”
LOCA	Loss-of-Coolant Accident
NPP	Nuclear Power Plant
PCMI	Pellet-Cladding Mechanical Interaction
SFD	Severe Fuel Damage

## CONTRIBUTORS TO DRAFTING AND REVIEW

Aszódi, A.	Hungary, BME NTI
Boros, I.	Hungary, BME NTI
Guillard, V.	France, IRSN
Gyóri, Cs.	Hungary, AEKI
Hegy, G	Hungary, AEKI
Horváth, G. L.	Hungary, VEIKI
Hózer, Z. (editor)	Hungary, AEKI
Nagy, I.	Hungary, AEKI
Junninen, P.	Finland, VTT
Kobzar, V.	Russia, KI
Légrádi, G.	Hungary, BME NTI
Molnár, A.	Hungary, AEKI
Pietarinen, K.	Finland, VTT
Perneckzy, L.	Hungary, AEKI
Makihara, Y.	IAEA
Matejovic, P.	Slovak Republic, IVS
Szabó, E.	Hungary, AEKI
Trambauer, K.	Germany, GRS
Trosztel, I.	Hungary, AEKI
Varpoorten, J.	Belgium, Suez – Tractebel Engineering
Vitanza, C.	OECD/NEA
Vogel, M.	Slovak Republic, VUJE
Volchek, A.	Russia, KI
Wagner, K.C.	USA, SNL
Zvonarev, Y.	Russia, KI